

BIS Working Papers No 1052

Systemic risk in markets with multiple central counterparties

by Luitgard A M Veraart and Iñaki Aldasoro

Monetary and Economic Department

November 2022

JEL classification: C60, C62, G18, G21, G23.

Keywords: Central counterparties, systemic risk, contagion, stress testing, Cover 2.

BIS Working Papers are written by members of the Monetary and Economic Department of the Bank for International Settlements, and from time to time by other economists, and are published by the Bank. The papers are on subjects of topical interest and are technical in character. The views expressed in them are those of their authors and not necessarily the views of the BIS.

This publication is available on the BIS website (www.bis.org).

© *Bank for International Settlements 2022. All rights reserved. Brief excerpts may be reproduced or translated provided the source is stated.*

ISSN 1020-0959 (print)
ISSN 1682-7678 (online)

Systemic Risk in Markets with Multiple Central Counterparties*

Luitgard A. M. Veraart[†] Iñaki Aldasoro[‡]

October 31, 2022

Abstract

We provide a framework for modelling risk and quantifying payment shortfalls in cleared markets with multiple central counterparties (CCPs). Building on the stylised fact that clearing membership is shared among CCPs, we show how this can transmit stress across markets through multiple CCPs. We provide stylised examples to lay out how such stress transmission can take place, as well as empirical evidence to illustrate that the mechanisms we study could be relevant in practice. Furthermore, we show how stress mitigation mechanisms such as variation margin gains haircutting by one CCP can have spillover effects on other CCPs. The framework can be used to enhance CCP stress-testing, which currently relies on the “Cover 2” standard requiring CCPs to be able to withstand the default of their two largest clearing members. We show that who these two clearing members are can be significantly affected by higher-order effects arising from interconnectedness through shared clearing membership. Looking at the full network of CCPs and shared clearing members is therefore important from a financial stability perspective.

JEL classification: C60, C62, G18, G21, G23.

Key words: Central counterparties, systemic risk, contagion, stress testing, Cover 2.

*The views expressed in this article are those of the authors and do not necessarily reflect those of the Bank for International Settlements (BIS). Parts of this research were carried out while Luitgard Veraart was a BIS Research Fellow at the Bank for International Settlements, whose hospitality and funding are gratefully acknowledged. We thank Wenqian Huang, Nikola Tarashev, participants at the IMSI Workshop on Systemic Risk and Stress Testing, the UCL Financial Computing and Analytics Seminar, the 11th World Congress of the Bachelier Finance Society, the 2022 SIAM Annual Meeting as well as seminar participants at the BIS and ESMA for helpful comments and suggestions.

[†]*Corresponding author.* London School of Economics and Political Science, Department of Mathematics, Houghton Street, London WC2A 2AE, UK. Email: l.veraart@lse.ac.uk.

[‡]Bank for International Settlements, Centralbahnplatz 2, 4051 Basel, Switzerland. Email: inaki.aldasoro@bis.org.

1 Introduction

Central clearing has become a key feature of global derivatives markets in the aftermath of the Global Financial Crisis. The mandates to centrally clear derivatives have significantly altered the shape of financial networks – in centrally cleared markets a central counterparty (CCP) sits at the centre, becoming the buyer to every seller and the seller to every buyer. Much of the academic and policy effort in understanding and managing risks in centrally cleared markets has been on the CCPs themselves and their ability to withstand a severe shock.¹ In theory, there are efficiency gains arising from having a single CCP (Duffie & Zhu, 2011). In practice, however, derivatives clearing is characterised not by a single CCP, but by a small set of CCPs. Importantly, linking these CCPs is a limited number of large banks representing the joint clearing membership that together account for the lion’s share of clearing volumes.²

In this paper, we analyse the role of joint clearing membership at multiple CCPs for stress transmission and financial stability. Joint clearing membership affects the structure of interconnections in financial networks, connecting CCPs via their shared clearing members and connecting the latter via CCPs. As such, it can affect risk transmission (see e.g. Faruqui et al. (2018) for a discussion of the economic mechanisms characterising the nexus between CCPs and clearing members). In this context, the default management mechanism of CCPs plays a central role.³ This is usually described in terms of the “default waterfall”, which specifies the order of loss absorption for the resources available to CCPs (see e.g., Duffie (2014)).

We show how joint clearing membership can affect several layers of the default waterfall. The exact structure of a waterfall varies between CCPs, but as outlined in Gregory (2014), it can be split into losses paid by defaulters and by survivors. In particular, initial losses are paid for by the defaulting clearing members (in the form of initial margins and their default fund contributions) and higher losses are paid for by the CCP (skin-in-the-game) and surviving clearing members (via their default fund contributions and potentially additional contributions). We show that joint clearing membership affects both parts of the default waterfall, i.e., how the defaulters pay and how the survivors pay, giving rise to different contagion channels.

We consider two contagion channels associated with the default waterfall. The first is the fire-sale channel of initial margins. Initial margins, typically in the form of collateral, serve as the first line of defense in the waterfall to cover losses associated with individual positions cleared via CCPs. A simultaneous default at more than one CCP by a joint clearing member can lead to losses larger than those covered by initial margins at all the CCPs where the member clears – a situation which is only worsened if collateral is illiquid.⁴ The second channel we consider is associated with one of the last layers of the default waterfall:

¹See Menkveld & Vuillemeij (2021) for a recent literature survey. A large part of the literature on central clearing focuses on counterparty credit risk and netting efficiency. Duffie & Zhu (2011) show that clearing different products in separate CCPs decreases netting efficiency and increases counterparty credit exposure, compared to clearing all products in one CCP. Despite the theoretical advantages, central clearing today is done by a group of CCPs and not just a single CCP. Cont & Kokholm (2014) consider a generalisation of the Duffie & Zhu (2011) framework and show that some of the conclusions depend on distributional assumptions on exposures. Garratt & Zimmerman (2015) generalise this framework further by considering more general network structures (e.g., scale free networks).

²(BCBS-CPMI-FSB-IOSCO, 2018) show that, empirically, central clearing is characterised by a strong concentration around clearing members. These tend to be the largest global dealer banks that have long dominated derivatives trading. The central role of these banks implies that they tend to be connected to more than one CCP, as they facilitate trading across both markets and jurisdictions.

³While CCP defaults are very rare events, they are not without historical precedent (Faruqui et al., 2018; Bignon & Vuillemeij, 2020). Furthermore, recent empirical evidence based on European repo market data suggests the potential failure of a CCP is perceived as a real possibility by market participants and is priced into repo rates (Boissel et al., 2017).

⁴Glasserman et al. (2015), who refer to this mechanism as “hidden illiquidity”, show that convex margin requirements incentivise clearing members to split their positions among several CCPs. They analyse existence and characteristics of equilibria of margin schedules, such that CCPs collect sufficient margins in the presence of optimising clearing members. However, they do not model the contagion mechanism itself that arises from illiquid collateral, which is what we study here. Throughout the paper we use the short-hand of “illiquid margins” to refer to the illiquidity of the collateral with which margins are met.

variation margin gains haircutting (VMGH).⁵ If a stressed CCP uses VMGH, then all clearing members that owe variation margin to this CCP are required to make full payments, but the CCP itself only pays out a fraction of the variation margin it owes. We show that one CCP's VMGH can transmit losses to another CCP via their joint clearing members. In the extreme, a clearing member could cause the default of an unrelated CCP if the CCP where it clears employs VMGH.

Finally, we show how illiquid collateral and VMGH interact, potentially leading to even larger losses, notably when the CCP-bank nexus consists of cycles (i.e. when CCPs are connected to each other via joint clearing members).⁶

To illustrate these channels we build a network model where clearing members are connected to multiple CCPs through derivatives market obligations. The trigger for contagion is an exogenous change in market conditions giving rise to variation margins between clearing members and CCPs. As variation margins come due, counterparties attempt to meet them. If they cannot, then they are put on "technical default" and initial margins and default fund contributions will be used. But if the collateral underpinning initial margins is illiquid (Ghamami et al., 2022), the realised equilibrium price will likely be smaller than originally anticipated – further fuelling shock transmission. If payment obligations cannot be met, clearing members effectively default, whereas CCPs can rely on VMGH, which in turn may curtail effective payments to other clearing members and further contribute to contagion. Along the way, at each stage stress can be transmitted across CCPs and clearing members due to the shared membership across CCPs. The model builds on the literature on systemic risk in financial networks and is particularly related to approaches that consider CCPs or the presence of collateral. Concretely, we build on Ghamami et al. (2022), who derive a modelling framework for clearing payments in collateralised networks (without a central counterparty) based on the seminal contribution by Eisenberg & Noe (2001). We adapt this framework to markets with multiple central counterparties, allow for a more detailed default mechanism of CCPs, and include frictions such as default costs (in the spirit of Rogers & Veraart (2013)) and the possibility of variation margin gains haircutting by CCPs.⁷

The modelling framework we present works for general network structures and does not make any assumptions on the magnitudes of different layers of the default waterfall. A growing literature considers design aspects of central clearing. For example, Amini et al. (2015) study the problem of designing central clearing such that it reduces systemic risk and is consistent with the preferences of those using it. Biais et al. (2016) study the optimal design for central clearing and margin calls to increase resilience in derivatives markets. Lopez et al. (2017) propose a methodology for estimating margin requirements that accounts for interdependencies of market participants. Wang et al. (2022) propose a normative analysis on the design of collateral requirements for central clearing. They consider both initial margins and default funds in their analysis. Huang (2019) consider the incentive problem of thin skin-in-the-game of CCPs. In contrast to these approaches, we take the design as given and analyse the outcome for a given design. There is considerable flexibility, however, in the specific design that can be considered in our analysis.

We use three stylised examples to illustrate how contagion through joint clearing membership and multiple CCPs operates in the model. The first and most simple has a clearing member jointly clearing in two CCPs and two additional clearing members clearing only at each of the two CCPs. The default of the joint

⁵We over details of the default waterfall below. ISDA (2013) advocates the use of Variation Margin Gains Haircutting for failing CCPs: "For Default Losses, this paper advocates Variation Margin Gains Haircutting ("VMGH") as a robust recovery and continuity mechanism which will operate as part of the default waterfall following the exhaustion of all other layers of the default waterfall".

⁶Throughout, the default of a clearing member (given by an inability to meet payments due on derivatives) is invariably at the root of a CCP's default.

⁷Our work also relates to Paddrik et al. (2020) and Paddrik & Young (2021), who model payment shortfalls in centrally cleared markets with a single CCP. In contrast, we consider markets with multiple CCPs, model in more detail the CCP default waterfall and include additional frictions such as default costs and different magnitudes of variation margin gains haircutting into the modelling framework.

clearing member can cause large losses to both CCPs, in the extreme potentially leading to their default if the collateral posted by the defaulting member is illiquid.⁸ The second example has a similar structure, but the default is of a clearing member that only clears at one CCP. This example helps to illustrate the possibility that the default of a clearing member can adversely affect a CCP in which the member *does not* clear. The third example involves a cycle where two clearing members jointly clear at two CCPs, and it helps to illustrate how the interaction of illiquid collateral and VMGH can help propagate distress and default in the network. Our analysis extends earlier work on the nexus between CCPs and clearing members (as analysed for example in Faruqui et al. (2018)) by providing a quantitative model to measure the magnitude of losses arising from the feedback loops between these agents.

Beyond these stylised examples, we provide empirical evidence of CCP-clearing member interconnectivity by analysing public data on interest rate and credit default swaps (IRS and CDS respectively). Indeed, as described in BCBS-CPMI-FSB-IOSCO (2018), several banks are clearing members at multiple CCPs. This is in line with results by Demange & Piquard (2021), who provide empirical evidence of competition between CCPs in Europe.⁹

We use the data to provide case studies that show how the different contagion channels can play out in the IRS and CDS markets. We calibrate our model based on data on clearing membership, notional amounts cleared (for both members and CCPs), default funds, skin-in-the-game and aggregate initial margins, as well as estimates of the network of payments obligations and liquidity buffers. We use this to quantify the shortfall in payments when accounting for higher order effects and the different contagion channels discussed above. We find that these contagion channels can cause the default of CCPs and we quantify the magnitude of the losses. Our analysis helps to illustrate that the mechanisms captured by the model could be of relevance when calibrated to real-world data. That said, our exercises are meant as illustrative of the mechanisms we model, rather than a real-world stress test – in other words, we cannot quantify the likelihood of any scenario leading to an actual CCP default.

Our results carry important implications from a policy perspective, in particular regarding CCP stress-testing.¹⁰ At the heart of current practice is the Cover-2 standard, which, generally speaking, seeks to identify the two groups of clearing members that would lead to the largest shortfall of prefunded resources for a given CCP or alternatively across all CCPs.¹¹ Paddrik & Young (2021) argue that the Cover-2 standard can underestimate the vulnerability of the system because it does not consider network effects. They provide empirical evidence for such network effects in a single-CCP market, allowing for variation margin gains haircutting. By considering only one CCP, however, their analysis abstracts from the effects of joint clearing members in loss transmission between several CCPs – what we analyse here. For the specific simulations we conduct – which are only meant as illustrative – the total loss can increase by a factor of around four when considering network effects with multiple CCPs, shared clearing members and the contagion channels discussed above.

We argue that who the top two clearing members are (that cause the highest losses) will significantly depend on the contagion mechanisms included in the modelling framework. In particular, we show that the ranking of institutions according to first order losses can differ notably from that obtained when considering

⁸In both the model and the simulations that follow, a CCP can default if it is not able to meet its payment obligations to clearing members (after recourse to available elements from the default waterfall).

⁹There is also theoretical work modelling competition between CCPs. Huang (2019) studies incentives of for-profit CCPs with limited liabilities, analysing the trade-off between maximising fee income and counterparty credit risk. A CCP that requires higher collateral from its clearing members (which reduces the probability of a CCP's default), will attract fewer clearing members. A key result is that if there are no capital requirements for CCPs, a profit-maximising CCP will hold no capital and will only ask for small collateral requirements from its clearing members. If, however, a CCP is user-owned, i.e., owned by its clearing members, then it has incentives to hold more capital.

¹⁰See CPMI-IOSCO (2018) for a general framework of supervisory stress testing of CCPs. For details on current market practice for stress testing CCPs in the European Union, we refer to ESMA (2020).

¹¹See Section 5 for details on the two different types of applications of the Cover-2 standard.

higher order losses that account for shared clearing membership.¹² From a financial stability perspective it is thus important to take into account the network of joint clearing membership across multiple CCPs.

The main contributions of our paper are three-fold. First, we develop a framework to quantify payment shortfalls in centrally cleared markets with multiple CCPs and identify different roles of joint clearing members for loss transmission. Furthermore, we show how stress mitigation mechanisms such as variation margin gains haircutting by one CCP can have spill-over effects to other CCPs. Second, we complement existing empirical evidence of CCP interconnectedness via their joint clearing members by analysing data from the interest rate and credit default swaps markets. Third, we discuss policy implications for stress testing central counterparties focusing in particular on the Cover-2 standard. We show that who the two top clearing members are varies significantly depending on whether one accounts for contagion effects via joint clearing membership and defaults at multiple CCPs. Our analysis therefore can serve as a tool to select stress scenarios in markets with multiple central counterparties.

The rest of the paper is structured follows. Section 2 presents the modelling framework and its various variants. Section 3 provides simple stylised examples to illustrate how contagion unfolds in the model. Section 4 presents evidence of CCP interconnectedness through joint clearing membership in interest rate and credit default swap markets, and applies our contagion model to these data. Section 5 discusses policy implications for CCP stress-testing. Finally, Section 6 concludes.

2 Modelling contagion in markets with multiple CCPs

We develop a model for a clearing equilibrium in derivatives markets when variation margins become due. Our model is a generalised version of the model proposed by Ghamami et al. (2022), which itself builds on the clearing framework developed by Eisenberg & Noe (2001). We adapt this to markets with multiple central counterparties and introduce additional frictions to account for risk-mitigation tools available to CCPs, in particular variation margin gains haircutting.

Ghamami et al. (2022) propose a clearing mechanism for collateralised markets that proceeds in two rounds. The first round determines who defaults, as well as the initial payments made between counterparties. In the second round, collateral (initial margin) that was not used is returned to the nodes that originally set it aside and is used to make additional payments if those made in the first round fell short of obligations. We will generalise the first round of clearing to allow for market frictions (such as exogenous default costs) or different magnitudes of variation margin gains haircutting by CCPs, and will then use the second round of clearing as proposed in Ghamami et al. (2022).¹³

We consider a financial market consisting of $n_M \in \mathbb{N}$ clearing members, with indices in $\mathcal{M} = \{1, \dots, n_M\}$ and $n_C \in \mathbb{N}$ central counterparties with indices in $\mathcal{C} = \{n_M + 1, \dots, n_M + n_C\}$. We write $\mathcal{N} = \mathcal{M} \cup \mathcal{C}$ and set $N = n_M + n_C$. We assume that every clearing member clears their trades with at least one of the CCPs. Clearing members can have trading relationships with more than one CCP and indeed this can be observed in practice, as we will discuss in detail in Section 4.

We assume that clearing members and CCPs are connected through a network of obligations arising from derivative positions. For example, these could represent a network of obligations arising from CDS written on a specific reference entity. Then, if the reference entity defaults, payments become due from the protection seller to the protection buyer in the CDS contract. But even if no default occurs, changes to market conditions can trigger payment obligations between the counterparties in the form of variation

¹²Cont (2017) highlights the importance of addressing liquidity risk in stress tests of CCPs rather than focusing only on counterparty credit risk and insolvency risk. Indeed, more recent stress tests, e.g., ESMA (2020) explicitly consider liquidity risk in their stress test. Our analysis focuses on liquidity stress testing as well.

¹³As our setting is similar to that in Ghamami et al. (2022), we try to use the same notation whenever possible, with adjustments to allow for the existence of CCPs.

margin payments. In the following, we focus on networks of variation margin payment obligations, as e.g. in Paddrik et al. (2020) who consider such a setting in a market with one CCP.¹⁴

2.1 First round of clearing and assessment of defaults

We assume that due to changes in market conditions, variation margins become due. We denote by $\bar{p}^{\text{R1}} \in [0, \infty)^{N \times N}$ the variation margin obligations matrix, with element \bar{p}_{ij}^{R1} , where $i, j \in \mathcal{N}$, capturing the *variation margin (VM) payment obligation* from i to j . Since variation margins are usually bilaterally netted, we assume that for all $i, j \in \mathcal{N}$ with $i \neq j$ at most one of p_{ij} and p_{ji} is strictly positive and $p_{ii} = 0$ for all $i \in \mathcal{N}$. Furthermore,

$$\bar{p}_i^{\text{R1}} = \sum_{j=1}^N \bar{p}_{ij}^{\text{R1}}$$

denotes the *total variation payment obligation* of firm $i \in \mathcal{N}$.

There are a number of resources available to the nodes in the system to meet payment obligations. For one, as part of the contractual arrangement that gives rise to potential payment obligations, counterparties post initial margin (IM). As in Ghamami et al. (2022), we denote by $m_{ki} \geq 0$ the amount of IM posted by k to i , where $k, i \in \mathcal{N}$, $k \neq i$ and $m_{ii} = 0$ for all $i \in \mathcal{N}$. An important difference between CCPs and clearing members is that the latter are required to provide initial margins to the CCP at which they clear, whereas CCPs do not provide initial margins to their clearing members (Ghamami et al., 2022, Appendix B). Hence, in our setting with multiple CCPs, we have $m_{ki} = 0$ for all $k \in \mathcal{C}$ and for all $i \in \mathcal{N}$. Furthermore, clearing members also have liquidity buffers to deal with fluctuations in payment obligations and receipts (e.g. cash). We assume that $b^{\text{M}} \in [0, \infty)^{n_{\text{M}}}$ is the vector capturing such liquidity buffers, i.e., each clearing member $i \in \{1, \dots, n_{\text{M}}\}$ has a *liquidity buffer* $b_i^{\text{M}} \geq 0$.

In contrast to Ghamami et al. (2022), our model contains CCPs and we account for the special structure of their liquidity buffers. As discussed above, a key feature of CCPs' risk-management is the so-called default waterfall, which sets out the hierarchy and sequence of resources that CCPs can draw from to meet payment obligations arising from the default of one or more clearing members.

We explicitly model two pre-funded resources that form part of the default waterfall of a CCP (in addition to the initial margins), namely the default fund and the skin-in-the-game. The default fund refers to the contribution of clearing members to the financial resources of the CCP, whereas the skin-in-the-game refers to the (usually very thin) CCP's equity.¹⁵ This part of our model is a slight generalisation of the model by Paddrik et al. (2020), who – in addition to modelling contagion in a single-CCP setting – consider only the default fund as a liquidity buffer. We denote by $\delta \in [0, \infty)^{n_{\text{C}}}$ the vector of CCPs' default funds, i.e., δ_j is the default fund of CCP j . In particular,

$$\delta^{\text{T}} = \mathbf{1}_{n_{\text{M}}}^{\text{T}} \tilde{\delta},$$

where $\mathbf{1}_{n_{\text{M}}}$ is the n_{M} -dimensional unit vector and $\tilde{\delta} \in [0, \infty)^{n_{\text{M}} \times n_{\text{C}}}$ is the matrix with element $\tilde{\delta}_{ij}$ representing the default fund contribution of member i to CCP j .

We denote by $\sigma \in [0, \infty)^{n_{\text{C}}}$ the skin-in-the-game vector, i.e., σ_j is the skin-in-the-game of CCP j . We then define a vector $b \in [0, \infty)^N$ as follows:

$$b_i = \begin{cases} b_i^{\text{M}}, & \text{if } i \in \mathcal{M}, \\ \delta_i + \sigma_i, & \text{if } i \in \mathcal{C}. \end{cases}$$

¹⁴It would be possible to explicitly model how the original obligations network can be mapped into a network of variation margin payments as in Veraart (2022), but for the purpose of our analysis this is not strictly necessary.

¹⁵Huang & Takats (2020) provide empirical evidence that higher skin-in-the-game – even though very limited in size – is associated with more prudent risk management of CCPs (e.g., fewer margin breaches).

Hence, b represents additional resources that are in principle available to cover payment shortfalls that are not covered by initial margins.

Figure 1 depicts the stylised CCP waterfall considered in our model. The pre-funded layers of the default waterfall are included in a solid frame, whereas the last layer (indicated by a dashed frame) represents unfunded resources (we discuss the unfunded layer in more detail when we define the first round of clearing). As mentioned in Faruqi et al. (2018), the skin-in-the game of the CCP “can come before, along with, and/or after the default fund contributions of non-defaulting members, depending on the CCP’s specific rules”. In our analysis, the order in which the skin-in-the-game is used relative to the default fund contributions of the surviving members does not matter.

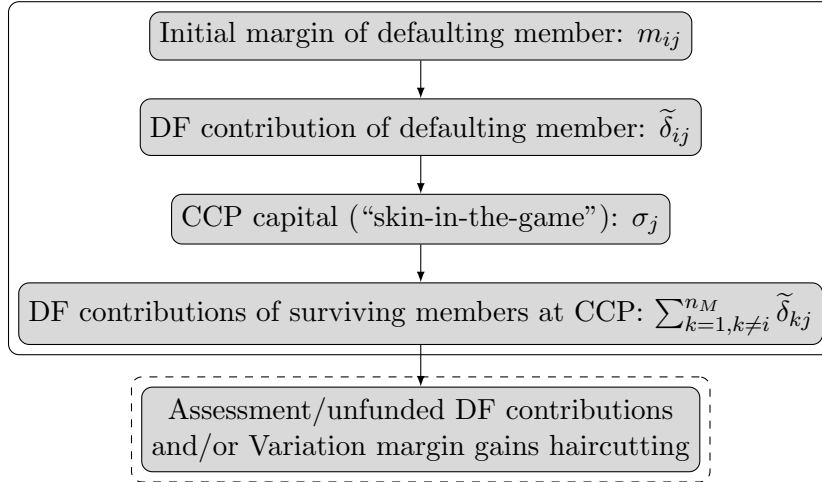


Figure 1: A stylised default waterfall of CCP j in a situation where only clearing member i defaults. The first four layers (included in a solid frame), are the prefunded resources of CCP j . The remaining layer (in a dashed frame), indicates unfunded resources of CCP j .

In practice, if a clearing member defaults, its portfolio will be sold by the CCP in an auction (CPMI-IOSCO, 2020). The design of auction mechanisms and their implications have been studied in e.g., Huang & Zhu (2021); Ferrara et al. (2020). Huang & Zhu (2021) show that juniorisation of the guarantee fund contributions of those clearing members that submit bad bids in the auction increases the auction price. In our model, any possible difference in seniority of the guarantee fund contributions of the surviving members will not affect the contagion mechanism, since we assume that each CCP i will use its full resources b_i (in addition to the initial margins that correspond to defaulted positions) before it transmits any losses to clearing members directly. We will therefore not consider aspects of mechanism design in our contagion model.

First round price - payment - equilibrium. We are now interested in determining a price-payment-equilibrium in the first clearing round ($R1$), i.e., we aim to determine an $N \times N$ -matrix $p^{*,R1}$, where each component $p_{ij}^{*,R1}$ represents the variation margin payments made from i to j . In addition, some collateral will need to be liquidated if defaults occur, potentially affecting its market price. Accordingly, we also aim to determine the price $\pi^{*,R1}$ of the collateral in equilibrium. To do so, we consider an inverse demand function modelled along the lines of Cifuentes et al. (2005) which returns the price of the collateral as a function of the amount of collateral sold.

The price-payment-equilibrium can be characterised by a suitable fixed-point. Considering a function $\Phi^{R1} : [0, 1] \times [0, \bar{p}^{R1}] \rightarrow [0, 1] \times [0, \bar{p}^{R1}]$, the goal is to obtain a fixed point of this function, i.e., we want to

find $(\pi^{*,R1}, p^{*,R1})$ such that

$$(\pi^{*,R1}, p^{*,R1}) = \Phi^{R1}(\pi^{*,R1}, p^{*,R1}).$$

Here, Φ^{R1} is defined as follows:

$$\begin{aligned} \Phi_1^{R1}(\pi, p) &= \exp(-\alpha \Delta(\pi, p)), \\ \Phi_{2,(ij)}^{R1}(\pi, p) &= \begin{cases} \min \left\{ \bar{p}_{ij}^{R1}, \pi m_{ij} + a_{ij}^{R1}(\pi) \left(\gamma_i^{(1)} b_i + \gamma_i^{(2)} \sum_{k=1}^N p_{ki} \right) \right\}, & \text{if } i \in \mathcal{D}(p), \\ \bar{p}_{ij}^{R1}, & \text{if } i \in \mathcal{N} \setminus \mathcal{D}(p), \end{cases} \end{aligned} \quad (1)$$

where

$$\mathcal{D}(p) = \{i \in \mathcal{N} \mid A_i(p) < \bar{p}_i^{R1}\},$$

specifies the nodes in default in a system with payments $p \in [0, \bar{p}^{R1}]$, i.e., these are the nodes that have fewer assets than payment obligations, where

$$A_i(p) = b_i + \sum_{k=1}^N p_{ki}$$

denotes the available assets of node $i \in \mathcal{N}$.

The matrix $a^{R1}(\pi) \in [0, 1]^{N \times N}$ specifies the repayment proportions and is given by

$$a_{ij}^{R1}(\pi) = \begin{cases} \frac{\max\{0, \bar{p}_{ij}^{R1} - \pi m_{ij}\}}{\sum_{k=1}^N \max\{0, \bar{p}_{ik}^{R1} - \pi m_{ik}\}}, & \text{if } \sum_{k=1}^N \max\{0, \bar{p}_{ik}^{R1} - \pi m_{ik}\} > 0, \\ 0 & \text{otherwise,} \end{cases}$$

for all $i, j \in \mathcal{N}$, where $a_{ij}^{R1}(\pi)$ specifies the relative payment obligations due from i to j while accounting for initial margins. In other words, $a_{ij}^{R1}(\pi)$ describes the relative payment obligations from i to j that are not covered by collateral (i.e., initial margins) when the price of the collateral per share is π .

The parameter $\alpha \geq 0$ is used to model the price impact of (fire) sales of collateral.¹⁶ If $\alpha = 0$, then there is no price impact and $\Phi_1^{R1}(\pi, p) = 1$ for all $p \in [0, \bar{p}^{R1}]$. If $\alpha > 0$ and $\Delta(\pi, p) > 0$, then $\Phi_1^{R1}(\pi, p) < 1$ for all $p \in [0, \bar{p}^{R1}]$, hence capturing the decline in the price of collateral when the share $\Delta(\pi, p)$ of collateral is sold. In particular, $\Delta(\pi, p)$ is given by

$$\Delta(\pi, p) = \sum_{i=1}^N \sum_{j=1}^N \Delta_{ij}(\pi, p),$$

where the total share of collateral seized and sold by node j after the default of node i is given by

$$\Delta_{ij}(\pi, p) = \begin{cases} \min \left\{ m_{ij}, \frac{\bar{p}_{ij}^{R1}}{\pi} \right\}, & \text{if } i \in \mathcal{D}(p), \\ 0, & \text{if } i \in \mathcal{N} \setminus \mathcal{D}(p), \end{cases}$$

¹⁶For a discussion and further results related to the choice of the parameter α for the exponential inverse demand function we refer to Amini et al. (2016). In particular, they show that the function modelling the cash proceeds from liquidation $\Delta \mapsto \Delta \exp(-\alpha \Delta)$ is increasing in $[0, \Delta_{\text{total}}]$ if and only if $\alpha \leq \frac{1}{\Delta_{\text{total}}}$. Here, $\Delta_{\text{total}} > 0$ denotes the maximum collateral available for sale, i.e., $\Delta_{\text{total}} = \sum_{i=1}^N \sum_{j=1}^N m_{ij}$.

if $\pi > 0$, and when $\pi = 0$ it is given by

$$\Delta_{ij}(\pi, p) = \begin{cases} m_{ij}, & \text{if } i \in \mathcal{D}(p) \text{ and } \bar{p}_{ij}^{\text{R1}} > 0, \\ 0, & \text{otherwise.} \end{cases}$$

Hence, only collateral of nodes that default (i.e., which are in $\mathcal{D}(p)$) can in principle be sold. The amount of collateral sold is capped by the collateral available for a given position m_{ij} and by the payment obligations due relative to the price of the collateral.

The parameters $\gamma_i^{(1)}, \gamma_i^{(2)} \in [0, 1], i \in \mathcal{N}$ are used to model further market frictions such as exogenous default costs or the severity of variation margin gains haircutting. Mathematically, they are similar to the model by Rogers & Veraart (2013). The special case $\gamma_1^{(1)} = \dots, \gamma_N^{(1)} = 1$ and $\gamma_1^{(2)} = \dots, \gamma_N^{(2)} = 1$ corresponds to the model proposed by Ghamami et al. (2022). When $\gamma_i^{(1)} < 1$ or $\gamma_i^{(2)} < 1$, we can capture the effect that, in case of default, not all assets are available or used to pay counterparties.

The parameters $\gamma_i^{(1)}, \gamma_i^{(2)}, i \in \mathcal{N}$ only play a role if there are defaulting nodes. Every node i that defaults (i.e., is in $\mathcal{D}(p)$), uses the proportion $\gamma_i^{(1)}$ of its liquidity buffer b_i and the proportion $\gamma_i^{(2)}$ of the payments it received ($\sum_{k=1}^N p_{ki}$) to make payments to other nodes. How much an individual node j receives from i is determined both by the proportion $a_{ij}^{\text{R1}}(\pi)$, which is used to distribute the cash available to j , and the initial margin evaluated at the market price πm_{ij} .

If a node $i \in \mathcal{D}(p)$ is a CCP¹⁷, then, formula (1) simplifies to

$$\Phi_{2,(ij)}^{\text{R1}}(\pi, p) = \min \left\{ \bar{p}_{ij}^{\text{R1}}, \frac{\bar{p}_{ij}^{\text{R1}}}{\bar{p}_i^{\text{R1}}} \left(\gamma_i^{(1)} b_i + \gamma_i^{(2)} \sum_{k=1}^N p_{ki} \right) \right\},$$

since CCPs do not post initial margin to their clearing members. In particular, the payments of CCP i to its clearing members do not directly depend on the price of the collateral π .

For each CCP i we will assume that $\gamma_i^{(1)} = 1$, which means that the full pre-funded resources from the default waterfall b_i are used to make payments to its clearing members.

If all prefunded resources are not enough to meet its payment obligations, then we think of CCP i as being in default (i.e., $i \in \mathcal{D}(p)$). What this implies is that not all due payments are made in full. In this case we distinguish two sub-cases, which we refer to as variants of variation margin gains haircutting (VMGH). The severity of the VMGH is modelled by the parameter $\gamma_i^{(2)}$. If $\gamma_i^{(2)} = 1$, then node i pays out the full amount of variation margins received from its clearing members to clearing members to which payments are due, but this is still not enough to meet payment obligations – we refer to this situation as one of *soft* VMGH. If $\gamma_i^{(2)} < 1$, however, then node i does not pay out the full amount of variation margins received to clearing members to which payments are due – a situation we refer to as *severe* VMGH.¹⁸ In practice, VMGH is done pro rata (Gregory, 2014) and this is captured by the proportion $\frac{\bar{p}_{ij}^{\text{R1}}}{\sum_{k=1}^N \bar{p}_{ik}^{\text{R1}}}$.

For each clearing member i , we will also consider different choices of $\gamma_i^{(1)}, \gamma_i^{(2)}$. In particular, $\gamma_i^{(1)} = \gamma_i^{(2)} = 1$ would correspond to a *soft* default and $\gamma_i^{(1)} = \gamma_i^{(2)} = 0$ would correspond to a *hard* default of the clearing member as in Paddrik & Young (2021). We will allow for intermediate cases, i.e., $\gamma_i^{(1)}, \gamma_i^{(2)} \in (0, 1)$ as well.

The introduction of the parameters $\gamma_i^{(1)}, \gamma_i^{(2)} \in [0, 1], i \in \mathcal{N}$ has implications for the fire sale of collateral as well. If some of these parameters are strictly smaller than one, this can increase the losses spreading through the system. If those losses cause additional defaults of clearing members, then more collateral will

¹⁷Since $i \in \mathcal{D}(p)$, we have that $\sum_{k=1}^N \bar{p}_{ik}^{\text{R1}} > 0$.

¹⁸Strictly speaking, this second variant is closer to VMGH as commonly discussed.

be liquidated, causing a stronger price decline of the collateral which itself can feed back to further losses and defaults. Therefore these two channels interact and can amplify the contagion effects.

Using Tarksi's fixed point theorem, we show in Appendix B that the set of fixed points of the function Φ^{R1} is a non-empty complete lattice. Throughout this paper we will always consider the greatest fixed point of Φ^{R1} and denote this by $(\pi^{*,R1}, p^{*,R1})$.

Definition 2.1 (Defaults). *We will refer to all nodes in the set*

$$\mathcal{D}(p^{*,R1}) = \{i \in \mathcal{N} \mid A_i(p^{*,R1}) < \bar{p}_i^{R1}\} = \{i \in \mathcal{N} \mid b_i + \sum_{k=1}^N p_{ki}^{*,R1} < \bar{p}_i^{R1}\}$$

as nodes in default. *We refer to all nodes in the set $\mathcal{F} = \mathcal{D}(\bar{p}^{R1}) = \{i \in \mathcal{N} \mid b_i + \sum_{k=1}^N \bar{p}_{ki}^{R1} < \bar{p}_i^{R1}\}$ as fundamental defaults. We refer to all nodes in the set $\mathcal{D}(p^{*,R1}) \setminus \mathcal{F}$ as contagious defaults.*

Hence, all nodes that cannot satisfy their payment obligations even if all other nodes satisfy theirs are referred to as fundamental defaults. We show in Corollary B.3 in the Appendix that $\mathcal{F} \subseteq \mathcal{D}(p^{*,R1})$.

Remark 2.2 (No fundamental defaults among CCPs). CCPs have matched books, i.e., for each $i \in \mathcal{C}$ it holds that $\sum_{k=1}^N \bar{p}_{ki}^{R1} = \bar{p}_i^{R1}$, which means that the total variation margins that $i \in \mathcal{C}$ is due to pay (\bar{p}_i^{R1}) coincide with the variation margin payments that the clearing members are due to pay to CCP i (namely, $\sum_{k=1}^N \bar{p}_{ki}^{R1}$). This implies (together with $b_i \geq 0$ for all $i \in \mathcal{C}$), that the set of fundamental defaults \mathcal{F} cannot contain CCPs, i.e., $\mathcal{F} \cap \mathcal{C} = \emptyset$.

Second round price - payment - equilibrium. Next, we consider the same mechanism for a second round of clearing ($R2$), as proposed in Ghamami et al. (2022). The main idea of the second round of clearing is that collateral not used in the first round is freed and becomes available to make still-outstanding payments. This can be modelled by considering a second fixed point problem. Payments outstanding at the start of the second round are given by $\bar{p}^{R2} = \bar{p}^{R1} - p^{*,R1} \in [0, \bar{p}^{R1}]$. We define a function $\Phi^{R2} : [0, \pi^{*,R1}] \times [0, \bar{p}^{R2}] \rightarrow [0, \pi^{*,R1}] \times [0, \bar{p}^{R2}]$, and our aim is to determine a fixed point of this function, i.e., we want to find $(\pi^{*,R2}, p^{*,R2})$ such that

$$(\pi^{*,R2}, p^{*,R2}) = \Phi^{R2}(\pi^{*,R2}, p^{*,R2}),$$

where $\Phi^{R2}(\pi, p)$ is defined in Appendix A.

The existence of a greatest fixed point of Φ^{R2} for the second round of clearing follows directly from (Ghamami et al., 2022, Proposition 3.1), in addition to the arguments provided in the Appendix for the modified first round of clearing.

Remark 2.3 (Seniority of payments). The definitions of Φ^{R1} and Φ^{R2} reflect the fact that all payment obligations have the same seniority. It is possible to change this assumption to allow e.g. for situations in which clearing members pay CCPs according to a pecking order rather than based on a proportionality assumption. In Appendix D we discuss this modification in detail. While this change in clearing method will lead to different price-payment-equilibria, we show that the key insights developed in this paper remain the same under both types of clearing mechanisms.

3 Joint clearing members and loss transmission

With the fundamentals of the model behind us, we now provide stylised examples that illustrate different types of loss transmissions arising from multiple CCPs with joint clearing members. To do this, we compute

the clearing payments and clearing price of the collateral in both rounds and consider the pair-specific payment shortfalls S_{ij} , where $i, j \in \mathcal{N}$, after the two rounds of clearing, given by

$$S_{ij} = \max\{0, \bar{p}_{ij}^{\text{R1}} - p_{ij}^{*,\text{R1}} - p_{ij}^{*,\text{R2}}\}, \quad i, j \in \mathcal{N},$$

and the total payment shortfall S , which measures the amount of unfulfilled payment obligations after the two clearing rounds (using the initial margins where applicable), defined as

$$S = \sum_{i=1}^N \sum_{j=1}^N S_{ij}.$$

3.1 Example #1: Default of a joint clearing member

First, we consider the situation where a joint clearing member defaults simultaneously at two CCPs. We show that this can result in both CCPs suffering severe losses and could potentially even cause their default if the collateral posted by the defaulting clearing member is illiquid.

We consider a system consisting of $n_C = 2$ CCPs and $n_M = 3$ clearing members. Figure 2 provides an illustration of the network of payment obligations. The weights along the edges represent the payment obligation due from i to j in the first round, i.e., \bar{p}_{ij}^{R1} , and the numbers in parentheses represent the corresponding initial margins (m_{ij}). For simplicity, we assume that the liquidity buffers are zero, but the example can be easily generalised to include positive liquidity buffers, default funds and skin-in-the-game.

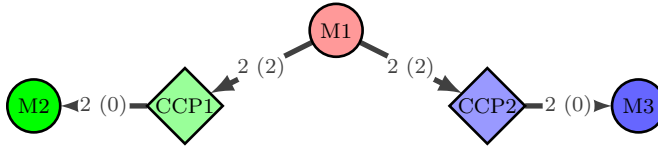


Figure 2: Example #1 – Default of a joint clearing member affecting several CCPs.

There is one joint clearing member (M1) that clears at both CCPs. The other two clearing members only clear at one CCP each (M2 at CCP1 and M3 at CCP2). We label the clearing members M_i with index i for $i \in \{1, 2, 3\}$, CCP1 with index 4 and CCP2 with index 5 in the matrices and vectors below.

Formally,

$$\bar{p}^{\text{R1}} = \begin{pmatrix} 0 & 0 & 0 & 2 & 2 \\ 0 & 0 & 0 & 0 & 0 \\ 0 & 0 & 0 & 0 & 0 \\ 0 & 2 & 0 & 0 & 0 \\ 0 & 0 & 2 & 0 & 0 \end{pmatrix}, \quad m = \begin{pmatrix} 0 & 0 & 0 & 2 & 2 \\ 0 & 0 & 0 & 0 & 0 \\ 0 & 0 & 0 & 0 & 0 \\ 0 & 0 & 0 & 0 & 0 \\ 0 & 0 & 0 & 0 & 0 \end{pmatrix}, \quad b = (0, 0, 0, 0, 0)^\top.$$

The joint clearing member M1 is the only node in fundamental default, i.e., $\mathcal{F} = \{1\} = \{M1\}$.

We assume that $\gamma_i^{(1)}, \gamma_i^{(2)} \in [0, 1]$ for all $i \in \mathcal{N}$. We consider various cases,

1. First, we consider the case of fully liquid collateral that can be liquidated at no discount, i.e., $\alpha = 0$.

In this scenario, the price of the collateral cannot change, i.e., $\pi^{*,R1} = \pi^{*,R2} = 1$. Furthermore, we obtain that $p^{*,R1} = \bar{p}^{R1}$ and $p^{*,R2} = 0$, implying that all payments are made in full (the total shortfall is $S = 0$). Here, $\mathcal{D}(p^{*,R1}) = \mathcal{F} = \{1\}$. Hence, even though clearing member M1 is in fundamental default, CCP1 still receives 2 from M1 by seizing the initial margin $m_{14} = 2$ and the same situation arises for CCP2, which seizes $m_{15} = 2$. Therefore, both CCP1 and CCP2 are able to satisfy their payment obligations of 2 to M2 and M3, respectively, in full.

Note that in this example the values of $\gamma_i^{(1)}$ and $\gamma_i^{(2)}$ do not matter, since the joint clearing member M1 does not pay the CCPs directly (these payment would be affected by the parameters $\gamma_i^{(1)}, \gamma_i^{(2)}$) as it does not have any resources to use. The CCPs seize the initial margins instead, and therefore the clearing payments $p^{*,R1} = \bar{p}^{R1}$ correspond to the full payment obligations in Round 1 and there is nothing left to be paid in Round 2, i.e., $p^{*,R2} = 0$.

2. Second, we assume that the collateral is illiquid by setting $\alpha = 0.25 > 0$.

The total shares of collateral sold in the first round are $\Delta = 4$, and in the second round $\Gamma = 0$, see Appendix A for details on the second round of clearing and the formal definition of Γ . Furthermore, the clearing price of the collateral in both rounds is given by $\pi^{*,R1} = \pi^{*,R2} = \exp(-4\alpha) \approx 0.3679$. It does not decrease from the first to the second round, since no collateral is sold in the second round in this case. The clearing payments in the first round are given by

$$p^{*,R1} = \begin{pmatrix} 0 & 0 & 0 & 2\pi^{*,R1} & 2\pi^{*,R1} \\ 0 & 0 & 0 & 0 & 0 \\ 0 & 0 & 0 & 0 & 0 \\ 0 & \gamma_4^{(2)}2\pi^{*,R1} & 0 & 0 & 0 \\ 0 & 0 & \gamma_5^{(2)}2\pi^{*,R1} & 0 & 0 \end{pmatrix}$$

and the clearing payments in the second round are given by the zero matrix, i.e., $p^{*,R2} = 0$.

This implies that the total shortfall is $S = 2(2 - 2\pi^{*,R1}) + (2 - 2\gamma_4^{(2)}\pi^{*,R1}) + (2 - 2\gamma_5^{(2)}\pi^{*,R1})$. In particular, the total shortfall depends on $\gamma_i^{(2)}, i \in \{4, 5\}$. For example, for $\gamma_4^{(2)} = \gamma_5^{(2)} = 1$, $S \approx 5.057$ and for $\gamma_4^{(2)} = \gamma_5^{(2)} = 0.5$, $S \approx 5.793$.

Furthermore, for all choices of $\gamma_4^{(2)}, \gamma_5^{(2)}$, both CCPs suffer a contagious default and $\mathcal{D}(p^{*,R1}) = \{1, 4, 5\}$. Hence, even though the liabilities of the joint clearing member were fully collateralised at both CCPs, the fact that this collateral was illiquid still caused the (contagious default) of both CCPs, which causes knock-on losses to clearing members that only clear at one CCP.

The scenario from this stylised example has been considered by Glasserman et al. (2015) before, but not in the context of a model involving different contagion channels. They show that convex initial margin schedules provide incentives for clearing members to split their positions across multiple CCPs. This gives rise to what they refer to as *hidden illiquidity* – i.e., the CCPs involved are not aware that the positions of some of their joint clearing members are in fact undercollateralised.

We demonstrate how this effect can be captured by the different contagion mechanisms in our model. In our example, CCP1 does not know that M1 has the same position at CCP1 and CCP2 and therefore for CCP1 it may appear that the position of M1 is sufficiently collateralised. For illiquid collateral, however, we find that both CCPs can default and if these two CCPs use more severe variation margin gains haircutting (achieved by setting $\gamma_4^{(2)} = \gamma_5^{(2)} = 0.5$ as in our last example) then other clearing members can suffer substantial additional losses.

3.2 Example #2: Default of clearing member at only one CCP

Next, we show that even if there is no fundamental default among the joint clearing members, they can still act as a transmission channel of losses from one CCP to another. To illustrate this effect, we consider a situation where there is only one fundamental default in a clearing member that only clears at one CCP.

As before, we consider an example consisting of $n_C = 2$ CCPs and $n_M = 3$ clearing members. Figure 3 provides an illustration of the network of payment obligations. The notation is the same as in Figure 2.

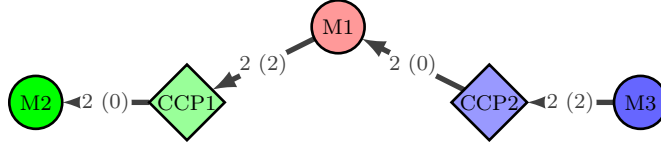


Figure 3: Example #2 – Loss transmission due to joint clearing members network.

Formally,

$$\bar{p}^{R1} = \begin{pmatrix} 0 & 0 & 0 & 2 & 0 \\ 0 & 0 & 0 & 0 & 0 \\ 0 & 0 & 0 & 0 & 2 \\ 0 & 2 & 0 & 0 & 0 \\ 2 & 0 & 0 & 0 & 0 \end{pmatrix}, \quad m = \begin{pmatrix} 0 & 0 & 0 & 2 & 0 \\ 0 & 0 & 0 & 0 & 0 \\ 0 & 0 & 0 & 0 & 2 \\ 0 & 0 & 0 & 0 & 0 \\ 0 & 0 & 0 & 0 & 0 \end{pmatrix}, \quad b = (0, 0, 0, 0, 0)^\top.$$

Here, $\mathcal{F} = \{3\} = \{M3\}$, hence the clearing member (labeled M3 in Figure 3) is the only fundamental default. As in the first example, we consider two alternative cases by varying the liquidity of the collateral.

1. First, we assume that the collateral is liquid, i.e., $\alpha = 0$. As above, this means that the price of the collateral cannot change (i.e., $\pi^{*,R1} = \pi^{*,R2} = 1$), $p^{*,R1} = \bar{p}^{R1}$ and $p^{*,R2} = 0$ and hence all payments are made in full (the total shortfall is $S = 0$). The default set is $\mathcal{D}(p^{*,R1}) = \mathcal{F} = \{3\} = \{M3\}$: there is only the original fundamental default and no contagious defaults.

Hence, even though clearing member M3 is in fundamental default, CCP2 still receives 2 from M3 by seizing the initial margin $m_{35} = 2$. Therefore, CCP2 is able to satisfy its payment obligations of 2 to M1 in full. As in the previous example, the value of $\gamma_3^{(2)}$ does not matter, since CCP2 seizes the collateral and there are no other payments from M3 to CCP2 (which would be affected by the parameter $\gamma_3^{(2)}$). Also note that, since $b_3 = 0$, the value of $\gamma_3^{(1)}$ does not matter either.

2. Second, we assume that the collateral is illiquid by setting $\alpha > 0$. We choose $\alpha = 0.01$ and find that both defaults and shortfall depend on $\gamma_1^{(2)}, \gamma_4^{(2)}, \gamma_5^{(2)}$. In particular, we find that both CCP2 and M1 suffer a contagious default for all choices of $\gamma_i^{(1)}, \gamma_i^{(2)}, i \in \mathcal{N}$, but whether CCP1 suffers a contagious default or not depends on the particular values of $\gamma_1^{(2)}, \gamma_4^{(2)}, \gamma_5^{(2)}$.

For all $\gamma_i^{(1)}, \gamma_i^{(2)} \in [0, 1]$, the total shares of collateral sold are $\Delta = 4, \Gamma = 0$, resulting in prices for

the collateral of $\pi^{*,R1} = \pi^{*,R2} = \exp(-4\alpha) \approx 0.9608$. Furthermore,

$$\begin{aligned} p_{14}^{*,R1} &= \min\{2, 2\pi^{*,R1}(1 + \gamma_1^{(2)}\gamma_5^{(2)})\}, \\ p_{35}^{*,R1} &= 2\pi^{*,R1}, \\ p_{42}^{*,R1} &= \min\{2, \gamma_4^{(2)}p_{14}^{*,R1}\} = \min\{2, \gamma_4^{(2)}\min\{2, 2\pi^{*,R1}(1 + \gamma_1^{(2)}\gamma_5^{(2)})\}\}, \\ p_{51}^{*,R1} &= \gamma_5^{(2)}2\pi^{*,R1}, \end{aligned}$$

and $p_{ij}^{*,R1} = 0$ for the remaining index pairs (i, j) and $p^{*,R2} = 0$. The shortfall is given by

$$\begin{aligned} S &= (2 - \min\{2, 2\pi^{*,R1}(1 + \gamma_1^{(2)}\gamma_5^{(2)})\}) + (2 - 2\pi^{*,R1}) \\ &\quad + (2 - \min\{2, \gamma_4^{(2)}\min\{2, 2\pi^{*,R1}(1 + \gamma_1^{(2)}\gamma_5^{(2)})\}\}) + (2 - \gamma_5^{(2)}2\pi^{*,R1}), \end{aligned}$$

i.e., it depends on $\gamma_1^{(2)}, \gamma_4^{(2)}, \gamma_5^{(2)}$. For example, for $\gamma_1^{(2)} = \gamma_4^{(2)} = \gamma_5^{(2)} = 1$, $S \approx 0.1568$ and $\mathcal{D}(p^{*,R1}) = \{1, 3, 5\} = \{M1, M3, CCP2\}$.

If CCP2 does very severe variation margin gains haircutting, achieved by e.g., setting $\gamma_5^{(1)} = 0$ (and $\gamma_1^{(2)} = \gamma_4^{(2)} = 1$), then $S \approx 2.2353$ and $\mathcal{D}(p^{*,R1}) = \{1, 3, 4, 5\} = \{M1, M3, CCP1, CCP2\}$. Hence, there is the additional default of CCP1.

If both CCPs do severe variation margin gains haircutting, by for example setting $\gamma_4^{(2)} = \gamma_5^{(2)} = 0$ and $\gamma_3^{(1)} = 1$, then the total shortfall increases even further to $S \approx 4.1568$, but the default set remains the same as in the situation in which only CCP2 does severe variation margin gains haircutting, i.e., $\mathcal{D}(p^{*,R1}) = \{1, 3, 4, 5\} = \{M1, M3, CCP1, CCP2\}$.

This example serves to illustrate that the default of an institution (M3) can trigger the default of a CCP (CCP1) at which it is not a clearing member. In particular, here the variation margin gains haircutting of CCP2 is one of the causes of the default of CCP1. So while variation margin gains haircutting can serve as a defense mechanism for CCP2 on a stand-alone basis, it can have contagion effects and ultimately lead to the default of another CCP.

3.3 Example #3: Circular loss transmission via joint clearing members and multiple CCPs

Finally, we consider a situation in which the existence of multiple joint clearing members creates a circle of loss transmission between them and CCPs, which can cause the default of both types of institutions.

In this example, we still consider a system with $n_C = 2$ CCPs, but now have $n_M = 6$ clearing members. Figure 4 provides an illustration of the network of payment obligations. The notation is the same as in Figure 2. In contrast to the previous examples, we now consider two joint clearing members that clear at both CCPs which leads to a circular structure of payment obligations.

Formally,

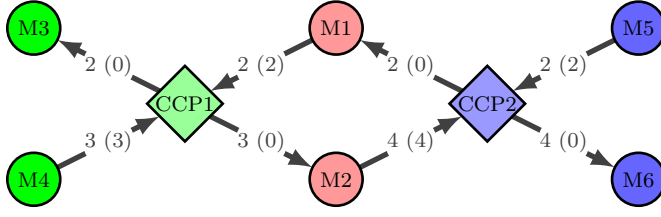


Figure 4: Example #3 – Cycle of loss transmission due to joint clearing members network.

$$\bar{p}^{R1} = \begin{pmatrix} 0 & 0 & 0 & 0 & 0 & 0 & 2 & 0 \\ 0 & 0 & 0 & 0 & 0 & 0 & 0 & 4 \\ 0 & 0 & 0 & 0 & 0 & 0 & 0 & 0 \\ 0 & 0 & 0 & 0 & 0 & 0 & 3 & 0 \\ 0 & 0 & 0 & 0 & 0 & 0 & 0 & 2 \\ 0 & 0 & 0 & 0 & 0 & 0 & 0 & 0 \\ 0 & 3 & 2 & 0 & 0 & 0 & 0 & 0 \\ 2 & 0 & 0 & 0 & 0 & 0 & 0 & 4 \end{pmatrix}, \quad m = \begin{pmatrix} 0 & 0 & 0 & 0 & 0 & 0 & 2 & 0 \\ 0 & 0 & 0 & 0 & 0 & 0 & 0 & 4 \\ 0 & 0 & 0 & 0 & 0 & 0 & 0 & 0 \\ 0 & 0 & 0 & 0 & 0 & 0 & 3 & 0 \\ 0 & 0 & 0 & 0 & 0 & 0 & 0 & 2 \\ 0 & 0 & 0 & 0 & 0 & 0 & 0 & 0 \\ 0 & 0 & 0 & 0 & 0 & 0 & 0 & 0 \\ 0 & 0 & 0 & 0 & 0 & 0 & 0 & 0 \end{pmatrix}, \quad b = (0, 0, 0, 0, 0, 0, 0, 0)^\top. \quad (2)$$

There are three fundamental defaults, $\mathcal{F} = \{2, 4, 5\} = \{M2, M4, M5\}$. The node M4 is only a clearing member of CCP1, the node M5 is only a clearing member of CCP2 and the node M2 is a joint clearing member of both CCPs, but only has payment obligations to CCP2. As before, we consider alternative cases:

1. First, we consider the case of liquid collateral, i.e., $\alpha = 0$, implying that the clearing price of collateral is fixed at $\pi^{*,R1} = \pi^{*,R2} = 1$. We now distinguish between two sub-cases: fully versus not fully collateralised obligations from clearing members to CCPs.
 - (a) Fully collateralised obligations from clearing members to CCPs correspond to the initial margins given by m in (2). In this case, we have $p^{*,R1} = \bar{p}^{R1}$ and $p^{*,R2} = 0$, implying that all payments are made in full and the total shortfall is zero. Collateral sold amounts to $\Delta = 9$ in the first round and $\Gamma = 0$ in the second round. There are thus no contagious defaults ($\mathcal{D}(p^{*,R1}) = \mathcal{F}$). As in previous examples, the values of $\gamma_i^{(1)}, \gamma_i^{(2)}$ do not matter in this case.
 - (b) If we reduce initial margins by considering $0.99m$ rather than m in (2), the situation changes. Fundamental defaults remain the same, but the overall default set is larger. In particular, $\mathcal{D}(p^{*,R1}) = \{M1, M2, M4, M5, CCP1, CCP2\}$, i.e., both CCPs and the additional joint clearing member M1 default as well (even for $\gamma_i^{(1)} = \gamma_i^{(2)} = 1$ for all $i \in \mathcal{N}$).
The total shortfall depends on the parameters $\gamma_i^{(1)}, \gamma_i^{(2)}$. For example, for $\gamma_i^1 = \gamma_i^{(2)} = 1$ for all $i \in \mathcal{N}$, the total shortfall is $S = 0.1$, whereas for $\gamma_7^{(2)} = \gamma_8^{(2)} = 0.5$ (and $\gamma_i^{(1)} = 1$ for all $i \in \mathcal{N}$ and $\gamma_i^{(2)} = 1$ for all $i \in \mathcal{M}$) the shortfall increases to $S = 5.575$. In this example the collateral sold is $\Delta = 11 \cdot 0.99 = 10.89$ in the first round and $\Gamma = 0$ in the second round.
2. Second, we assume that collateral is illiquid by setting $\alpha > 0$. We further assume that initial margins are given by m in (2), i.e., payment obligations of clearing members to the CCPs are fully collateralised. We then consider two sub-cases, based on differences in liquidity buffers.

- (a) First, we consider a liquidity buffer of 0 for all nodes, i.e., b as given in (2). For all $\gamma_i^{(1)}, \gamma_i^{(2)} \in [0, 1]$, $i \in \mathcal{N}$, the total shares of collateral sold in the two rounds are respectively $\Delta = 11$ and $\Gamma = 0$, resulting in collateral prices given by $\pi^{*,R1} = \pi^{*,R2} = \exp(-11\alpha)$. It is possible to check that choosing $\alpha = -\frac{\log(0.99)}{\Delta} \approx 0.00091$ as price impact yields the same outcome as in 1b) above. In other words, for $\gamma_i^{(1)} = \gamma_i^{(2)} = 1$ for all $i \in \mathcal{N}$, the shortfall is $S = 0.1$, whereas for $\gamma_7^{(2)} = \gamma_8^{(2)} = 0.5$ (and $\gamma_i^{(1)} = 1$ for all $i \in \mathcal{N}$ and $\gamma_i^{(2)} = 1$ for all $i \in \mathcal{M}$) the shortfall increases to $S = 5.575$ and again $\mathcal{D}(p^{*,R1}) = \{M1, M2, M4, M5, CCP1, CCP2\}$.
- (b) Second, we increase the liquidity buffers of two nodes. We take the buffer from $b_2 = 0$ to $b_2 = 1$ for joint clearing member M2, which removes this node from the fundamental default set. In addition, we increase the liquidity buffer of clearing member M4 from $b_4 = 0$ to $b_4 = 3$, which guarantees that this node cannot default since $\bar{p}_4^{R1} = 3 = b_4$. Hence, as M4 is no longer a fundamental default, we have $\mathcal{F} = \{M5\}$.

With $\alpha = 0.1$ and $\gamma_i^{(1)} = \gamma_i^{(2)} = 1$ for all $i \in \mathcal{N}$, the fundamental default of M5 causes the contagious default of CCP2 and the joint clearing member M1, i.e., $\mathcal{D}(p^{*,R1}) = \{M1, M5, CCP2\}$, and the shortfall amounts to $S \approx 1.3187$. Still, CCP1 does not default.

If we change $\gamma_8^{(2)} = 1$ to $\gamma_8^{(2)} = 0.25$, i.e., assume that CCP2 uses more severe variation margin gains haircutting, and keep all other parameters the same, we find that $\mathcal{D}(p^{*,R1}) = \{M1, M2, M5, CCP1, CCP2\}$ and the shortfall increases to $S \approx 7.2629$. Hence, the more severe variation margin gains haircutting by CCP2 triggers the additional default of CCP1 and the joint clearing member M2.

Hence, this is an example that shows that insufficient collateral, either because it was not posted in the first place (situation 1b)) or because it is illiquid (situation 2a)), can cause contagion and defaults of CCPs. Example 2b) shows how the default of a clearing member (M5) at one CCP (CCP2) can ultimately trigger the default of another CCP (CCP1) of which M5 is not a clearing member, conditional on the first affected CCP (CCP2) using variation margin gains haircutting. This then triggers the default of M2, in turn leading to further losses at CCP2 due to the circular structure arising from joint clearing membership.

3.4 Joint clearing members and trapped liquidity

So far we have assumed that when variation margins become due, both clearing members and CCPs make these payments at the same time. In practice, however, this might not be the case. As described in (ESRB, 2020, p. 51), “CCPs typically only pay out variation margin gains to counterparties the next morning [...]. In times of high market volatility, this practice results in liquidity being trapped in CCPs and could create or amplify liquidity stress in the financial system”. In the following we will illustrate consequences of trapped liquidity in situations with joint clearing members, revisiting the previous three examples.

In Example 3.1 (default of a joint clearing member, M1), the effects of trapped liquidity in the two CCPs would imply that clearing members M2 and M3 would not receive any payments at time 1, since both CCPs withhold their payments. But since the clearing members M2 and M3 do not have any payment obligations at time 1, there are no further contagion effects.

In Example 3.2, where we have one joint clearing member M1 that is due to receive payments from CCP2 and is due to make payments to CCP1, the payment delays of CCP2 can have consequences for CCP1. Suppose we equip clearing member M3 with a liquidity buffer of 2. Then, if all variation margin gains are passed through all CCPs simultaneously, then there are no defaults. If only clearing members make payments, however, then clearing member M1 only has its liquidity buffer (which we assume to be 0) as recourse to make the required variation margin payments of 2 to CCP1 and hence cannot make this payment at this point in time. Hence, a joint clearing member with a matched book can become a source

of liquidity stress to a CCP (here CCP2) due to another CCP (here CCP1) not passing through its variation margin gains.

This mechanism (i.e., joint clearing members becoming a liquidity stress to a CCP), can occur repeatedly if we have a circular structure as in Example 3.3.

4 Interconnectedness in centrally cleared markets – Empirical evidence

The presence of central counterparties affects financial interconnections in various ways. The most obvious, and the one that has attracted most attention, is the reconfiguration of the financial network to a star-shaped form – whereby the CCP stands in the middle as a large node centralising all traffic. While useful as a focal point to think about how CCPs affect the nature of counterparty and liquidity risks, this is still a stylised representation. In practice, the CCP ecosystem gives rise to layers of interconnections. As discussed above, CCP membership consists of a reduced group of large financial institutions that simultaneously clears in multiple CCPs. Quite often, these same institutions will provide additional services to CCPs giving rise to further interconnections, such as liquidity provision, credit lines and custodianship (BCBS-CPMI-FSB-IOSCO (2018)). In what follows, we focus on the interconnections arising from joint clearing membership in derivative markets, using publically available data for interest rate swaps and credit default swaps.

Figure 5 presents a time series of notional amounts cleared by different CCPs in both markets, confirming the well-documented fact that IRS are a considerably larger portion of derivatives markets – especially in the cleared space. A couple of observations are in order. For one, while concentrated, both markets feature a few CCPs, i.e. the network is not exactly star-shaped, although admittedly there is some geographic specialisation. In addition, some CCPs clear in both markets (LCH, JSCC), whereas others do so only in one of the two markets (e.g., CME and Eurex clear only IRS, and e.g. ICE Clear Credit and ICE Clear Europe clear only CDS).

4.1 The bipartite network of clearing members and CCPs

Next, we analyse interconnections between CCPs through shared clearing membership.¹⁹ Figure 6 presents the bipartite network of clearing members (left)²⁰ and CCPs (right). An edge between a clearing member and a CCP indicates that the member clears at this particular CCP. As is evident, there is a strong overlap between the clearing members at multiple CCPs.

We investigate this overlap by considering one-mode projections of the bipartite network. One-mode projections are a way to condense information in bipartite networks.²¹ While the original bipartite network consists of two types of nodes (clearing members and CCPs), a one-mode projection projects this bipartite network onto a network that consists only of one of the two groups. Edges appear between the nodes in the new network if there is a relationship between those two nodes in the dimension that is no longer directly visible. So an edge in the network of clearing members means that they are joint clearing members in at least one CCP. An edge in the network of CCPs means that they share at least one clearing member. We describe these one-mode projections in more detail next.

First, we consider a one-mode projection that will create a network whose nodes are all the clearing members. The edges in the new network are undirected and weighted, where the weights represent the number of CCPs at which both clearing members clear. Formally, this is computed as follows. The original bipartite network consists of clearing members and CCPs. We consider the incidence matrix B for n_C

¹⁹We consider data from end-2019, with reported notional amounts in million USD.

²⁰We focus on clearing members that are large global systemic banks.

²¹For background on one-mode projections see Newman (2010).

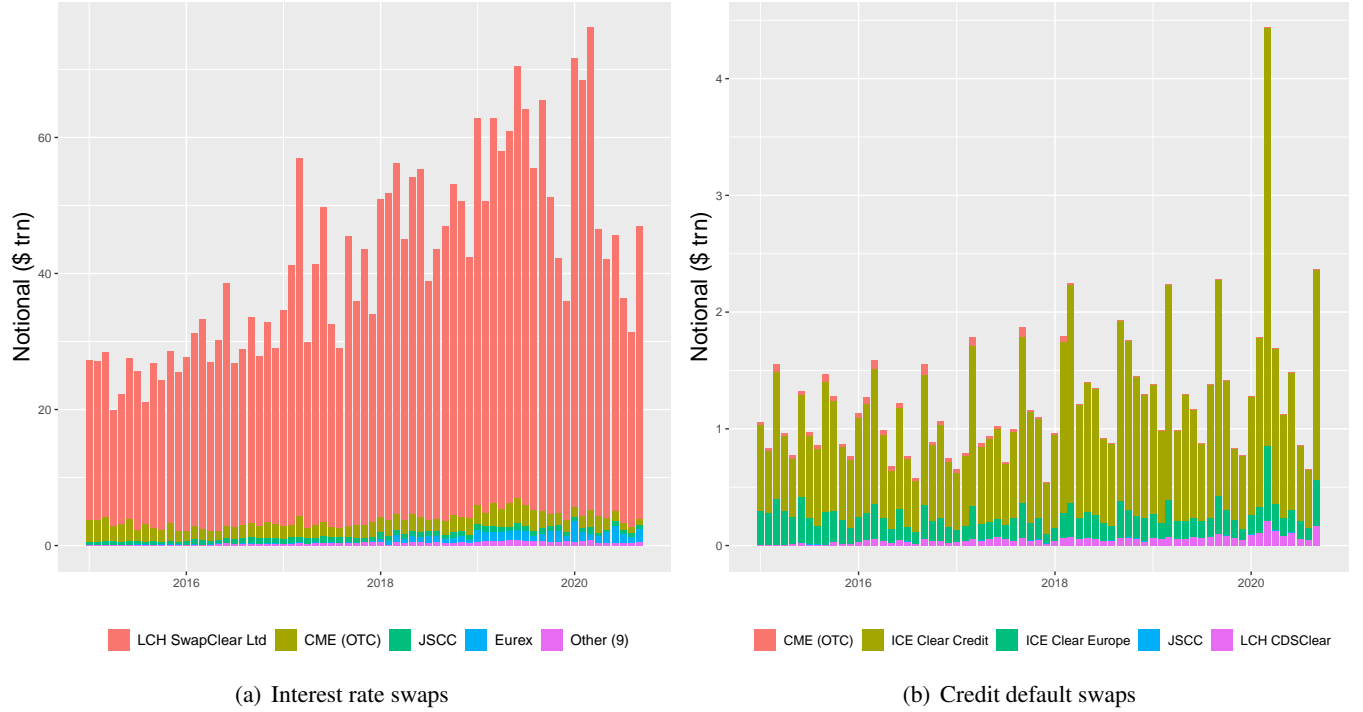


Figure 5: Notional amounts of derivatives cleared by market. (Note that the y-axes are on different scales due to the large volume of the IRS market.) *Source*: Clarus FT.

groups (the CCPs) and n_M participants (the clearing members) which is given by $B \in \{0, 1\}^{n_C \times n_M}$, where

$$B_{ij} = \begin{cases} 1, & \text{if institution } j \text{ is a clearing member of CCP } i, \\ 0, & \text{otherwise.} \end{cases}$$

Then, for $i, j \in \{1, \dots, n_M\}$ and $k \in \{1, \dots, n_C\}$ it holds that $B_{ki}B_{kj} = 1$ if and only if both institutions i and j clear at CCP k . Therefore, the total number of CCPs where both i and j are clearing members is given by

$$P_{ij}^{\text{members}} = \sum_{k=1}^{n_C} B_{ki}B_{kj} = \sum_{k=1}^{n_C} B_{ik}^\top B_{kj}.$$

In particular, $P^{\text{members}} = B^\top B \in \{0, 1, \dots, n_C\}^{n_M \times n_M}$ and its diagonal element

$$P_{ii}^{\text{members}} = \sum_{k=1}^{n_C} B_{ki}B_{ki} = \sum_{k=1}^{n_C} B_{ki}$$

represents the total number of CCPs where $i \in \{1, \dots, n_M\}$ is a clearing member.

Figure 7(a) presents the network of the first one-mode projection. Most clearing members have at least two interconnections. Figure 7(b) in turn presents a heatmap of P^{members} : roughly half of all institutions are clearing members of all six CCPs (red area).

The second one-mode projection creates a network that consists only of CCPs. Its edges are again undirected and weighted, with weights representing the number of shared clearing members. Formally, the

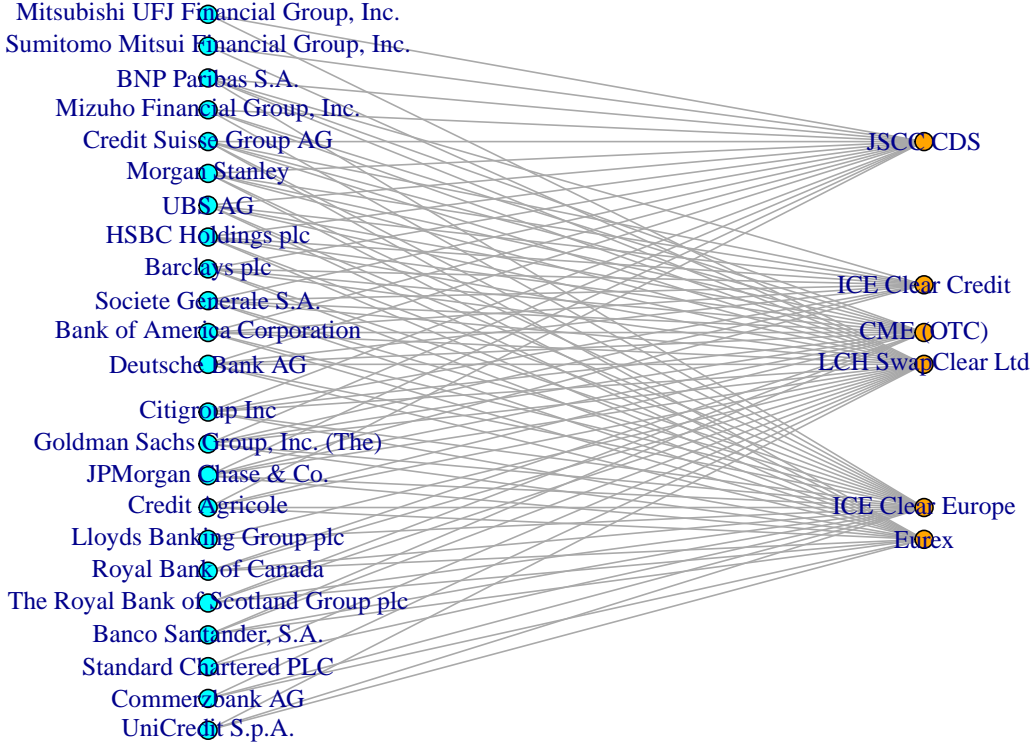


Figure 6: Bipartite network of clearing members and CCPs.

total number of institutions that are clearing members at both CCPs i and j is given by

$$P_{ij}^{\text{CCPs}} = \sum_{k=1}^{n_M} B_{ik} B_{jk} = \sum_{k=1}^{n_M} B_{ik} B_{kj}^{\top}.$$

In particular, $P^{\text{CCPs}} = BB^{\top} \in \{0, 1, \dots, n_M\}^{n_C \times n_C}$ and its diagonal element

$$P_{ii}^{\text{CCPs}} = \sum_{k=1}^{n_M} B_{ik}$$

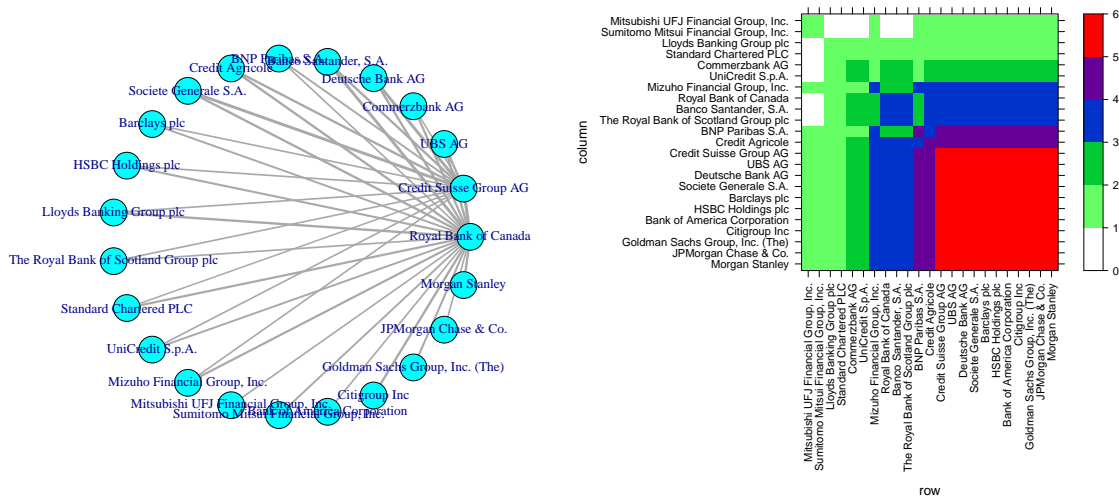
represents the total number of clearing members that CCP $i \in \{1, \dots, n_C\}$ has.

Figure 8(b) presents a heatmap of P^{CCPs} . There exists exactly one CCP, namely LCH, which has all 23 institutions considered here as its clearing members.

For both one-mode projections P^{members} and P^{CCPs} , if we consider the corresponding networks (shown in Figures 7(a) and 8(a)), then we obtain a complete network in both cases. This implies that losses from one CCP can in principle spill over to all other CCPs and losses of clearing members can in principle spill over to all other clearing members, if the corresponding liquidity buffers/initial margins/default funds/etc. are not large enough to stop the loss transmission.

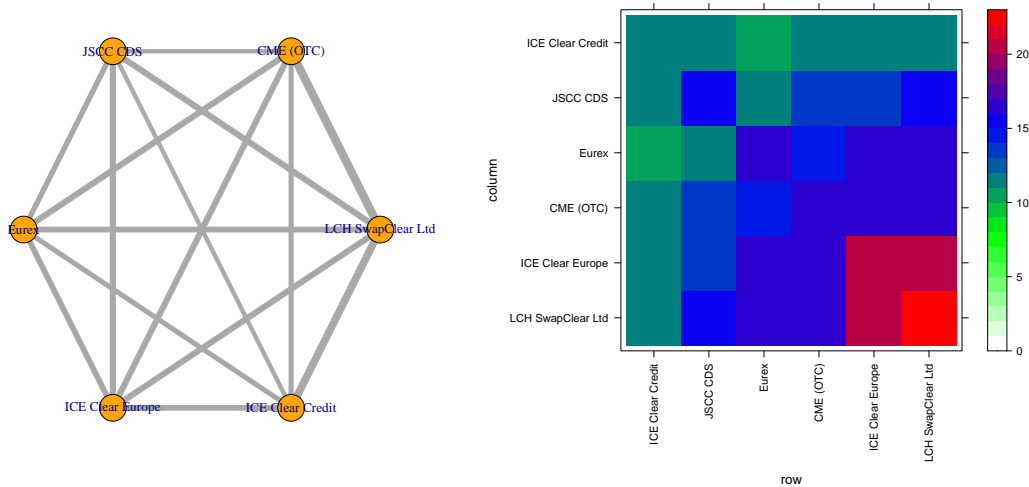
4.2 Case studies

We now provide two case studies (for IRS and CDS respectively) that bring together model and data to illustrate contagion via joint clearing members. Our data, available from public disclosures and sourced



(a) Network of clearing members corresponding to (b) Levelplot of P^{members} ; each cell shows the total number of CCPs at which both institutions i and j clear. Edge weight between i and j is proportional to the number of CCPs at which both clear.

Figure 7: Graphical illustrations of P^{members} , i.e., the one mode projection of the bipartite network of clearing members and CCPs on clearing members. The resulting network consists of 23 nodes representing the clearing members.



(a) Network of CCPs corresponding to P^{CCPs} ; edge weight between i and j is proportional to the number of joint clearing members for each pair of CCPs. (b) Levelplot of P^{CCPs} ; each cell shows the total number of joint clearing members for each pair of CCPs.

Figure 8: Graphical illustration of P^{CCPs} , i.e., the one mode projection of the bipartite network of clearing members and CCPs on CCPs. The resulting network consists of 6 nodes representing the CCPs.

from Clarus FT, contain information on the CCPs (total notional cleared, default funds δ_i , skin-in-the-game σ_i , aggregate initial margins $\sum_{j=1}^{n_M} m_{ji}$ for all $i \in \mathcal{C}$) and the clearing members (total notional cleared). Furthermore, for each CCP we observe its clearing members.

There are, however, two key model quantities that we do not observe in the data. The first is the network of payment obligations (\bar{p}^{R1}) and the second is the liquidity buffer of clearing members b^M .²² Accordingly, we reconstruct the matrix \bar{p}^{R1} from available information. Appendix C provides details on the network reconstruction approach, as well as on how we choose the liquidity buffers of clearing members.

4.2.1 Contagion in the IRS market

We start with the IRS market. Figure 9(a) presents the reconstructed payment obligations arising from observed IRS positions. The network consists of four CCPs and 23 clearing members, with nodes in either group only linked with nodes of the other group – hence any directed weighted edge has a CCP on one end and a clearing member on the other. We choose clearing members’ liquidity buffers such that there are two fundamental defaults among them. These are Credit Suisse Group AG and Deutsche Bank AG, both clearing members at all CCPs.²³ In what follows, we study the effects of these two fundamental defaults.

We start by assuming that the collateral is liquid, i.e., $\alpha = 0$. Within this setting, we work with three alternative scenarios and report the results in Figure 9. First, we assume that $\gamma_i^{(1)} = \gamma_i^{(2)} = 1$ for all $i \in \mathcal{N}$. This means that there are no additional frictions in the model. After computing the greatest fixed point, in addition to the two clearing members (see above), two CCPs (LCH Swap Clear and JSCC) also default. Hence, even without additional frictions that could amplify contagion, two CCPs suffer a contagious default. Figure 9(b) presents a heatmap of the matrix of shortfalls $(S_{ij})_{i,j \in \mathcal{N}}$ under this hypothetical scenario. Four rows (corresponding to the four defaulting institutions) are not white and hence indicate the payment shortfall between the defaulting institutions and their creditors.

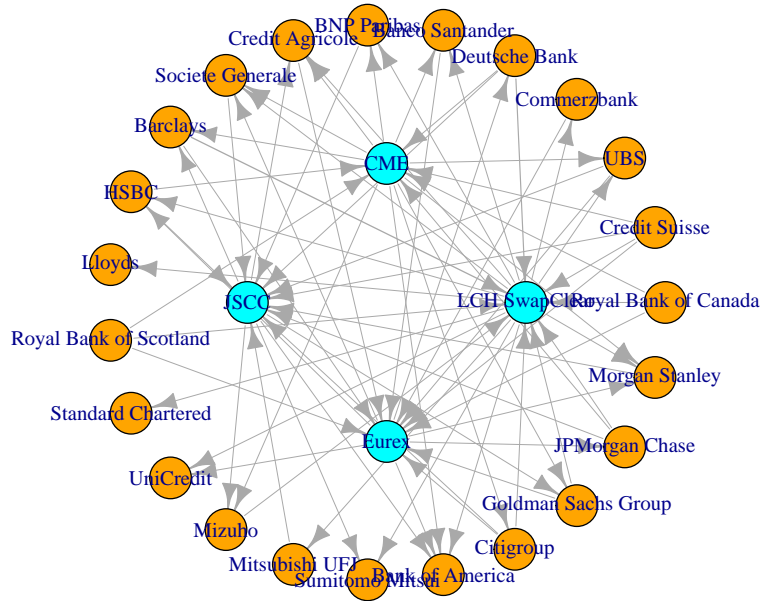
Second, we add frictions to the default process by setting $\gamma_i^{(1)} = \gamma_i^{(2)} = 0$ for all $i \in \mathcal{M}$. This means, that in case of default, clearing members do not make any payments to CCPs beyond their initial margins. For the CCPs, we continue to assume that $\gamma_i^{(1)} = \gamma_i^{(2)} = 1$ for all $i \in \mathcal{C}$, i.e., there are no additional frictions when CCPs default. Figure 9(b) shows the shortfalls for this scenario: they generally increase and there is one additional contagious default of a CCP (Eurex).

Third, we assume for clearing members that $\gamma_i^{(1)} = \gamma_i^{(2)} = 0$ for all $i \in \mathcal{M}$ and for CCPs that $\gamma_i^{(1)} = 1$ and $\gamma_i^{(2)} = 0.8$ for all $i \in \mathcal{C}$, i.e. CCPs use more severe variation margin gains haircutting ($\gamma_i^{(2)} = 0.8 < 1$) in case of default, but still use their pre-funded resources of the default waterfall in full ($\gamma_i^{(1)} = 1$). In this case, we find that three clearing members (JP Morgan Chase in addition to the two other members defaulting in the previous case) and four CCPs (CME in addition to LCH Swap Clear, JSCC and Eurex) default. Hence, there are two additional contagious defaults compared to the situation without more severe variation margin gains haircutting. Figure 9(d) shows a heatmap of the matrix of shortfalls. These increased compared to the situation without VMGH, and there are two more rows (corresponding to JP Morgan Chase and CME) where shortfalls occur.

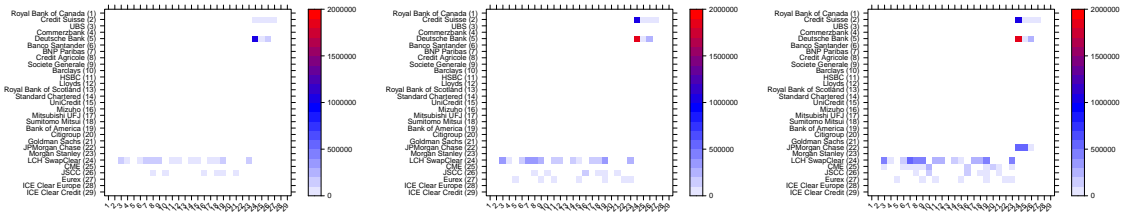
When relaxing the liquidity assumption on the collateral, we find that the total shortfall increases, but there are no additional contagious defaults. We consider the case $\alpha = 1000$ in the following, which essentially reduces the price of collateral from 1 to 0 (i.e., illiquid collateral). In particular, we find that in the first scenario, i.e., without default frictions, the total shortfall with liquid collateral is given by $S = 2,345,279$ (million USD) and this increases to $S = 2,409,927$ (million USD) for illiquid collateral. In the second

²²Note that it is in principle possible to collect or estimate this information, though this requires access to proprietary data (see e.g. Paddrik et al. (2020)).

²³To be sure, this represents an illustrative exercise: we are not suggesting that these institutions are the most likely to default across CCPs in the real world.



(a) Reconstructed payment obligations in the IRS network



(b) No frictions. Shortfall $S = 2,345,279$. (c) Frictions for default of clearing members. $S = 6,281,260$ (for $\alpha =$ members and CCPs. Shortfall $S = 1000 S = 6,346,000$) (d) Frictions for defaults of clearing members and CCPs. Shortfall $S = 9,632,085$.

Figure 9: Case study IRS: Reconstructed network of payment obligations (top) and shortfall of actual payments made under different scenarios (bottom). Shortfall (in million USD) without frictions (left), i.e., $\gamma_i^{(1)} = \gamma_i^{(2)} = 1 \forall i \in \mathcal{N}$, with frictions for defaults of clearing members (middle), i.e., $\gamma_i^{(1)} = \gamma_i^{(2)} = 0$ for all $i \in \mathcal{M}$ and $\gamma_i^{(1)} = \gamma_i^{(2)} = 1.0$ for all $i \in \mathcal{C}$, and with frictions for defaults of clearing members and CCPs (right), i.e., $\gamma_i^{(1)} = \gamma_i^{(2)} = 0$ for all $i \in \mathcal{M}$ and $\gamma_i^{(1)} = 1, \gamma_i^{(2)} = 0.8$ for all $i \in \mathcal{C}$. All figures of shortfalls are for the case of liquid collateral ($\alpha = 0$).

scenario with frictions for defaults of clearing members, the total shortfall corresponding to liquid collateral is given by $S = 6,281,260$ (million USD) and increases to $S = 6,346,000$ (million USD) for illiquid collateral. Similarly, in the third scenario with frictions for both defaults of clearing members and defaults of CCPs, the shortfall with liquid collateral is $S = 9,632,085$ (million USD) and increases to $S = 9,748,324$ (million USD) for illiquid collateral.

Overall we find that default frictions of clearing members or CCPs (or both), increase the total shortfall considerably more than assuming that collateral is illiquid.

4.2.2 Contagion in the CDS market

Next, we explore the model in the context of data on the CDS market. Figure 10(a) illustrates the reconstructed payment obligations given observable CDS positions. There are four CCPs (only two of which also clear IRS) and 23 clearing members trading in the CDS market in our data set. The clearing members are exactly the same as in the IRS case.

For this case study we chose clearing members' liquidity buffers such that there is only one fundamental default – Barclays, a clearing member shared by all CCPs. As before, we initially assume that there are no frictions, i.e., no bankruptcy costs and no severe form of variation margin gains haircutting, i.e., $\gamma_i^{(1)} = \gamma_i^{(2)} = 1$ for all $i \in \mathcal{N}$. Figure 10(b) presents the corresponding shortfalls for the case of liquid collateral ($\alpha = 0$). In this scenario, even though there is a fundamental default (by assumption), there are no shortfalls in payments (even for Barclays), i.e., $S = 0$. This means that the initial margins that were posted by the defaulting member were sufficient to cover all payments due (together with the liquidity buffer and the payments received from other CCPs). Hence, the initial fundamental default does not lead to any contagion effects.

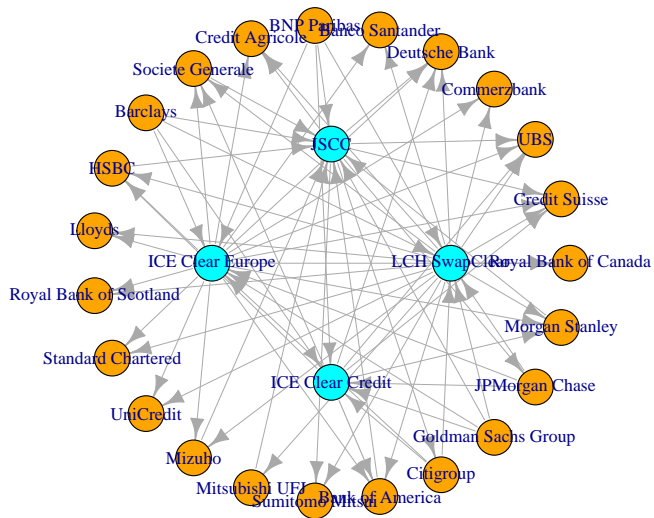
The situation changes, however, when we assume that the collateral is no longer liquid. Figure 10(c) shows the corresponding shortfalls in this case (where we set $\alpha = 10$). Now Barclays has payment shortfalls to all four CCPs, with the largest being towards ICE Clear Credit, which nonetheless is able to withstand the shock. LCH Swap Clear, however, defaults as a consequence of the payment shortfall. Therefore, the illiquidity of the collateral causes one contagious default at a CCP and a total shortfall of $S = 1,580$ (million USD).

Finally, when considering additional frictions we find additional contagious defaults among CCPs (both with and without illiquid collateral). For example, when setting $\gamma_i^{(1)} = \gamma_i^{(2)} = 0.75$ for all $i \in \mathcal{M}$ (and $\gamma_i^{(1)} = \gamma_i^{(2)} = 1$ for all $i \in \mathcal{C}$), then one member (Barclays) and three CCPs default (LCH Swap Clear, ICE Clear Europe, ICE Clear Credit) and the total shortfall is $S = 10,971$ (million USD) for $\alpha = 0$ and it increases to $S = 19,432$ (million USD) for $\alpha = 10$.

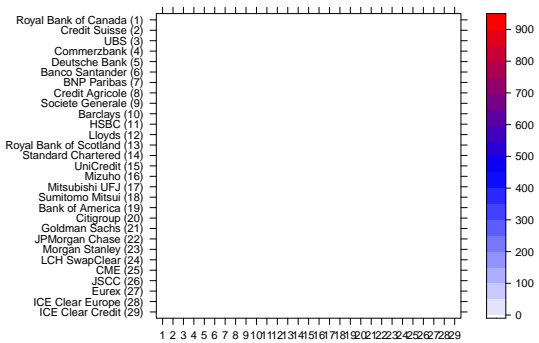
5 Policy implications for CCP stress-testing

Our model and findings have implications for CCP stress-testing. CCPs run regular in-house stress tests to ensure they have adequate resources to withstand a variety of stress scenarios. In addition, authorities conduct system-wide stress tests that apply to several CCPs simultaneously.

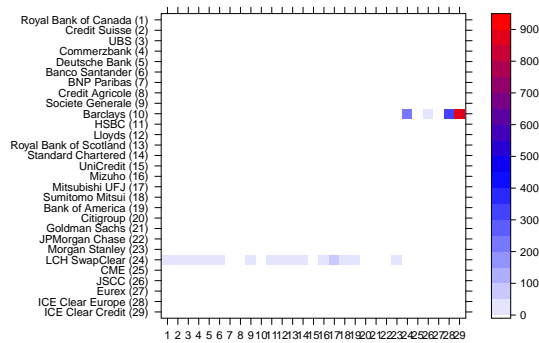
The most notable feature of CCP stress-testing is the Cover-2 standard, used in practice both for single CCP and system stress-testing (ESMA, 2020). The European Securities and Markets Authority (ESMA) coordinates EU-wide stress-testing of CCPs and has used the Cover-2 standard. In particular, ESMA distinguishes between two different types: the ‘‘Cover-2 groups per CCP’’ and ‘‘EU-wide Cover-2 groups’’. Under the first type, the top 2 clearing members *for each* CCP are assumed to default only for that individual CCP and not for others. Under the second type, the top 2 clearing members chosen to be in default are identified



(a) Reconstructed payment obligations in the network of Credit Default Swaps.



(b) Shortfall with liquid collateral ($\alpha = 0$)



(c) Shortfall with illiquid collateral ($\alpha = 10$)

Figure 10: Case study Credit Default Swaps: Comparison of the shortfall with liquid (left) and illiquid (right) collateral without severe variation margin gains haircutting or bankruptcy costs ($\gamma_i^{(1)} = \gamma_i^{(2)} = 1$ for all $i \in \mathcal{N}$).

based on exposures *across all* CCPs, and are assumed to default at all CCPs (see (ESMA, 2020, p. 20/21) for details).

Importantly, stress tests do not consider second round effects arising from joint clearing membership (ESMA, 2020). We illustrate how accounting for such higher order effects can affect stress-testing results. Two key insights emerge: higher order effects increase losses, and, when coupled with frictions such as default costs or severe variation margin gains haircutting, they can affect the choice of which the top 2 clearing members are that cause the largest losses.

Figure 11 presents the total shortfall in a stress-testing exercise based on the IRS data, considering all possible clearing member pairs being shocked. The x -axis represents the different clearing member pairs shocked and the y -axis represents the shortfalls (in million USD). Since there are $n_M = 23$ clearing members in our data, there are $\binom{n_M}{2} = 253$ ways to select two clearing members to be shocked.²⁴

We consider first the shortfall computed based only on first order effects (black line), which we use to sort the pairs as benchmark. We then compute the corresponding shortfalls in equilibrium (i.e., accounting for higher order effects) and additionally consider fire sales of collateral (i.e., $\alpha > 0$), default frictions (i.e., $\gamma_i^{(1)} < 1$ and/or $\gamma_i^{(2)}$ for some i) and combinations of them.

Figure 11 shows that accounting for higher order effects indeed results in higher shortfalls, as evident when contrasting the black and red lines in Figure 11. More interesting, however, is the fact that the red line is no longer monotonically decreasing. If we account for additional frictions ($\gamma_i^{(1)} < 1$ and or $\gamma_i^{(2)} < 1$ for some $i \in \mathcal{N}$) then this non-monotonicity becomes even more evident (e.g., blue and purple lines in Figure 11). This implies that a pair that leads to high first order losses need not rank equally high when considering higher order effects (with or without frictions). The very large spike in Figure 11 indicates that there is one pair of clearing members that has very small losses when only considering first order effects, but very high losses when accounting for higher order effects. Figure 11 also shows that – in this example at least – illiquid collateral increases the shortfall, but the effect of frictions caused by choosing $\gamma_i^{(1)}$ and/or $\gamma_i^{(2)}$ strictly smaller than 1 is generally more severe.

Default frictions are particularly powerful in affecting the pair-specific shortfalls. When considering default frictions of clearing members by setting $\gamma_i^{(1)} = \gamma_i^{(2)} = 0$ for all $i \in \mathcal{M}$ (blue line in Figure 11), shortfalls increase significantly, and the ordering of pairs leading to highest losses changes. When frictions are only associated with CCPs (purple line in Figure 11), i.e., $\gamma_i^{(1)} = 1$ and $\gamma_i^{(2)} = 0$ for all $i \in \mathcal{C}$ (and $\gamma_i^{(1)} = \gamma_i^{(2)} = 1$ for all $i \in \mathcal{M}$), then shortfalls increase even more and similarly the ordering of pairs leading to largest losses again varies considerably. In particular, the pair leading to the largest shortfalls is not the same as the pair that leads to the largest first order shortfalls. When combining these two frictions for liquid collateral (black dotted line) or for illiquid collateral (green dotted line) shortfalls increase even further.

We next look at shortfalls for two particular pairs of clearing members. On the one side, the pair linked to the largest loss when looking at first order effects; on the other, the pair linked to the largest losses when accounting for higher order effects with illiquid collateral, and default frictions of clearing members and CCPs. We consider the parameters corresponding to Figure 11. In this example, there is no fundamental default before any pair is shocked. Under this scenario, the first pair (first order effects only) is Deutsche Bank and Barclays, whereas the second pair is Deutsche Bank and the Royal Bank of Scotland.

Figure 12 presents the results, with the first two panels focusing on the first pair and the last two panels focusing on the second pair. Figure 12(a) shows the first order shortfall when Deutsche Bank and Barclays have their liquidity buffers set to 0, and Figure 12(b) shows the corresponding higher order shortfall that accounts for illiquid collateral, hard defaults of clearing members and severe variation margin gain hair-

²⁴In our example 18 clearing members have positive payment obligations. Hence, there are at most $\binom{18}{2} = 153$ combinations of 2 clearing members that can lead to shortfalls when their buffers are wiped out. That is why we observe 0 shortfalls beyond the 153rd pair in Figure 11.

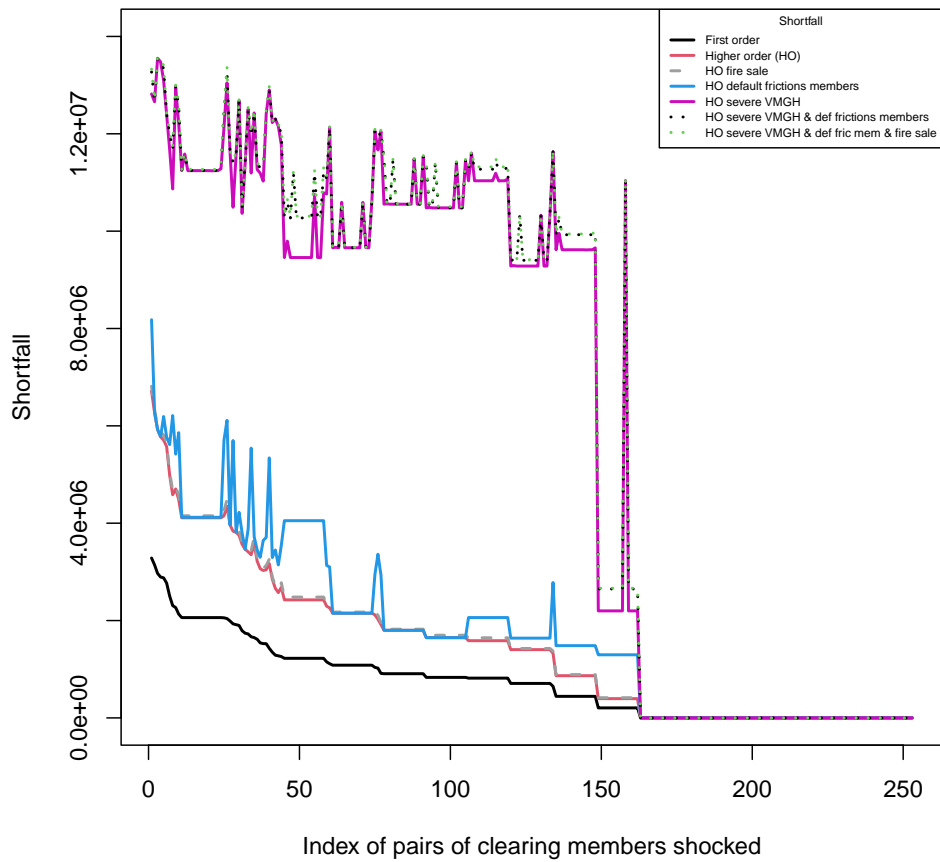
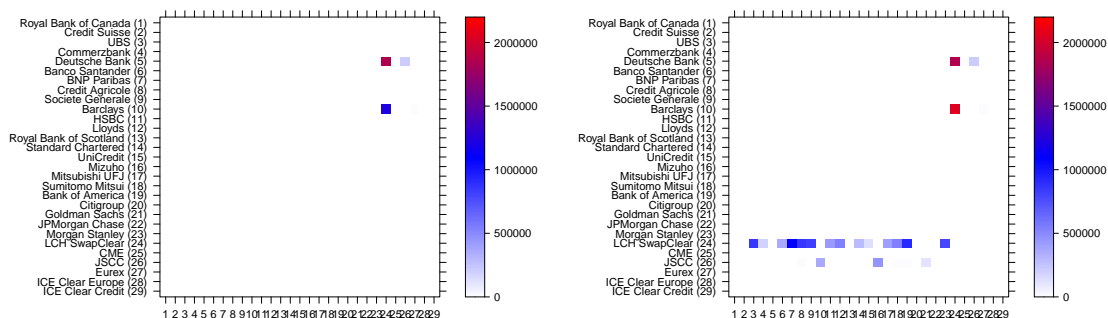


Figure 11: First order and higher order shortfalls when different pairs of clearing members are shocked for different parameter choices in Φ^{R1} . All numbers in million USD.

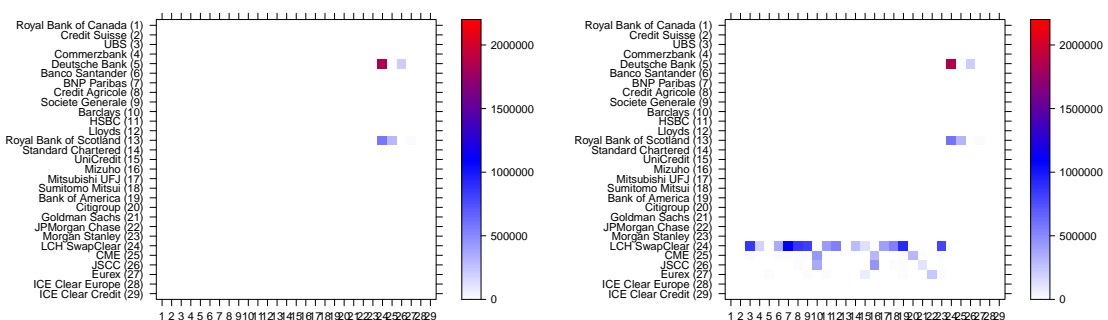
cutting, i.e., $\alpha = 1000 > 0$, $\gamma_i^{(1)} = \gamma^{(2)} = 0$ for all $i \in \mathcal{M}$, and $\gamma_i^{(1)} = 1$, $\gamma^{(2)} = 0$ for all $i \in \mathcal{C}$. In this example, accounting for these higher order effects increases the total shortfall from 3,284,789 (million USD) to 13,327,776 (million USD), i.e., the shortfall is more than four times larger.

For the second pair, the picture that emerges is similar. Figure 12(c) shows the first order shortfall when Deutsche Bank and the Royal Bank of Scotland have their liquidity buffers set to 0, and Figure 12(d) shows the corresponding higher order shortfall that accounts for the same frictions as before. In this example, accounting for these higher order effects increases the total shortfall from 2,968,599 (million USD) to 13,585,060 (million USD), i.e., the shortfall is more than 4.5 times larger. In particular, four CCPs default under this scenario.

Taken together, these results illustrate that the combination of higher order effects and frictions interacts and affects the ordering of pairs causing the largest losses. By considering only first order effects one would select the pair consisting of Deutsche Bank and Barclays, with an associated shortfall of 3,284,789 (million USD) (Figure 12(a)). The largest possible shortfall, however, would be achieved by a different pair (Deutsche Bank and the Royal Bank of Scotland) when accounting for higher order effects and frictions, resulting in a total shortfall of 13,585,060 (million USD) (Figure 12(d)). This highlights the importance of considering higher order effects, as well as potential market-related frictions, when performing CCP stress-testing exercises.



(a) First order shortfall for stress to Deutsche Bank and (b) Higher order shortfall (with illiquid collateral and de-Barclays; total first order shortfall is 3,284,789 million fault frictions of both clearing members and CCPs) for stress to Deutsche Bank and Barclays; total shortfall is 13,327,776 million USD.



(c) First order shortfall for stress to Deutsche Bank and (d) Higher order shortfall (with illiquid collateral and de-the Royal Bank of Scotland; total first order shortfall is 2,968,599 million USD. total shortfall is 13,585,060 million USD.

Figure 12: First order (left) and higher order (right) shortfall when two different pairs of clearing members have their liquidity buffer set to 0. In the first row, Deutsche Bank and Barclays are selected to have 0 liquidity buffer, in the second row Deutsche Bank and the Royal Bank of Scotland are selected. The liquidity buffers are chosen such that there is no fundamental default prior to the stress-testing exercise.

6 Conclusion

This paper underscores the important role that joint clearing members can have in loss transmission between several CCPs, especially in a context where realistic frictions potentially affecting contagion are present. As such, it serves to highlight the need to incorporate these features into current CCP stress testing practice. Furthermore, it also highlights the importance of stress testing CCPs simultaneously and not just in isolation.

As our case studies illustrate, in the presence of joint clearing members it is even theoretically possible that a clearing member triggers the default of a CCP at which it does not clear. This can happen indirectly via fire sales of collateral, or directly via variation margin gains haircutting of the CCP at which it clears, or a combination of both mechanisms. Admittedly, situations like this would be rare, but nevertheless they illustrate the importance of accounting for second and higher order interconnections between CCPs in their risk management.

It is important to bear in mind that our model is stylised and results are illustrative of the mechanisms we aim to highlight. Throughout we analyse how the effects of a clearing members' default play out mechanically through CCP's rulebooks, by incorporating key elements of the latter on an enhanced version of standard network contagion model. When interpreting results, it should be clear that we are not able to quantify the likelihood of any scenario leading to an actual CCP default.

That said and despite the stylised nature of the model, we are able to illustrate important issues regarding contagion in markets with multiple CCPs and joint clearing membership. In our case studies we made a number of simplifying assumptions not required by our key results to go through, such as clearing members novating all their trades to CCPs, having no bilateral positions with other clearing members, or disregarding the links between clearing members and the clients they clear for. Even under these assumptions, which essentially remove several additional ways in which contagion can spread through the network of payment obligations, we still found strong contagion effects that amplified losses considerably. Furthermore, these contagion effects significantly changed the ranking of clearing members that would cause the largest losses in case of default.

These results suggest that any Cover-2 standard that excludes network effects has the risk of being not conservative enough. One of the key lessons after the Great Financial Crisis was that stress scenarios need to be "sufficiently severe" (Basel Committee on Banking Supervision, 2018, Principle 4). Our paper provides evidence that accounting for network effects and joint clearing membership can be crucial to achieve this objective.

Appendices

A The second round of clearing

In this appendix we review the details of the second round of clearing in the model, developed in Ghamami et al. (2022), which can be summarised as a second fixed point problem.

Let $(\pi^{*,R1}, p^{*,R1}) \in [0, 1] \times [0, \bar{p}^{R1}]$ be the greatest fixed point of Φ^{R1} defined in (1). Then, the payments that are still outstanding at the start of the second round are given by $\bar{p}^{R2} = \bar{p}^{R1} - p^{*,R1} \in [0, \bar{p}^{R1}]$. We define a function $\Phi^{R2} : [0, \pi^{*,R1}] \times [0, \bar{p}^{R2}] \rightarrow [0, \pi^{*,R1}] \times [0, \bar{p}^{R2}]$ and the aim is to determine a fixed point of this function, i.e., we want to find $(\pi^{*,R2}, p^{*,R2})$ such that

$$(\pi^{*,R2}, p^{*,R2}) = \Phi^{R2}(\pi^{*,R2}, p^{*,R2}),$$

where $\Phi^{R2}(\pi, p)$ is defined as follows:

$$\begin{aligned} \Phi_1^{R2}(\pi, p) &= \pi^{*,R1} \exp(-\alpha \Gamma(\pi, p)), \\ \Phi_{2,(ij)}^{R2}(\pi, p) &= \min \left\{ \bar{p}_{ij}^{R2}, a_{ij}^{R2} \left(\pi r_i(\pi^{*,R1}, p^{*,R1}) + \sum_{k=1}^N p_{ki} \right) \right\}, \end{aligned} \quad (3)$$

where

$$a_{ij}^{R2} = \begin{cases} \frac{\bar{p}_{ij}^{R2}}{\sum_{k=1}^N \bar{p}_{ik}^{R2}}, & \text{if } \sum_{k=1}^N \bar{p}_{ik}^{R2} > 0, \\ 0, & \text{otherwise,} \end{cases}$$

denotes the repayment proportions for $i, j \in \mathcal{N}$ in the second round and $\Gamma(\pi, p)$ denotes the total shares of collateral sold in the second round, i.e.,

$$\Gamma(\pi, p) = \sum_{i=1}^N \Gamma_i(\pi, p),$$

where the total share of collateral sold by node $i \in \mathcal{N}$ is given by

$$\Gamma_i(\pi, p) = \min \left\{ r_i(\pi^{*,R1}, p^{*,R1}), \frac{1}{\pi} \max \left\{ 0, \sum_{j=1}^N \bar{p}_{ij}^{R2} - \sum_{j=1}^N p_{ji} \right\} \right\},$$

if $\pi > 0$. For $\pi = 0$, we set

$$\Gamma_i(\pi, p) = \begin{cases} r_i(\pi^{*,R1}, p^{*,R1}), & \text{if } i \in \mathcal{D}(p^{*,R1}) \text{ and } \max \left\{ 0, \sum_{j=1}^N \bar{p}_{ij}^{R2} - \sum_{j=1}^N p_{ji} \right\} > 0, \\ 0, & \text{otherwise.} \end{cases}$$

Furthermore, $r_i(\pi^{*,R1}, p^{*,R1})$ is the collateral returned to node $i \in \mathcal{N}$ and is defined as

$$r_i(\pi^{*,R1}, p^{*,R1}) = \begin{cases} \sum_{j=1}^N (m_{ij} - \Delta_{ij}(\pi^{*,R1}, p^{*,R1})), & \text{if } i \in \mathcal{D}(p^{*,R1}), \\ \sum_{j \in \mathcal{D}(p^{*,R1})} m_{ij}, & \text{if } i \in \mathcal{N} \setminus \mathcal{D}(p^{*,R1}). \end{cases}$$

In our setting, the market consists of clearing members and CCPs. Since we assume that CCPs do not post initial margins to their clearing members, only clearing members can have collateral returned to them in Round 2. In particular, this implies that $r_i(\pi^{*,R1}, p^{*,R1}) = 0$ for all $i \in \mathcal{C}$.

B Existence results and proofs

Lemma B.1 (Properties of Φ^{R1}). *Let $\Phi^{R1} : [0, 1] \times [0, \bar{p}^{R1}] \rightarrow [0, 1] \times [0, \bar{p}^{R1}]$ be the function defined in (1), then Φ^{R1} is order-preserving, i.e., for all $\tilde{\pi}, \pi \in [0, 1]$ with $\tilde{\pi} \leq \pi$ and for all $\tilde{p}, p \in [0, \bar{p}^{R1}]$ with $\tilde{p}_{ij} \leq p_{ij}$ for all $i, j \in \mathcal{N}$ it holds that*

$$\begin{aligned}\Phi_1^{R1}(\tilde{\pi}, \tilde{p}) &\leq \Phi_1^{R1}(\pi, p), \\ \Phi_{2,(ij)}^{R1}(\tilde{\pi}, \tilde{p}) &\leq \Phi_{2,(ij)}^{R1}(\pi, p) \quad \forall i, j \in \mathcal{N}.\end{aligned}$$

Proof of Lemma B.1. Let $\tilde{\pi}, \pi \in [0, 1]$ with $\tilde{\pi} \leq \pi$ and let $\tilde{p}, p \in [0, \bar{p}^{R1}]$ with $\tilde{p}_{ij} \leq p_{ij}$ for all $i, j \in \mathcal{N}$.

We show that Φ_1^{R1} is order-preserving. The total assets satisfy

$$A_i(\tilde{p}) = b_i + \sum_{k=1}^N \tilde{p}_{ki} \leq b_i + \sum_{k=1}^N p_{ki} = A_i(p).$$

This implies that all nodes that default under p also default under \tilde{p} , in particular

$$\mathcal{D}(p) \subseteq \mathcal{D}(\tilde{p}), \quad (4)$$

since for $i \in \mathcal{D}(p)$, it holds that $\bar{p}_i^{R1} > A_i(p) \geq A_i(\tilde{p})$, and hence $i \in \mathcal{D}(\tilde{p})$.

Next, we need to show that the number of shares of collateral sold satisfies

$$\Delta_{ij}(\tilde{\pi}, \tilde{p}) \geq \Delta_{ij}(\pi, p) \quad \forall i, j \in \mathcal{N}. \quad (5)$$

Once this has been shown, we immediately obtain that

$$\Delta(\tilde{\pi}, \tilde{p}) = \sum_{i=1}^N \sum_{j=1}^N \Delta_{ij}(\tilde{\pi}, \tilde{p}) \geq \sum_{i=1}^N \sum_{j=1}^N \Delta_{ij}(\pi, p) = \Delta(\pi, p),$$

and hence

$$\Phi_1^{R1}(\tilde{\pi}, \tilde{p}) = \exp(-\alpha \Delta(\tilde{\pi}, \tilde{p})) \leq \exp(-\alpha \Delta(\pi, p)) = \Phi_1^{R1}(\pi, p),$$

since $\alpha \geq 0$.

We now prove (5). Let $i, j \in \mathcal{N}$.

- First, let $i \in \mathcal{D}(p)$. By (4), $i \in \mathcal{D}(\tilde{p})$. We distinguish between three cases:

Case 1: Let $\tilde{\pi} > 0$, then, $\Delta_{ij}(\tilde{\pi}, \tilde{p}) = \min \left\{ m_{ij}, \frac{\bar{p}_{ij}^{R1}}{\tilde{\pi}} \right\}$ and $\Delta_{ij}(\pi, p) = \min \left\{ m_{ij}, \frac{\bar{p}_{ij}^{R1}}{\pi} \right\}$. Since

$0 < \tilde{\pi} \leq \pi$, it holds that $\frac{\bar{p}_{ij}^{R1}}{\tilde{\pi}} \geq \frac{\bar{p}_{ij}^{R1}}{\pi}$ which implies that

$$\Delta_{ij}(\tilde{\pi}, \tilde{p}) = \min \left\{ m_{ij}, \frac{\bar{p}_{ij}^{R1}}{\tilde{\pi}} \right\} \geq \min \left\{ m_{ij}, \frac{\bar{p}_{ij}^{R1}}{\pi} \right\} = \Delta_{ij}(\pi, p).$$

Case 2: Let $\tilde{\pi} = \pi = 0$, then if $\bar{p}_{ij}^{R1} > 0$, it holds that $\Delta_{ij}(\tilde{\pi}, \tilde{p}) = m_{ij} = \Delta_{ij}(\pi, p)$. If $\bar{p}_{ij}^{R1} = 0$, then $\Delta_{ij}(\tilde{\pi}, \tilde{p}) = 0 = \Delta_{ij}(\pi, p)$.

Case 3: Let $0 = \tilde{\pi} < \pi$, then if $\bar{p}_{ij}^{R1} > 0$, it holds that $\Delta_{ij}(\tilde{\pi}, \tilde{p}) = m_{ij} \geq \min \left\{ m_{ij}, \frac{\bar{p}_{ij}^{R1}}{\pi} \right\} =$

$\Delta_{ij}(\pi, p)$. If $\bar{p}_{ij}^{R1} = 0$, then $\Delta_{ij}(\tilde{\pi}, \tilde{p}) = 0 = \min \left\{ m_{ij}, \frac{\bar{p}_{ij}^{R1}}{\pi} \right\} = \Delta_{ij}(\pi, p)$.

- Second, let $i \in \mathcal{N} \setminus \mathcal{D}(p)$. Then, $\Delta_{ij}(\pi, p) = 0 \leq \Delta_{ij}(\tilde{\pi}, \tilde{p})$. Hence, (5) holds.

Next, we show that Φ_2^{R1} is order-preserving. Let $i, j \in \mathcal{N}$. We distinguish between two cases.

Case 1: Let $i \in \mathcal{N} \setminus \mathcal{D}(p)$. Then,

$$\Phi_{2,(ij)}^{\text{R1}}(\pi, p) = \bar{p}_{ij}^{\text{R1}} \geq \Phi_{2,(ij)}^{\text{R1}}(\tilde{\pi}, \tilde{p}).$$

Case 2: Let $i \in \mathcal{D}(p)$. Then, $i \in \mathcal{D}(\tilde{p})$. Then,

$$\begin{aligned} \Phi_{2,(ij)}^{\text{R1}}(\tilde{\pi}, \tilde{p}) &= \min \left\{ \bar{p}_{ij}^{\text{R1}}, \tilde{\pi} m_{ij} + a_{ij}^{\text{R1}}(\tilde{\pi}) \left(\gamma_i^{(1)} b_i + \gamma_i^{(2)} \sum_{k=1}^N \tilde{p}_{ki} \right) \right\}, \\ \Phi_{2,(ij)}^{\text{R1}}(\pi, p) &= \min \left\{ \bar{p}_{ij}^{\text{R1}}, \pi m_{ij} + a_{ij}^{\text{R1}}(\pi) \left(\gamma_i^{(1)} b_i + \gamma_i^{(2)} \sum_{k=1}^N p_{ki} \right) \right\}. \end{aligned}$$

We distinguish between two cases.

First, let $\Phi_{2,(ij)}^{\text{R1}}(\pi, p) = \bar{p}_{ij}^{\text{R1}}$, then $\Phi_{2,(ij)}^{\text{R1}}(\pi, p) = \bar{p}_{ij}^{\text{R1}} \geq \Phi_{2,(ij)}^{\text{R1}}(\tilde{\pi}, \tilde{p})$.

Second, let

$$\bar{p}_{ij}^{\text{R1}} > \Phi_{2,(ij)}^{\text{R1}}(\pi, p) = \pi m_{ij} + a_{ij}^{\text{R1}}(\pi) \left(\gamma_i^{(1)} b_i + \gamma_i^{(2)} \sum_{k=1}^N p_{ki} \right). \quad (6)$$

We show that

$$\bar{p}_{ij}^{\text{R1}} > \Phi_{2,(ij)}^{\text{R1}}(\tilde{\pi}, \tilde{p}) = \tilde{\pi} m_{ij} + a_{ij}^{\text{R1}}(\tilde{\pi}) \left(\gamma_i^{(1)} b_i + \gamma_i^{(2)} \sum_{k=1}^N \tilde{p}_{ki} \right). \quad (7)$$

Rearranging (6) gives $\bar{p}_{ij}^{\text{R1}} - \pi m_{ij} > a_{ij}^{\text{R1}}(\pi) \left(\gamma_i^{(1)} b_i + \gamma_i^{(2)} \sum_{k=1}^N p_{ki} \right) \geq 0$ and hence

$$0 < \frac{\bar{p}_{ij}^{\text{R1}} - \pi m_{ij}}{\sum_{k=1}^N \max\{0, \bar{p}_{ik}^{\text{R1}} - \pi m_{ik}\}} = a_{ij}^{\text{R1}}(\pi),$$

which implies that

$$\begin{aligned} \bar{p}_{ij}^{\text{R1}} - \pi m_{ij} &> a_{ij}^{\text{R1}}(\pi) \left(\gamma_i^{(1)} b_i + \gamma_i^{(2)} \sum_{k=1}^N p_{ki} \right) = \frac{\bar{p}_{ij}^{\text{R1}} - \pi m_{ij}}{\sum_{k=1}^N \max\{0, \bar{p}_{ik}^{\text{R1}} - \pi m_{ik}\}} \left(\gamma_i^{(1)} b_i + \gamma_i^{(2)} \sum_{k=1}^N p_{ki} \right), \\ \iff 1 &> \frac{\left(\gamma_i^{(1)} b_i + \gamma_i^{(2)} \sum_{k=1}^N p_{ki} \right)}{\sum_{k=1}^N \max\{0, \bar{p}_{ik}^{\text{R1}} - \pi m_{ik}\}}. \end{aligned} \quad (8)$$

It also holds that $a_{ij}^{\text{R1}}(\tilde{\pi}) > 0$. We prove this by contradiction. Assume that $a_{ij}^{\text{R1}}(\tilde{\pi}) = 0$. This implies that $\bar{p}_{ij}^{\text{R1}} \leq \tilde{\pi} m_{ij}$. But since $0 = a_{ij}^{\text{R1}}(\tilde{\pi}) < a_{ij}^{\text{R1}}(\pi)$, we obtain

$$\tilde{\pi} m_{ij} + a_{ij}^{\text{R1}}(\tilde{\pi}) \left(\gamma_i^{(1)} b_i + \gamma_i^{(2)} \sum_{k=1}^N \tilde{p}_{ki} \right) \leq \pi m_{ij} + a_{ij}^{\text{R1}}(\pi) \left(\gamma_i^{(1)} b_i + \gamma_i^{(2)} \sum_{k=1}^N p_{ki} \right) = \Phi_{2,(ij)}^{\text{R1}}(\pi, p) < \bar{p}_{ij}^{\text{R1}},$$

which is a contradiction to $\bar{p}_{ij}^{\text{R1}} \leq \tilde{\pi} m_{ij}$. Hence, $a_{ij}^{\text{R1}}(\tilde{\pi}) > 0$.

From $a_{ij}^{\text{R1}}(\tilde{\pi}) > 0$ it follows directly that

$$\sum_{k=1}^N \max\{0, \bar{p}_{ik}^{\text{R1}} - \tilde{\pi}m_{ik}\} > 0 \text{ and } \bar{p}_{ij}^{\text{R1}} - \tilde{\pi}m_{ij} > 0. \quad (9)$$

Then,

$$\begin{aligned} \tilde{\pi}m_{ij} + a_{ij}^{\text{R1}}(\tilde{\pi}) \left(\gamma_i^{(1)}b_i + \gamma_i^{(2)} \sum_{k=1}^N \tilde{p}_{ki} \right) &= \tilde{\pi}m_{ij} + \frac{\max\{0, \bar{p}_{ij}^{\text{R1}} - \tilde{\pi}m_{ij}\}}{\sum_{k=1}^N \max\{0, \bar{p}_{ik}^{\text{R1}} - \tilde{\pi}m_{ik}\}} \left(\gamma_i^{(1)}b_i + \gamma_i^{(2)} \sum_{k=1}^N \tilde{p}_{ki} \right) \\ &\leq \tilde{\pi}m_{ij} + \frac{\max\{0, \bar{p}_{ij}^{\text{R1}} - \tilde{\pi}m_{ij}\}}{\sum_{k=1}^N \max\{0, \bar{p}_{ik}^{\text{R1}} - \pi m_{ik}\}} \left(\gamma_i^{(1)}b_i + \gamma_i^{(2)} \sum_{k=1}^N p_{ki} \right) < \tilde{\pi}m_{ij} + \max\{0, \bar{p}_{ij}^{\text{R1}} - \tilde{\pi}m_{ij}\} = \bar{p}_{ij}^{\text{R1}}, \end{aligned} \quad (10)$$

where the last inequality follows from (8). Observe that (6) implies that indeed $\sum_{k=1}^N \max\{0, \bar{p}_{ik}^{\text{R1}} - \pi m_{ik}\} > 0$. Hence, (7) holds.

It remains to show that

$$\begin{aligned} \Phi_{2,(ij)}^{\text{R1}}(\tilde{\pi}, \tilde{p}) &= \tilde{\pi}m_{ij} + a_{ij}^{\text{R1}}(\tilde{\pi}) \left(\gamma_i^{(1)}b_i + \gamma_i^{(2)} \sum_{k=1}^N \tilde{p}_{ki} \right) \\ &\leq \pi m_{ij} + a_{ij}^{\text{R1}}(\pi) \left(\gamma_i^{(1)}b_i + \gamma_i^{(2)} \sum_{k=1}^N p_{ki} \right) = \Phi_{2,(ij)}^{\text{R1}}(\pi, p). \end{aligned}$$

It is clear that $\Phi_{2,(ij)}^{\text{R1}}$ is order-preserving in the argument p . So we only need to show that it is also order-preserving in π . If $m_{ij} = 0$, then it follows directly that $a_{ij}^{\text{R1}}(\tilde{\pi}) \leq a_{ij}^{\text{R1}}(\pi)$ and hence $\Phi_{2,(ij)}^{\text{R1}}(\tilde{\pi}, \tilde{p}) \leq \Phi_{2,(ij)}^{\text{R1}}(\pi, p)$. If $m_{ij} > 0$, we define a function $f_{ij}(\cdot; \hat{p}) : [\tilde{\pi}, \pi] \rightarrow [0, \bar{p}_{ij}^{\text{R1}}]$ by

$$f_{ij}(\hat{\pi}; \hat{p}) = \hat{\pi}m_{ij} + a_{ij}^{\text{R1}}(\hat{\pi}) \underbrace{\left(\gamma_i^{(1)}b_i + \gamma_i^{(2)} \sum_{k=1}^N \hat{p}_{ki} \right)}_{=A_i(\hat{p}; \gamma_i^{(1)}, \gamma_i^{(2)})} = \hat{\pi}m_{ij} + a_{ij}^{\text{R1}}(\hat{\pi})A_i(p; \gamma_i^{(1)}, \gamma_i^{(2)}),$$

where $\hat{p} \in [\tilde{p}, p]$. In particular, $f_{ij}(\hat{\pi}; \hat{p}) = \Phi_{2,(ij)}^{\text{R1}}(\hat{\pi}, \hat{p})$ under the given constraints on the parameters.

Furthermore, since $a^{\text{R1}}(\tilde{\pi}) > 0$ and $a^{\text{R1}}(\pi) > 0$, we obtain for all $\hat{\pi} \in [\tilde{\pi}, \pi]$ that $\tilde{\pi}m_{ij} \leq \hat{\pi}m_{ij} \leq \pi m_{ij} < \bar{p}_{ij}^{\text{R1}}$ and hence $a_{ij}^{\text{R1}}(\hat{\pi}) > 0$.

From (6) and (7), it follows directly that $A_i(p; \gamma_i^{(1)}, \gamma_i^{(2)}) < \sum_{k=1}^N \max\{0, \bar{p}_{ik}^{\text{R1}} - \pi m_{ik}\}$ and $A_i(\tilde{p}; \gamma_i^{(1)}, \gamma_i^{(2)}) < \sum_{k=1}^N \max\{0, \bar{p}_{ik}^{\text{R1}} - \tilde{\pi}m_{ik}\}$. Hence, for all $\hat{p} \in [\tilde{p}, p]$ we obtain

$$\begin{aligned} A_i(\tilde{p}; \gamma_i^{(1)}, \gamma_i^{(2)}) &\leq A_i(\hat{p}; \gamma_i^{(1)}, \gamma_i^{(2)}) \leq A_i(p; \gamma_i^{(1)}, \gamma_i^{(2)}) < \sum_{k=1}^N \max\{0, \bar{p}_{ik}^{\text{R1}} - \pi m_{ik}\} \\ &\leq \sum_{k=1}^N \max\{0, \bar{p}_{ik}^{\text{R1}} - \hat{\pi}m_{ik}\} \leq \sum_{k=1}^N \max\{0, \bar{p}_{ik}^{\text{R1}} - \tilde{\pi}m_{ik}\}. \end{aligned} \quad (11)$$

The function f_{ij} is continuous and piecewise differentiable.²⁵ Similarly to the argument used in (Ghamami et al., 2022, Proof of Lemma A.1), we can consider the derivative of f_{ij} , and obtain

$$\begin{aligned}\frac{\partial f_{ij}(\hat{\pi}; \hat{p})}{\partial \hat{\pi}} &= m_{ij} + \frac{\partial a_{ij}^{\text{R1}}(\hat{\pi})}{\partial \hat{\pi}} A_i(\hat{p}; \gamma_i^{(1)}, \gamma_i^{(2)}), \\ \frac{\partial a_{ij}^{\text{R1}}(\hat{\pi})}{\partial \hat{\pi}} &= \frac{\left(\sum_{k=1}^N \max\{0, \bar{p}_{ik}^{\text{R1}} - \hat{\pi} m_{ik}\} \right) (-m_{ij}) + (\bar{p}_{ij}^{\text{R1}} - \hat{\pi} m_{ij})^+ \sum_{k=1}^N m_{ik} \mathbb{I}_{\{\bar{p}_{ik}^{\text{R1}} > \hat{\pi} m_{ik}\}}}{\left(\sum_{k=1}^N \max\{0, \bar{p}_{ik}^{\text{R1}} - \hat{\pi} m_{ik}\} \right)^2},\end{aligned}$$

and hence,

$$\frac{\partial f_{ij}(\hat{\pi}; \hat{p})}{\partial \hat{\pi}} = m_{ij} \left(1 - \frac{A_i(\hat{p}; \gamma_i^{(1)}, \gamma_i^{(2)})}{\sum_{k=1}^N \max\{0, \bar{p}_{ik}^{\text{R1}} - \hat{\pi} m_{ik}\}} \right) + \frac{(\bar{p}_{ij}^{\text{R1}} - \hat{\pi} m_{ij})^+ \sum_{k=1}^N m_{ik} \mathbb{I}_{\{\bar{p}_{ik}^{\text{R1}} > \hat{\pi} m_{ik}\}}}{\left(\sum_{k=1}^N \max\{0, \bar{p}_{ik}^{\text{R1}} - \hat{\pi} m_{ik}\} \right)^2} A_i(\hat{p}; \gamma_i^{(1)}, \gamma_i^{(2)}).$$

The first term of the derivative satisfies

$$1 - \frac{A_i(\hat{p}; \gamma_i^{(1)}, \gamma_i^{(2)})}{\sum_{k=1}^N \max\{0, \bar{p}_{ik}^{\text{R1}} - \hat{\pi} m_{ik}\}} \geq 0,$$

because of (11). Furthermore, it is clear that the second term of the derivative is non-negative. Hence, the derivative is non-negative. Together with the continuity of f_{ij} , this implies that f_{ij} is order-preserving on $[\tilde{\pi}, \pi]$ and hence $\Phi_{2,(ij)}^{\text{R1}}(\tilde{\pi}, \tilde{p}) \leq \Phi_{2,(ij)}^{\text{R1}}(\pi, p)$. \square

Theorem B.2 (Existence of a least and greatest price-payment equilibrium in Round 1). *Let $\Phi^{\text{R1}} : [0, 1] \times [0, \bar{p}^{\text{R1}}] \rightarrow [0, 1] \times [0, \bar{p}^{\text{R1}}]$ be the function defined in (1).*

1. *The set of fixed points of Φ^{R1} is a complete lattice. In particular Φ^{R1} admits a greatest and a least fixed point.*
2. *Let $(\pi^{(0)}, p^{(0)}) = (1, \bar{p}^{\text{R1}})$ and define recursively for $k \in \mathbb{N}_0$*

$$(\pi^{(k+1)}, p^{(k+1)}) = \Phi^{\text{R1}}(\pi^{(k)}, p^{(k)}).$$

Then,

- (a) *$(\pi^{(k)}, p^{(k)})_{k \in \mathbb{N}_0}$ is a monotonically non-increasing sequence, that is, $\pi^{(k+1)} \leq \pi^{(k)}$ and $p_{ij}^{(k+1)} \leq p_{ij}^{(k)}$ for all $i, j \in \mathcal{N}$ and for all $k \in \mathbb{N}_0$.*
- (b) *The limit $\lim_{k \rightarrow \infty} (\pi^{(k)}, p^{(k)})$ exists and is the greatest fixed point of Φ^{R1} .*

Proof of Theorem B.2. 1. We will prove the statement using Tarski's fixed point theorem (Tarski, 1955). First, $[0, 1] \times [0, \bar{p}^{\text{R1}}]$ is a complete lattice with respect to the component-wise ordering. Second, it follows directly from the definition of Φ^{R1} in (1) that indeed $\Phi^{\text{R1}} : [0, 1] \times [0, \bar{p}^{\text{R1}}] \rightarrow [0, 1] \times [0, \bar{p}^{\text{R1}}]$. Third, Φ^{R1} is an order-preserving function by Lemma B.1. By Tarski's fixed point theorem, the set of fixed points of Φ^{R1} is a complete lattice and hence a least and greatest fixed point exist.

2. Next, we show that the greatest fixed point can be obtained by fixed point iteration.

²⁵The only points where f_{ij} is not differentiable are points $\bar{p}_{ik}^{\text{R1}}/m_{ik} \in [\tilde{\pi}, \pi]$ with $m_{ik} > 0$, $k \in \mathcal{N}$.

(a) We prove that $\pi^{(k+1)} \leq \pi^{(k)}$ and $p_{ij}^{(k+1)} \leq p_{ij}^{(k)}$ for all $i, j \in \mathcal{N}$ and for all $k \in \mathbb{N}_0$ by induction.

For $k = 0$, it follows directly from the definition of Φ^{R1} in (1) that $\pi^{(1)} = \Phi_1^{\text{R1}}(\pi^{(0)}, p^{(0)}) = \exp(-\alpha \Delta(\pi^{(0)}, p^{(0)})) \leq 1 = \pi^{(0)}$ and $p_{ij}^{(1)} = \Phi_{2,(ij)}^{\text{R1}}(\pi^{(0)}, p^{(0)}) \leq \bar{p}_{ij}^{\text{R1}} = p_{ij}^{(0)}$ for all $i, j \in \mathcal{N}$.

Our induction hypothesis is that $\pi^{(k+1)} \leq \pi^{(k)}$ and $p_{ij}^{(k+1)} \leq p_{ij}^{(k)}$ for all $i, j \in \mathcal{N}$ and for a $k \in \mathbb{N}_0$.

Then, by the definition of the sequence

$$(\pi^{(k+2)}, p^{(k+2)}) = \Phi^{\text{R1}}(\pi^{(k+1)}, p^{(k+1)}) \leq \Phi^{\text{R1}}(\pi^{(k)}, p^{(k)}) = (\pi^{(k+1)}, p^{(k+1)}),$$

where the inequality follows from the induction hypothesis and the fact that Φ^{R1} is order-preserving by Lemma B.1. Hence, this completes the induction step.

It follows directly from the definition of Φ^{R1} that it is bounded from below by $(0, 0)$ (where the first 0 is 1-dimensional and the second zero is the $N \times N$ zero matrix). Hence, there exists a monotone limit $(\hat{\pi}, \hat{p}) = \lim_{k \rightarrow \infty} (\pi^{(k)}, p^{(k)})$. This limit is a fixed point of Φ^{R1} , since

$$\Phi^{\text{R1}}(\hat{\pi}, \hat{p}) = \Phi^{\text{R1}}(\lim_{k \rightarrow \infty} (\pi^{(k)}, p^{(k)})) = \lim_{k \rightarrow \infty} \Phi^{\text{R1}}(\pi^{(k)}, p^{(k)}) = \lim_{k \rightarrow \infty} (\pi^{(k+1)}, p^{(k+1)}) = (\hat{\pi}, \hat{p}),$$

where the second equality follows from the right-continuity of Φ^{R1} . It remains to show that $(\hat{\pi}, \hat{p}) = (\pi^{*,\text{R1}}, p^{*,\text{R1}})$, i.e., that it is the greatest fixed point of Φ^{R1} .

We show by induction that $(\pi^{(k)}, p^{(k)}) \geq (\pi^{*,\text{R1}}, p^{*,\text{R1}})$ for all $k \in \mathbb{N}_0$. It is clear, that $(\pi^{(0)}, p^{(0)}) = (1, \bar{p}^{\text{R1}}) \geq (\pi^{*,\text{R1}}, p^{*,\text{R1}})$. Suppose $(\pi^{(k)}, p^{(k)}) \geq (\pi^{*,\text{R1}}, p^{*,\text{R1}})$ for a $k \in \mathbb{N}_0$. Then,

$$(\pi^{(k+1)}, p^{(k+1)}) = \Phi^{\text{R1}}(\pi^{(k)}, p^{(k)}) \geq \Phi^{\text{R1}}(\pi^{*,\text{R1}}, p^{*,\text{R1}}) = (\pi^{*,\text{R1}}, p^{*,\text{R1}}),$$

where the inequality follows from the induction hypothesis and the fact that Φ^{R1} is order-preserving. The last equality holds because $(\pi^{*,\text{R1}}, p^{*,\text{R1}})$ is a fixed point of Φ^{R1} .

Hence,

$$(\hat{\pi}, \hat{p}) = \lim_{k \rightarrow \infty} (\pi^{(k)}, p^{(k)}) \geq (\pi^{*,\text{R1}}, p^{*,\text{R1}})$$

and since $(\hat{\pi}, \hat{p}) = \Phi^{\text{R1}}(\hat{\pi}, \hat{p})$, we obtain that $(\hat{\pi}, \hat{p}) = (\pi^{*,\text{R1}}, p^{*,\text{R1}})$. □

Corollary B.3. *It holds that $\mathcal{F} \subseteq \mathcal{D}(p^{*,\text{R1}})$.*

Proof of Corollary B.3. From Theorem B.2, $\mathcal{F} = \mathcal{D}(p^{(0)})$. Since, $(p^{(k)})_{k \in \mathbb{N}_0}$ is monotonically non-increasing, it holds that for all $k \in \mathbb{N}$

$$\mathcal{D}(p^{(k)}) = \{i \in \mathcal{N} \mid b_i + \sum_{\nu=1}^N p_{\nu i}^{(k)} < \bar{p}_i^{\text{R1}}\} \subseteq \{i \in \mathcal{N} \mid b_i + \sum_{\nu=1}^N p_{\nu i}^{(k+1)} < \bar{p}_i^{\text{R1}}\} = \mathcal{D}(p^{(k+1)}).$$

Hence, in particular $\mathcal{F} = \mathcal{D}(p^{(0)}) \subseteq \mathcal{D}(p^{*,\text{R1}})$. □

Remark B.4. The existence of a greatest and least fixed point for the second round of clearing was proved in Ghamami et al. (2022). In particular, $[0, \pi^{*,\text{R1}}] \times [0, \bar{p}^{\text{R2}}]$ is a complete lattice with respect to the component-wise ordering and Φ^{R2} is order-preserving. The greatest fixed point of Φ^{R2} therefore exists by Tarksi's fixed point theorem.

Additionally, since Φ^{R2} is also right-continuous, one can show using the same type of arguments as for Φ^{R1} , that the greatest fixed point $(\pi^{*,\text{R2}}, p^{*,\text{R2}})$ of Φ^{R2} can be obtained by setting $(\pi^{(0)}, p^{(0)}) = (\pi^{*,\text{R1}}, \bar{p}^{\text{R2}})$ and then defining recursively for $k \in \mathbb{N}_0$

$$(\pi^{(k+1)}, p^{(k+1)}) = \Phi^{\text{R2}}(\pi^{(k)}, p^{(k)}),$$

which is a non-increasing sequence that is bounded from below by $(0, 0)$ (as it was the case for Φ^{R1}). In particular, $(\pi^{*,\text{R2}}, p^{*,\text{R2}}) = \lim_{k \rightarrow \infty} \Phi^{\text{R2}}(\pi^{(k)}, p^{(k)})$, i.e., it converges to the greatest fixed point.

C Data description and network reconstruction for the case studies

Our case studies rely on data from CCP public disclosures, which we source from Clarus FT. These data provide a substantial amount of information that can be directly used to calibrate our model. For each CCP $i \in \{1, \dots, n_C\}$, we know its clearing members and we observe the total notional cleared (denoted by a_i), the default fund (δ_i), the CCP's capital (i.e., skin-in-the-game σ_i), and the aggregate initial margins ($\sum_{j=1}^{n_M} m_{ji}$). This is enough to have a well-rounded picture of CCP's waterfalls, which we illustrate in Figure 13 for the CCPs in our sample (aggregated over both IRS and CDS data). As the Figure shows, the bulk of loss absorbing resources are given by initial margins and the default fund, whereas skin-in-the-game is thin to a level that is almost imperceptible in the graphs. In addition, we also obtain, for each clearing member $i \in \{1, \dots, n_M\}$ the total notional cleared by market (denoted by l_i).

There are however some important model objects that we do not observe, most notably the network of variation margin payment obligations (\bar{p}^{R1}). Accordingly, we need to estimate it based on observable data. In the following, we describe how we estimate this network.

We start with a matrix of notional positions, $X \in [0, \infty)^{N \times N}$, where X_{ij} is the total liability from i to j arising from a derivative contract. We assume that the first n_M rows and columns correspond to the clearing members, and the last n_C rows and columns correspond to CCPs. Hence,

$$X = \left(\begin{array}{ccc|ccc} X_{1,1} & \cdots & X_{1,n_M} & X_{1,(n_M+1)} & X_{1,(n_M+2)} & \cdots & X_{1,(n_M+n_C)} \\ \cdots & \cdots & \cdots & \cdots & \cdots & \cdots & \cdots \\ X_{n_M,1} & \cdots & X_{n_M,n_M} & X_{n_M,(n_M+1)} & X_{n_M,(n_M+2)} & \cdots & X_{n_M,(n_M+n_C)} \\ \hline X_{(n_M+1),1} & \cdots & X_{(n_M+1),n_M} & X_{(n_M+1),(n_M+1)} & X_{(n_M+1),(n_M+2)} & \cdots & X_{(n_M+1),(n_M+n_C)} \\ \cdots & \cdots & \cdots & \cdots & \cdots & \cdots & \cdots \\ X_{(n_M+n_C),1} & \cdots & X_{(n_M+n_C),n_M} & X_{(n_M+n_C),(n_M+1)} & X_{(n_M+n_C),(n_M+2)} & \cdots & X_{(n_M+n_C),(n_M+n_C)} \end{array} \right)$$

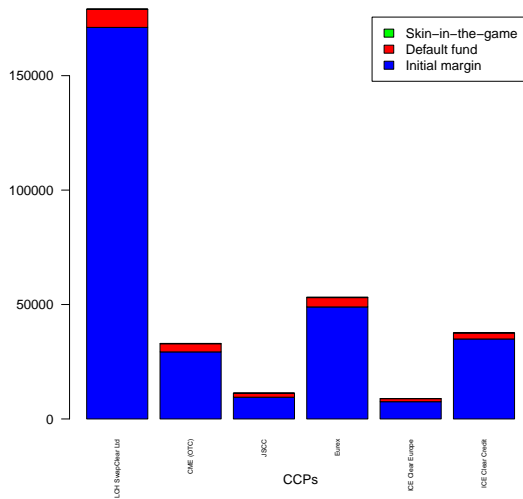
$$= \left(\begin{array}{c|c} A & B \\ \hline C & D \end{array} \right),$$

where $A \in [0, \infty)^{n_M \times n_M}$, $B \in [0, \infty)^{n_M \times n_C}$, $C \in [0, \infty)^{n_C \times n_M}$, $D \in [0, \infty)^{n_C \times n_C}$.

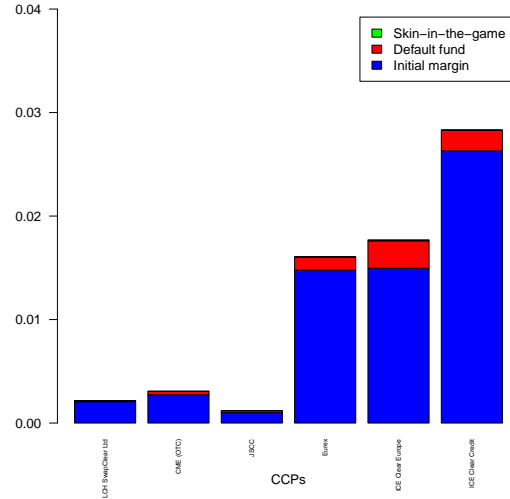
In our empirical analyses we assume that clearing members do not trade bilaterally. This implies that the upper left $n_M \times n_M$ -dimensional submatrix A is the zero matrix. Similarly, since the CCPs do not have any trading relationships with other CCPs, the lower right $n_C \times n_C$ -dimensional submatrix D is also the zero matrix. Hence, we need to estimate the following two submatrices

$$B = \begin{pmatrix} X_{1,(n_M+1)} & \cdots & X_{1,(n_M+n_C)} \\ \cdots & \cdots & \cdots \\ X_{n_M,(n_M+1)} & \cdots & X_{n_M,(n_M+n_C)} \end{pmatrix},$$

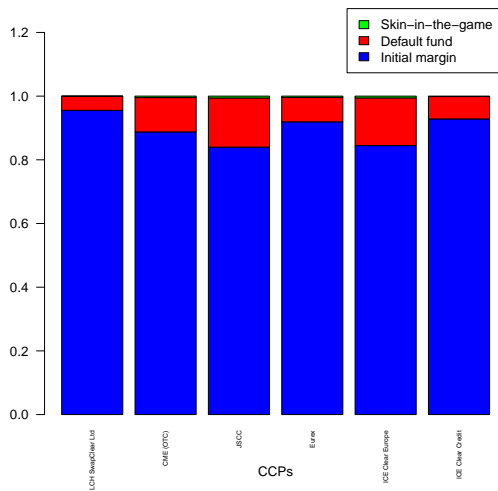
$$C = \begin{pmatrix} X_{(n_M+1),1} & \cdots & X_{(n_M+1),n_M} \\ \cdots & \cdots & \cdots \\ X_{(n_M+n_C),1} & \cdots & X_{(n_M+n_C),n_M} \end{pmatrix}.$$



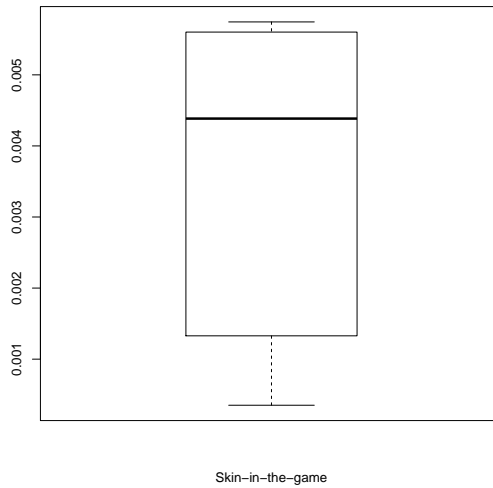
(a) Default waterfall for each CCP (in million USD).



(b) Default waterfall normalised by total exposure cleared for each CCP.



(c) Default waterfall normalised by total size of the default waterfall for each CCP.



(d) Boxplot of Skin-in-the-game normalised by total size of the default waterfall for each CCP.

Figure 13: Default waterfall for the six CCPs (original (top left), normalised by total exposure (top right) and by size of the default waterfall (bottom left)), and boxplot of the normalised skin-in-the game (bottom right).

Since positions at CCPs are netted, we assume that there are no index pairs $i, j \in \mathcal{N}$ such that both $X_{ij} > 0$ and $X_{ji} > 0$ for $i, j \in \mathcal{N}$. This implies, that there are no index pairs for which both $B_{ij} > 0$ and $C_{ji} > 0$, where $i \in \{1, \dots, n_M\}$ and $j \in \{1, \dots, n_C\}$.

Hence, we can estimate the two matrices B, C simultaneously, by estimating the matrix $Y \in \mathbb{R}^{n_M \times n_C}$, where $Y = B - C^\top$. In particular, Y can take positive and negative entries. Fix $i \in \{1, \dots, n_M\}$ and $j \in \{1, \dots, n_C\}$. First, if $Y_{i,j} \geq 0$, we set $B_{ij} = X_{i,(n_M+j)} = Y_{i,j}$ which means that clearing member i has an obligation to CCP j and we set $C_{j,i} = X_{(n_M+j),i} = 0$ (i.e., no obligation from CCP j to clearing member i). Second, if $Y_{i,j} < 0$, then we set $B_{ij} = X_{i,(n_M+j)} = 0$, i.e., clearing member i does not have any obligations to CCP j , and we set $C_{j,i} = X_{(n_M+j),i} = |Y_{i,j}|$, i.e., the CCP j has an obligation to clearing member i .

We have the following information about Y . From public disclosures, we know the clearing members of each CCP. This means that we know the adjacency matrix that corresponds to Y , which we denote by $A^{\text{observed}} \in \{0, 1\}^{n_M \times n_C}$. In particular,

$$A_{ij}^{\text{observed}} = \begin{cases} 1, & \text{if } i \text{ is a clearing member of } j, \\ 0, & \text{else.} \end{cases}$$

Furthermore, as mentioned above, for each clearing member $i \in \{1, \dots, n_M\}$ we know the total notional amount that it clears (l_i). In turn, for each CCP $j \in \{1, \dots, n_C\}$ we know the total notional that it clears, denoted by a_j . Moreover, we also know that each CCP has a matched book, as that is the essence of their business model. These considerations together give rise to the following mathematical constraints on matrix Y :

$$\begin{aligned} \sum_{j=1}^{n_C} |Y_{ij} A_{ij}^{\text{observed}}| &= l_i \quad \forall i \in \{1, \dots, n_M\} \quad (\text{total notional cleared by clearing member}) \\ \sum_{i=1}^{n_M} |Y_{ij} A_{ij}^{\text{observed}}| &= a_j \quad \forall j \in \{1, \dots, n_C\} \quad (\text{total notional cleared by CCP}) \\ \sum_{i=1}^{n_M} Y_{ij} A_{ij}^{\text{observed}} &= 0 \quad \forall j \in \{1, \dots, n_C\} \quad (\text{matched book of CCP}). \end{aligned} \tag{12}$$

Given these additional constraints, we cannot use standard methods available to reconstruct financial networks from observed row and column sums, see e.g. Gandy & Veraart (2017) and the references therein.

To obtain a matrix Y , we solve an optimisation problem that penalises deviations from the constraints formulated in (12). We consider the following objective function $f : \mathbb{R}^{n_M \times n_C} \rightarrow \mathbb{R}$, where

$$f(y) = \sum_{i=1}^{n_M} \left(l_i - \sum_{j=1}^{n_C} |Y_{ij} A_{ij}^{\text{observed}}| \right)^2 + \sum_{j=1}^{n_C} \left(a_j - \sum_{i=1}^{n_M} |Y_{ij} A_{ij}^{\text{observed}}| \right)^2 + P \sum_{j=1}^{n_C} \left(\sum_{i=1}^{n_M} Y_{ij} A_{ij}^{\text{observed}} \right)^2,$$

where $P > 0$ is a constant that we include to put an additional penalty weight on the term that captures how well the CCPs' books are matched. Then, we consider the following optimisation problem

$$\begin{aligned} &\min_{Y \in \mathbb{R}^{n_M \times n_C}} f(Y) \\ &\text{subject to } \text{Adj}(Y) = A^{\text{observed}}, \end{aligned}$$

where $\text{Adj}(Y)_{ij} = 1$ if $Y_{ij} > 0$ and 0 otherwise, hence it computes the adjacency matrix that corresponds to Y .²⁶

²⁶In fact, we only need to find those Y_{ij} for which $A_{ij}^{\text{observed}} = 1$. Hence, the number of unknown parameters can be reduced from $n_M \cdot n_C$ to $\sum_{i=1}^{n_M} \sum_{j=1}^{n_C} A_{ij}^{(Y)}$.

When solving this optimisation problem for our data for the IRS and CDS markets, we obtain in both cases matrices in which CCPs have indeed matched books and the deviations from the observed row and columns sums are very small. After having obtained the matrix Y , we can use it to compute the matrix X of notional positions as described before. Figures 14 and 15 show the reconstructed matrix of IRS notional amounts and of CDS notional amounts, respectively.

Finally, we then assume that the variation margin payments due from derivative positions are proportional to the original estimated position, i.e., if the derivative position is X_{ij} then we set $\bar{p}_{ij}^{R1} = \nu X_{ij}$ for some constant $\nu \geq 0$.

The final quantities we need are the liquidity buffers of the clearing members, i.e., b_i , where $i \in \mathcal{M}$. Since we do not have this information, we simulate numbers such that pre-shock (i.e., before setting some liquidity buffers to 0) there are no fundamental defaults.

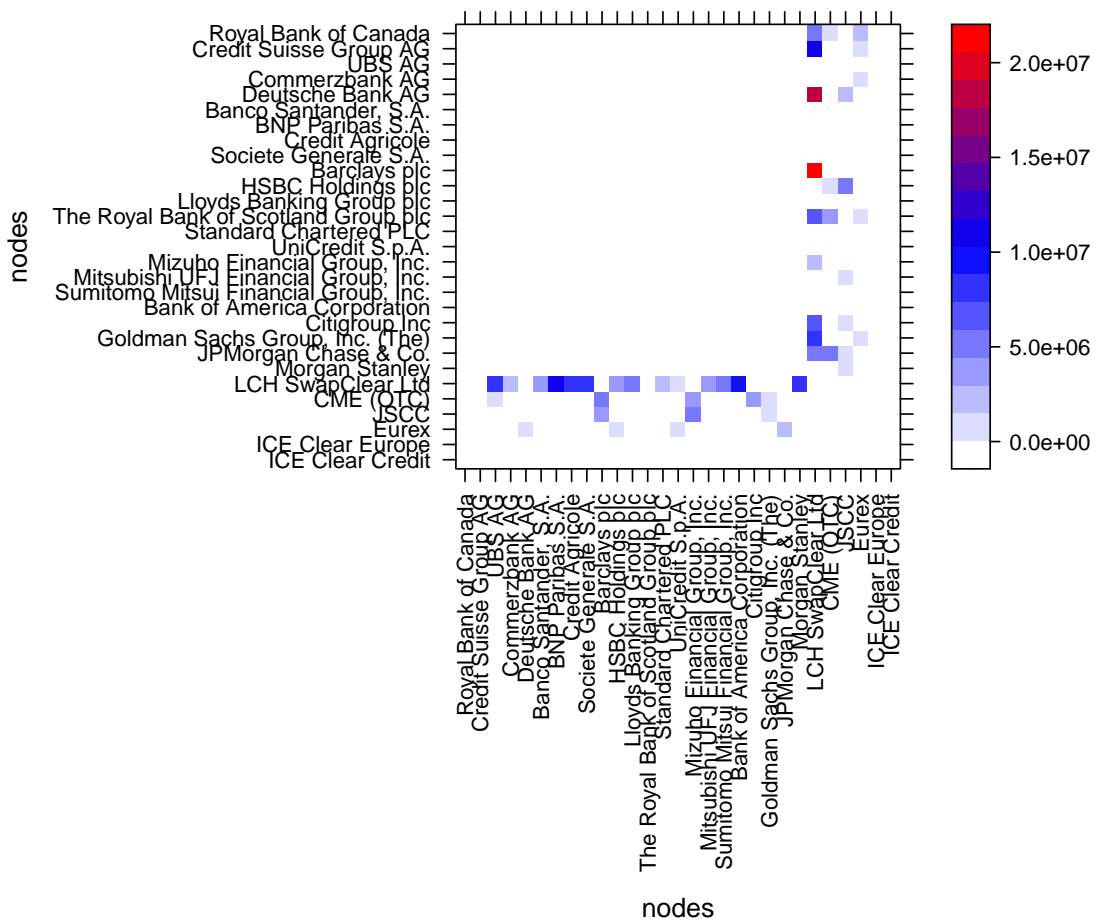


Figure 14: Reconstructed network of derivative positions for Interest Rate Swaps (in million USD).

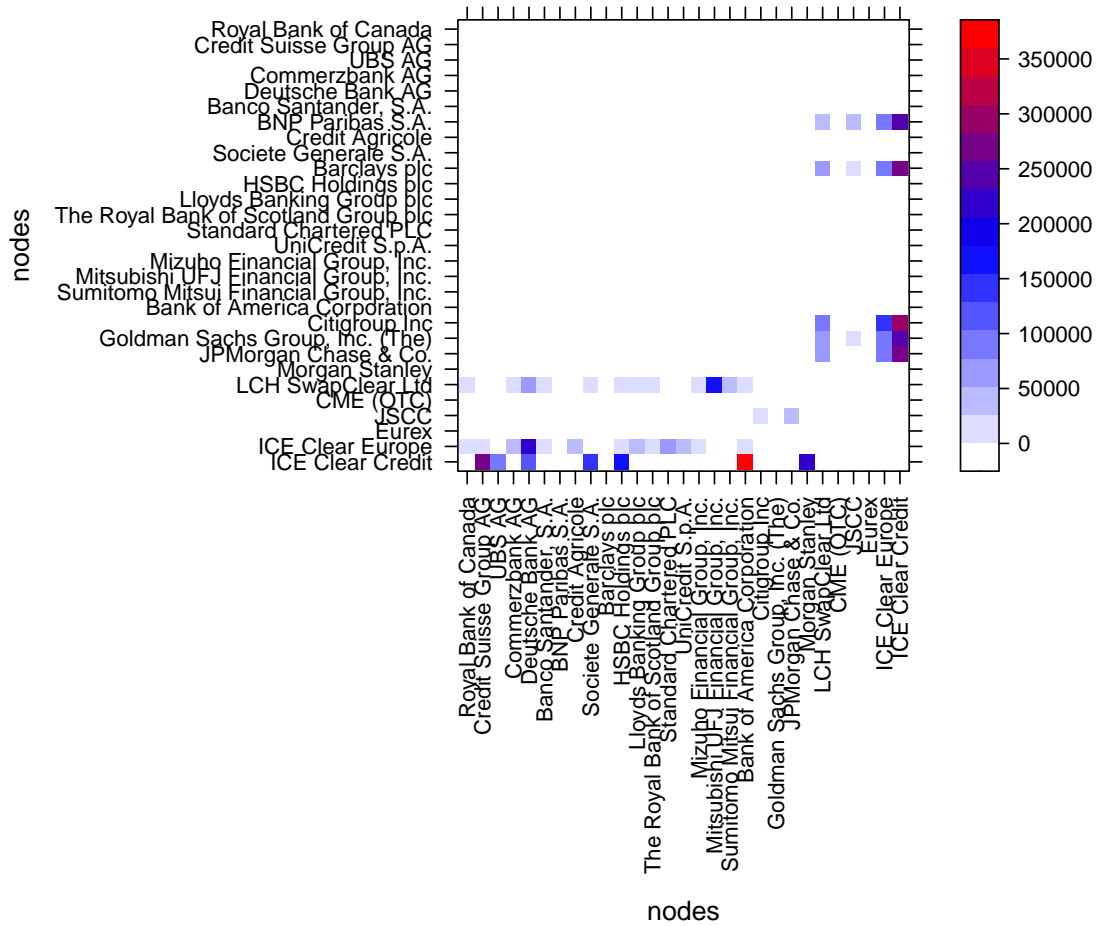


Figure 15: Reconstructed network of derivative positions for Credit Default Swaps (in million USD).

D Clearing with pecking order

In this appendix we develop a clearing mechanism in which clearing members that default do not pay the CCPs pro-rata (as assumed in our benchmark model) but according to a pecking order, and compare the results. We use ideas developed in Elsinger (2011) for clearing in networks with different seniorities of debt. We characterise the pecking order in terms of a matrix $\Omega \in \{0, 1, \dots, n_C\}^{n_M \times n_C}$, where Ω_{ij} represents the rank of CCP j in clearing member i 's pecking order. If $\Omega_{ij} = 1$, this means that CCP j is paid first by clearing member i , and payments to other CCPs are only made if assets are left after the payments to j are made. If $\Omega_{ij} = 0$, then this means that clearing member i does not have any payment obligations to CCP j . In the following we assume that each clearing member has a strict ranking of CCPs to which it makes payments, so no two CCPs are considered of equal seniority in a clearing member's pecking order.²⁷

Our mathematical model does not depend on which criteria are used by the clearing members to decide on their pecking order. For our case studies, we assume that the pecking order is obtained by considering the size of the payment obligations, i.e., a clearing member ranks the CCP to which it has the highest payment obligations first in the pecking order and then pays other CCPs according to decreasing nominal amounts of payments due. As before, we assume that CCPs still pay their clearing members pro rata and not according to a pecking order.

D.1 First round of clearing with pecking order

In the following, we assume that $\bar{p}_i^{\text{R1}} > 0$ for all $i \in \mathcal{C}$, i.e., all CCPs have strictly positive payment obligations. Since CCPs have matched books, this means that we do not have redundant CCPs in the model. To simplify notation, we assume that $\mathcal{M} = \{1, \dots, n_M\}$ and $\mathcal{C} = \{n_M + 1, \dots, n_M + n_C\}$, i.e., the first n_M indices correspond to the clearing members and the remaining indices to the CCPs.

We can characterise a price-payment equilibrium as a suitable fixed point. We consider a function $\Phi^{\text{R1, pecking}} : [0, 1] \times [0, \bar{p}^{\text{R1}}] \rightarrow [0, 1] \times [0, \bar{p}^{\text{R1}}]$, and are interested in a fixed point $(\pi^{\star, \text{R1, pecking}}, p^{\star, \text{R1, pecking}})$ such that

$$(\pi^{\star, \text{R1, pecking}}, p^{\star, \text{R1, pecking}}) = \Phi^{\text{R1, pecking}}(\pi^{\star, \text{R1, pecking}}, p^{\star, \text{R1, pecking}}),$$

where $\Phi^{\text{R1, pecking}}$ is defined as follows.

$$\Phi_1^{\text{R1}}(\pi, p) = \exp(-\alpha \Delta(\pi, p)),$$

$$\Phi_{2, (ij)}^{\text{R1, pecking}}(p) = \begin{cases} \min \left\{ \bar{p}_{ij}^{\text{R1}}, \frac{\bar{p}_{ij}^{\text{R1}}}{\sum_{k=1}^N \bar{p}_{ik}^{\text{R1}}} \left(\gamma_i^{(1)} b_i + \gamma_i^{(2)} \sum_{k=1}^N p_{ki} \right) \right\}, & \text{if } i \in \mathcal{C} \cap \mathcal{D}(p), \\ \min \left\{ \bar{p}_{ij}^{\text{R1}}, \pi m_{ij} + \left(\gamma_i^{(1)} b_i + \gamma_i^{(2)} \sum_{k=1}^N p_{ki} - W_{ij}(\pi) \right)^+ \right\}, & \text{if } i \in \mathcal{M} \cap \mathcal{D}(p), \\ \bar{p}_{ij}^{\text{R1}}, & \text{if } i \in \mathcal{N} \setminus \mathcal{D}(p), \end{cases} \quad (13)$$

where as before $\mathcal{D}(p) = \{i \in \mathcal{N} \mid A_i(p) < \bar{p}_i^{\text{R1}}\}$, specifies the nodes in default in a system with payments $p \in [0, \bar{p}^{\text{R1}}]$, and again $A_i(p) = b_i + \sum_{k=1}^N p_{ki}$ denotes the available assets of node $i \in \mathcal{N}$.

Furthermore,

$$W_{ij}(\pi) = \sum_{k=1}^{n_C} (\bar{p}_{i, n_M+k}^{\text{R1}} - \pi m_{i, n_M+k})^+ \mathbb{I}_{\{\Omega_{ik} < \Omega_{ij}\}},$$

²⁷Our model is related to that of Elsinger (2011), who adapt the Eisenberg & Noe (2001) framework to a setting with different seniorities of debt. In contrast to Elsinger (2011), our framework includes (possibly illiquid) collateral and bankruptcy costs and is therefore more general. We have formulated our model for a strict pecking order, but this assumption can be relaxed and one can consider a situation in which more than one CCP can have the same rank in the pecking order. This would lead to a slightly different definition of $\Phi^{\text{R1, pecking}}$.

i.e., $W_{ij}(\pi)$ are the payment obligations (that remain after seizing the initial margins for these position at a current price of $\pi \in [0, 1]$ per share) of clearing member i to the CCPs that are before CCP j in the pecking order. Again $\Delta(\pi, p)$ models the total amount of collateral sold in Round 1 and it is defined exactly as in Section 2.

When comparing $\Phi^{\text{R1, pecking}}$ in (13) to Φ^{R1} in (1), the only difference is for $i \in \mathcal{M} \cap \mathcal{D}(p)$, i.e., for defaulting clearing members. In (1) defaulting clearing members paid the CCPs pro rata, i.e., they distributed their available assets according to the proportions $a_{ij}^{\text{R1}}(\pi) = \frac{\max\{0, \bar{p}_{ij}^{\text{R1}} - \pi m_{ij}\}}{\sum_{k=1}^N \max\{0, \bar{p}_{ik}^{\text{R1}} - \pi m_{ik}\}}$. When there is a pecking order, this is no longer the case. A defaulting clearing member first uses all its assets to pay the CCP ranked first, then uses the remaining assets to pay the CCP ranked second, and so on. This is captured by the second branch of $\Phi^{\text{R1, pecking}}$ in (13). The term $(\gamma_i^{(1)} b_i + \gamma_i^{(2)} \sum_{k=1}^N p_{ki} - W_{ij}(\pi))^+$ captures the resources that clearing member i can use to pay the CCP j with pecking order rank Ω_{ij} on top of the initial margins.

Lemma D.1 (Properties of $\Phi^{\text{R1, pecking}}$). *Let $\Phi^{\text{R1, pecking}} : [0, 1] \times [0, \bar{p}^{\text{R1}}] \rightarrow [0, 1] \times [0, \bar{p}^{\text{R1}}]$ be the function defined in (13), then $\Phi^{\text{R1, pecking}}$ is order-preserving.*

Proof of Lemma D.1. Let $\tilde{\pi}, \pi \in [0, 1]$ with $\tilde{\pi} \leq \pi$ and let $\tilde{p}, p \in [0, \bar{p}^{\text{R1}}]$ with $\tilde{p}_{ij} \leq p_{ij}$ for all $i, j \in \mathcal{N}$.

Since $\Phi_1^{\text{R1, pecking}}$ is identical to Φ_1^{R1} , we know from the proof of Theorem B.2 that $\Phi_1^{\text{R1, pecking}}$ is order-preserving.

Next, we show that $\Phi_2^{\text{R1, pecking}}$ is order-preserving. Based on the same arguments as in the proof of Theorem B.2, it holds that

$$\mathcal{D}(p) \subseteq \mathcal{D}(\tilde{p}). \quad (14)$$

Next, we show that Φ_2^{R1} is order-preserving. Let $i, j \in \mathcal{N}$. We distinguish between three cases.

Case 1: Let $i \in \mathcal{N} \setminus \mathcal{D}(p)$. Then,

$$\Phi_{2,(ij)}^{\text{R1, pecking}}(\pi, p) = \bar{p}_{ij}^{\text{R1}} \geq \Phi_{2,(ij)}^{\text{R1, pecking}}(\tilde{\pi}, \tilde{p}).$$

Case 2: Let $i \in \mathcal{C} \cap \mathcal{D}(p)$. Then, $i \in \mathcal{C} \cap \mathcal{D}(\tilde{p})$. Then,

$$\begin{aligned} \Phi_{2,(ij)}^{\text{R1, pecking}}(\tilde{\pi}, \tilde{p}) &= \min \left\{ \bar{p}_{ij}^{\text{R1}}, \frac{\bar{p}_{ij}^{\text{R1}}}{\sum_{k=1}^N \bar{p}_{ik}^{\text{R1}}} \left(\gamma_i^{(1)} b_i + \gamma_i^{(2)} \sum_{k=1}^N \tilde{p}_{ki} \right) \right\}, \\ \Phi_{2,(ij)}^{\text{R1, pecking}}(\pi, p) &= \min \left\{ \bar{p}_{ij}^{\text{R1}}, \frac{\bar{p}_{ij}^{\text{R1}}}{\sum_{k=1}^N \bar{p}_{ik}^{\text{R1}}} \left(\gamma_i^{(1)} b_i + \gamma_i^{(2)} \sum_{k=1}^N p_{ki} \right) \right\}. \end{aligned}$$

We distinguish between two cases. First, let $\Phi_{2,(ij)}^{\text{R1, pecking}}(\pi, p) = \bar{p}_{ij}^{\text{R1}}$, then

$$\Phi_{2,(ij)}^{\text{R1}}(\pi, p) = \bar{p}_{ij}^{\text{R1}} \geq \Phi_{2,(ij)}^{\text{R1, pecking}}(\tilde{\pi}, \tilde{p}).$$

Second, let

$$\bar{p}_{ij}^{\text{R1}} > \Phi_{2,(ij)}^{\text{R1, pecking}}(\pi, p). \quad (15)$$

Then,

$$\begin{aligned} \bar{p}_{ij}^{\text{R1}} > \Phi_{2,(ij)}^{\text{R1, pecking}}(\pi, p) &= \frac{\bar{p}_{ij}^{\text{R1}}}{\sum_{k=1}^N \bar{p}_{ik}^{\text{R1}}} \left(\gamma_i^{(1)} b_i + \gamma_i^{(2)} \sum_{k=1}^N p_{ki} \right) \geq \frac{\bar{p}_{ij}^{\text{R1}}}{\sum_{k=1}^N \bar{p}_{ik}^{\text{R1}}} \left(\gamma_i^{(1)} b_i + \gamma_i^{(2)} \sum_{k=1}^N \tilde{p}_{ki} \right) \\ &= \Phi_{2,(ij)}^{\text{R1, pecking}}(\tilde{\pi}, \tilde{p}), \end{aligned}$$

where the last equality follows from assumption (15).

Case 3: Let $i \in \mathcal{M} \cap \mathcal{D}(p)$. Then, $i \in \mathcal{M} \cap \mathcal{D}(\tilde{p})$. Then,

$$\begin{aligned}\Phi_{2,(ij)}^{\text{R1, pecking}}(\tilde{\pi}, \tilde{p}) &= \min \left\{ \bar{p}_{ij}^{\text{R1}}, \tilde{\pi} m_{ij} + \left(\gamma_i^{(1)} b_i + \gamma_i^{(2)} \sum_{k=1}^N \tilde{p}_{ki} - W_{ij}(\tilde{\pi}) \right)^+ \right\}, \\ \Phi_{2,(ij)}^{\text{R1, pecking}}(\pi, p) &= \min \left\{ \bar{p}_{ij}^{\text{R1}}, \pi m_{ij} + \left(\gamma_i^{(1)} b_i + \gamma_i^{(2)} \sum_{k=1}^N p_{ki} - W_{ij}(\pi) \right)^+ \right\}.\end{aligned}$$

Again, we distinguish between two cases. First, let $\Phi_{2,(ij)}^{\text{R1, pecking}}(\pi, p) = \bar{p}_{ij}^{\text{R1}}$, then

$$\Phi_{2,(ij)}^{\text{R1}}(\pi, p) = \bar{p}_{ij}^{\text{R1}} \geq \Phi_{2,(ij)}^{\text{R1, pecking}}(\tilde{\pi}, \tilde{p}).$$

Second, let

$$\bar{p}_{ij}^{\text{R1}} > \Phi_{2,(ij)}^{\text{R1, pecking}}(\pi, p). \quad (16)$$

It follows directly from the definition of W_{ij} , that $W_{ij}(\pi) \leq W_{ij}(\tilde{\pi})$ and hence $-W_{ij}(\pi) \geq -W_{ij}(\tilde{\pi})$. Hence,

$$\begin{aligned}\bar{p}_{ij}^{\text{R1}} > \Phi_{2,(ij)}^{\text{R1, pecking}}(\pi, p) &= \min \left\{ \bar{p}_{ij}^{\text{R1}}, \pi m_{ij} + \left(\gamma_i^{(1)} b_i + \gamma_i^{(2)} \sum_{k=1}^N p_{ki} - W_{ij}(\pi) \right)^+ \right\} \\ &\geq \min \left\{ \bar{p}_{ij}^{\text{R1}}, \tilde{\pi} m_{ij} + \left(\gamma_i^{(1)} b_i + \gamma_i^{(2)} \sum_{k=1}^N \tilde{p}_{ki} - W_{ij}(\tilde{\pi}) \right)^+ \right\} \\ &= \Phi_{2,(ij)}^{\text{R1, pecking}}(\tilde{\pi}, \tilde{p}),\end{aligned}$$

where the last equality follows from assumption (16). Hence, indeed $\Phi^{\text{R1, pecking}}$ is order-preserving. \square

Theorem D.2 (Existence of a least and greatest price-payment equilibrium in Round 1 in the setting with a pecking order). *Let $\Phi^{\text{R1, pecking}} : [0, 1] \times [0, \bar{p}^{\text{R1}}] \rightarrow [0, 1] \times [0, \bar{p}^{\text{R1}}]$ be the function defined in (13).*

1. *The set of fixed points of $\Phi^{\text{R1, pecking}}$ is a complete lattice. In particular $\Phi^{\text{R1, pecking}}$ admits a greatest and a least fixed point.*
2. *Let $(\pi^{(0)}, p^{(0)}) = (1, \bar{p}^{\text{R1}})$ and define recursively for $k \in \mathbb{N}_0$*

$$(\pi^{(k+1)}, p^{(k+1)}) = \Phi^{\text{R1, pecking}}(\pi^{(k)}, p^{(k)}).$$

Then,

- (a) *$(\pi^{(k)}, p^{(k)})_{k \in \mathbb{N}_0}$ is a monotonically non-increasing sequence, that is, $\pi^{(k+1)} \leq \pi^{(k)}$ and $p_{ij}^{(k+1)} \leq p_{ij}^{(k)}$ for all $i, j \in \mathcal{N}$ and for all $k \in \mathbb{N}_0$.*
- (b) *The limit $\lim_{k \rightarrow \infty} (\pi^{(k)}, p^{(k)})$ exists and is the greatest fixed point of $\Phi^{\text{R1, pecking}}$.*

Proof of Theorem D.2. 1. We will prove the statement using Tarski's fixed point theorem (Tarski, 1955). First, $[0, 1] \times [0, \bar{p}^{\text{R1}}]$ is a complete lattice with respect to the component-wise ordering. Second, it follows directly from the definition of $\Phi^{\text{R1, pecking}}$ in (1) that indeed $\Phi^{\text{R1, pecking}} : [0, 1] \times [0, \bar{p}^{\text{R1}}] \rightarrow [0, 1] \times [0, \bar{p}^{\text{R1}}]$. Third, $\Phi^{\text{R1, pecking}}$ is an order-preserving function by Lemma D.1. By Tarski's fixed point theorem, the set of fixed points of $\Phi^{\text{R1, pecking}}$ is a complete lattice and hence a least and greatest fixed point exist.

2. This statement can be proved along the lines of the proof of Theorem B.2. We provide the details below.

(a) We prove that $\pi^{(k+1)} \leq \pi^{(k)}$ and $p_{ij}^{(k+1)} \leq p_{ij}^{(k)}$ for all $i, j \in \mathcal{N}$ and for all $k \in \mathbb{N}_0$ by induction.

For $k = 0$, it follows directly from the definition of $\Phi^{\text{R1, pecking}}$ in (13) that

$$\pi^{(1)} = \Phi_1^{\text{R1, pecking}}(\pi^{(0)}, p^{(0)}) = \exp(-\alpha \Delta(\pi^{(0)}, p^{(0)})) \leq 1 = \pi^{(0)} \text{ and}$$

$$p_{ij}^{(1)} = \Phi_{2,(ij)}^{\text{R1, pecking}}(\pi^{(0)}, p^{(0)}) \leq \bar{p}_{ij}^{\text{R1}} = p_{ij}^{(0)} \text{ for all } i, j \in \mathcal{N}.$$

Our induction hypothesis is that $\pi^{(k+1)} \leq \pi^{(k)}$ and $p_{ij}^{(k+1)} \leq p_{ij}^{(k)}$ for all $i, j \in \mathcal{N}$ and for a $k \in \mathbb{N}_0$.

Then, by the definition of the sequence

$$(\pi^{(k+2)}, p^{(k+2)}) = \Phi^{\text{R1, pecking}}(\pi^{(k+1)}, p^{(k+1)}) \leq \Phi^{\text{R1, pecking}}(\pi^{(k)}, p^{(k)}) = (\pi^{(k+1)}, p^{(k+1)}),$$

where the inequality follows from the induction hypothesis and the fact that $\Phi^{\text{R1, pecking}}$ is order-preserving by Lemma D.1. Hence, this completes the induction step.

It follows directly from the definition of $\Phi^{\text{R1, pecking}}$ that it is bounded from below by $(0, 0)$ (where the first 0 is 1-dimensional and the second zero is the $N \times N$ zero matrix). Hence, there exists a monotone limit $(\hat{\pi}, \hat{p}) = \lim_{k \rightarrow \infty} (\pi^{(k)}, p^{(k)})$. This limit is a fixed point of $\Phi^{\text{R1, pecking}}$, since

$$\begin{aligned} \Phi^{\text{R1, pecking}}(\hat{\pi}, \hat{p}) &= \Phi^{\text{R1, pecking}}\left(\lim_{k \rightarrow \infty} (\pi^{(k)}, p^{(k)})\right) = \lim_{k \rightarrow \infty} \Phi^{\text{R1, pecking}}(\pi^{(k)}, p^{(k)}) \\ &= \lim_{k \rightarrow \infty} (\pi^{(k+1)}, p^{(k+1)}) = (\hat{\pi}, \hat{p}), \end{aligned}$$

where the second equality follows from the right-continuity of $\Phi^{\text{R1, pecking}}$. It remains to show that $(\hat{\pi}, \hat{p}) = (\pi^{\star, \text{R1, pecking}}, p^{\star, \text{R1, pecking}})$, i.e., that it is the greatest fixed point of $\Phi^{\text{R1, pecking}}$.

We show by induction that $(\pi^{(k)}, p^{(k)}) \geq (\pi^{\star, \text{R1, pecking}}, p^{\star, \text{R1, pecking}})$ for all $k \in \mathbb{N}_0$. It is clear, that $(\pi^{(0)}, p^{(0)}) = (1, \bar{p}^{\text{R1}}) \geq (\pi^{\star, \text{R1, pecking}}, p^{\star, \text{R1, pecking}})$. Suppose $(\pi^{(k)}, p^{(k)}) \geq (\pi^{\star, \text{R1, pecking}}, p^{\star, \text{R1, pecking}})$ for a $k \in \mathbb{N}_0$. Then,

$$\begin{aligned} (\pi^{(k+1)}, p^{(k+1)}) &= \Phi^{\text{R1, pecking}}(\pi^{(k)}, p^{(k)}) \\ &\geq \Phi^{\text{R1, pecking}}(\pi^{\star, \text{R1, pecking}}, p^{\star, \text{R1, pecking}}) = (\pi^{\star, \text{R1, pecking}}, p^{\star, \text{R1, pecking}}), \end{aligned}$$

where the inequality follows from the induction hypothesis and the fact that $\Phi^{\text{R1, pecking}}$ is order-preserving. The last equality holds because $(\pi^{\star, \text{R1, pecking}}, p^{\star, \text{R1, pecking}})$ is a fixed point of $\Phi^{\text{R1, pecking}}$. Hence,

$$(\hat{\pi}, \hat{p}) = \lim_{k \rightarrow \infty} (\pi^{(k)}, p^{(k)}) \geq (\pi^{\star, \text{R1, pecking}}, p^{\star, \text{R1, pecking}})$$

and since $(\hat{\pi}, \hat{p}) = \Phi^{\text{R1, pecking}}(\hat{\pi}, \hat{p})$, we obtain $(\hat{\pi}, \hat{p}) = (\pi^{\star, \text{R1, pecking}}, p^{\star, \text{R1, pecking}})$.

□

D.2 Second round of clearing with pecking order

We now adapt the second round of clearing by Ghamami et al. (2022) to the pecking order setting. Let $(\pi^{*,R1, \text{pecking}}, p^{*,R1, \text{pecking}}) \in [0, 1] \times [0, \bar{p}^{R1}]$ be the greatest fixed point of $\Phi^{R1, \text{pecking}}$.

Again, the payments outstanding at the start of the second round are given by $\bar{p}^{R2, \text{pecking}} = \bar{p}^{R1} - p^{*,R1, \text{pecking}} \in [0, \bar{p}^{R1}]$. Consider the function $\Phi^{R2, \text{pecking}} : [0, \pi^{*,R1, \text{pecking}}] \times [0, \bar{p}^{R2}] \rightarrow [0, \pi^{*,R1, \text{pecking}}] \times [0, \bar{p}^{R2}]$. Our aim is to determine a fixed point of this function, i.e., we want to find $(\pi^{*,R2, \text{pecking}}, p^{*,R2, \text{pecking}})$ such that

$$(\pi^{*,R2, \text{pecking}}, p^{*,R2, \text{pecking}}) = \Phi^{R2, \text{pecking}}(\pi^{*,R2, \text{pecking}}, p^{*,R2, \text{pecking}}),$$

where $\Phi^{R2, \text{pecking}}(\pi, p)$ is defined as follows:

$$\begin{aligned} \Phi_1^{R2, \text{pecking}}(\pi, p) &= \pi^{*,R1, \text{pecking}} \exp(-\alpha \Gamma(\pi, p)), \\ \Phi_{2,(ij)}^{R2, \text{pecking}}(\pi, p) &= \begin{cases} \min \left\{ \bar{p}_{ij}^{R2}, \frac{\bar{p}_{ij}^{R2}}{\sum_{k=1}^N \bar{p}_{ik}^{R2}} \sum_{k=1}^N p_{ki} \right\}, & \text{if } i \in \mathcal{C}, \\ \min \left\{ \bar{p}_{ij}^{R2}, \left(\pi r_i(\pi^{*,\text{Round 1}}, p^{*,\text{Round 1}}) + \sum_{k=1}^N p_{ki} - \tilde{W}_{ij} \right)^+ \right\}, & \text{if } i \in \mathcal{M}, \end{cases} \end{aligned} \quad (17)$$

where

$$\tilde{W}_{ij} = \sum_{k=1}^{n_C} \bar{p}_{i, n_M+k}^{R2} \mathbb{I}_{\{\Omega_{ik} < \Omega_{ij}\}}$$

are the payment obligations of member i to CCPs that come before CCP j in the pecking order.

As before, $\Gamma(\pi, p)$ denotes the total shares of collateral sold in the second round, i.e.,

$$\Gamma(\pi, p) = \sum_{i=1}^N \Gamma_i(\pi, p),$$

where the total share of collateral sold by node $i \in \mathcal{N}$ is given by

$$\Gamma_i(\pi, p) = \min \left\{ r_i(\pi^{*,R1, \text{pecking}}, p^{*,R1, \text{pecking}}), \frac{1}{\pi} \max \left\{ 0, \sum_{j=1}^N \bar{p}_{ij}^{R2, \text{pecking}} - \sum_{j=1}^N p_{ji} \right\} \right\},$$

if $\pi > 0$. For $\pi = 0$, we set

$$\Gamma_i(\pi, p) = \begin{cases} r_i(\pi^{*,R1, \text{pecking}}, p^{*,R1, \text{pecking}}), & \text{if } i \in \mathcal{D}(p^{*,R1, \text{pecking}}) \text{ and } \max \left\{ 0, \sum_{j=1}^N \bar{p}_{ij}^{R2, \text{pecking}} - \sum_{j=1}^N p_{ji} \right\} > 0, \\ 0, & \text{otherwise.} \end{cases}$$

Furthermore, $r_i(\pi^{*,R1, \text{pecking}}, p^{*,R1, \text{pecking}})$ is the collateral returned to node $i \in \mathcal{N}$ and is defined as

$$r_i(\pi^{*,R1, \text{pecking}}, p^{*,R1, \text{pecking}}) = \begin{cases} \sum_{j=1}^N (m_{ij} - \Delta_{ij}(\pi^{*,R1, \text{pecking}}, p^{*,R1, \text{pecking}})), & \text{if } i \in \mathcal{D}(p^{*,R1, \text{pecking}}), \\ \sum_{j \in \mathcal{D}(p^{*,R1, \text{pecking}})} m_{ij}, & \text{if } i \in \mathcal{N} \setminus \mathcal{D}(p^{*,R1, \text{pecking}}). \end{cases}$$

In our setting, the market consists of clearing members and CCPs. Since we assume that CCPs do not post initial margins to their clearing members, only clearing members can have collateral returned to them in Round 2. In particular, $r_i(\pi^{*,R1, \text{pecking}}, p^{*,R1, \text{pecking}}) = 0$ for all $i \in \mathcal{C}$.

Lemma D.3 (Properties of $\Phi^{R2, \text{pecking}}$). *Let $\Phi^{R2, \text{pecking}} : [0, \pi^{*,R1, \text{pecking}}] \times [0, \bar{p}^{R2, \text{pecking}}] \rightarrow [0, \pi^{*,R1, \text{pecking}}] \times [0, \bar{p}^{R2, \text{pecking}}]$ be the function defined in (17), then $\Phi^{R2, \text{pecking}}$ is order-preserving.*

Proof of Lemma D.3. Let $\tilde{\pi}, \pi \in [0, \pi^{*,R1, \text{pecking}}]$ with $\tilde{\pi} \leq \pi$ and let $\tilde{p}, p \in [0, \bar{p}^{R2, \text{pecking}}]$ with $\tilde{p}_{ij} \leq p_{ij}$ for all $i, j \in \mathcal{N}$.

We first show that $\Phi_1^{R2, \text{pecking}}$ is order-preserving. To see that for all $i \in \mathcal{N}$ it holds that $\Gamma_i(\pi, p) \leq \Gamma_i(\tilde{\pi}, \tilde{p})$, we consider three cases.

Case 1: Let $\tilde{\pi} > 0$. Then, $0 < \tilde{\pi} \leq \pi$ and therefore

$$\begin{aligned} \Gamma_i(\pi, p) &= \min \left\{ r_i(\pi^{*,R1, \text{pecking}}, p^{*,R1, \text{pecking}}), \frac{1}{\pi} \max \left\{ 0, \sum_{j=1}^N \bar{p}_{ij}^{R2, \text{pecking}} - \sum_{j=1}^N p_{ji} \right\} \right\} \\ &\leq \min \left\{ r_i(\pi^{*,R1, \text{pecking}}, p^{*,R1, \text{pecking}}), \frac{1}{\pi} \max \left\{ 0, \sum_{j=1}^N \bar{p}_{ij}^{R2, \text{pecking}} - \sum_{j=1}^N \tilde{p}_{ji} \right\} \right\} \\ &\leq \min \left\{ r_i(\pi^{*,R1, \text{pecking}}, p^{*,R1, \text{pecking}}), \frac{1}{\tilde{\pi}} \max \left\{ 0, \sum_{j=1}^N \bar{p}_{ij}^{R2, \text{pecking}} - \sum_{j=1}^N \tilde{p}_{ji} \right\} \right\} = \Gamma_i(\tilde{\pi}, \tilde{p}). \end{aligned}$$

Case 2: Let $0 = \tilde{\pi} = \pi$, then it follows directly from the definition that $\Gamma_i(\pi, p) = \Gamma_i(\tilde{\pi}, \tilde{p})$.

Case 3: Let $0 = \tilde{\pi} < \pi$. If $i \in \mathcal{D}(p^{*,R1, \text{pecking}})$ and $\max \left\{ 0, \sum_{j=1}^N \bar{p}_{ij}^{R2, \text{pecking}} - \sum_{j=1}^N p_{ji} \right\} > 0$, then

$$\begin{aligned} \Gamma_i(\tilde{\pi}, \tilde{p}) &= r_i(\pi^{*,R1, \text{pecking}}, p^{*,R1, \text{pecking}}) \\ &\geq \min \left\{ r_i(\pi^{*,R1, \text{pecking}}, p^{*,R1, \text{pecking}}), \frac{1}{\pi} \max \left\{ 0, \sum_{j=1}^N \bar{p}_{ij}^{R2, \text{pecking}} - \sum_{j=1}^N p_{ji} \right\} \right\} = \Gamma(\pi, p), \end{aligned}$$

otherwise it holds that $\Gamma_i(\tilde{\pi}, \tilde{p}) = 0 = \Gamma(\pi, p)$.

Hence, $\Gamma(\pi, p) = \sum_{i=1}^N \Gamma_i(\pi, p) \leq \sum_{i=1}^N \Gamma_i(\tilde{\pi}, \tilde{p}) = \Gamma_i(\tilde{\pi}, \tilde{p})$ and therefore

$$\Phi_1^{R2, \text{pecking}}(\pi, p) = \pi^{*,R1, \text{pecking}} \exp(-\alpha \Gamma(\pi, p)) \geq \pi^{*,R1, \text{pecking}} \exp(-\alpha \Gamma(\tilde{\pi}, \tilde{p})) = \Phi_1^{R2, \text{pecking}}(\tilde{\pi}, \tilde{p}).$$

It is clear from the definition of $\Phi_2^{R2, \text{pecking}}$ that $\Phi_{2,(ij)}^{R2, \text{pecking}}(\tilde{\pi}, \tilde{p}) \leq \Phi_{2,(ij)}^{R2, \text{pecking}}(\pi, p)$ for all $i, j \in \mathcal{N}$. \square

Theorem D.4 (Existence of a least and greatest price-payment equilibrium in Round 2 in the setting with a pecking order). *Let $\Phi^{R2, \text{pecking}} : [0, \pi^{*,R1, \text{pecking}}] \times [0, \bar{p}^{R2, \text{pecking}}] \rightarrow [0, \pi^{*,R1, \text{pecking}}] \times [0, \bar{p}^{R2, \text{pecking}}]$ be the function defined in (17).*

1. *The set of fixed points of $\Phi^{R2, \text{pecking}}$ is a complete lattice. In particular $\Phi^{R2, \text{pecking}}$ admits a greatest and a least fixed point.*
2. *Let $(\pi^{(0)}, p^{(0)}) = (\pi^{*,R1, \text{pecking}}, \bar{p}^{R2})$ and define recursively for $k \in \mathbb{N}_0$*

$$(\pi^{(k+1)}, p^{(k+1)}) = \Phi^{R2, \text{pecking}}(\pi^{(k)}, p^{(k)}).$$

Then,

- (a) *$(\pi^{(k)}, p^{(k)})_{k \in \mathbb{N}_0}$ is a monotonically non-increasing sequence, that is, $\pi^{(k+1)} \leq \pi^{(k)}$ and $p_{ij}^{(k+1)} \leq p_{ij}^{(k)}$ for all $i, j \in \mathcal{N}$ and for all $k \in \mathbb{N}_0$.*

(b) The limit $\lim_{k \rightarrow \infty} (\pi^{(k)}, p^{(k)})$ exists and is the greatest fixed point of $\Phi^{R2, \text{pecking}}$.

Proof of Theorem D.4. 1. We will prove the statement using Tarski's fixed point theorem (Tarski, 1955). First, $[0, \pi^{*,R1, \text{pecking}}] \times [0, \bar{p}^{R2, \text{pecking}}]$ is a complete lattice with respect to the component-wise ordering. Second, it follows directly from the definition of $\Phi^{R2, \text{pecking}}$ in (17) that indeed $\Phi^{R2, \text{pecking}} : [0, \pi^{*,R1, \text{pecking}}] \times [0, \bar{p}^{R2, \text{pecking}}] \rightarrow [0, \pi^{*,R1, \text{pecking}}] \times [0, \bar{p}^{R2, \text{pecking}}]$. Third, $\Phi^{R2, \text{pecking}}$ is an order-preserving function by Lemma D.3. Hence, by Tarski's fixed point theorem, the set of fixed points of $\Phi^{R2, \text{pecking}}$ is a complete lattice and hence a least and greatest fixed point exist.

2. Since $\Phi^{R2, \text{pecking}}$ is right-continuous, the same arguments as in the proof of Theorem D.2 (part 2) can be used to prove the statement. □

D.3 Pecking order: two simple examples

We now show that clearing with a pecking order can lead to a different equilibrium compared to clearing based on the pro rata rule. We provide two examples, the first showing situations when a pecking order can reduce the number of contagious defaults, and the second illustrating that clearing with a pecking order can also increase the number of contagious defaults. We consider a similar situation as in Example 1 in Subsection 3.1, where a joint clearing member defaults.

D.3.1 Example #1: Clearing with a pecking order can reduce the number of contagious defaults

We consider a system consisting of $n_C = 2$ CCPs and $n_M = 3$ clearing members. Figure 16 provides an illustration of the network of payment obligations. The weights along the edges represent the payment obligation due from i to j in the first round, i.e., \bar{p}_{ij}^{R1} , and the numbers in parentheses represent the corresponding initial margins (m_{ij}). For simplicity, we assume that the liquidity buffers are zero for all nodes except for the joint clearing member M1 which has a liquidity buffer of 2.5.

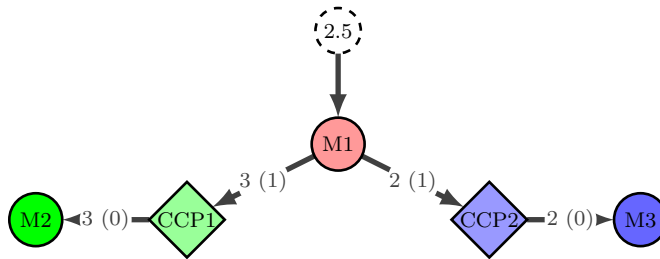


Figure 16: Example in which clearing with a pecking order can reduce the number of contagious defaults.

There is one joint clearing member (M1) that clears at both CCPs. The other two clearing members only clear at one CCP each (M2 at CCP1 and M3 at CCP2). Again we label the clearing members M_i with index i for $i \in \{1, 2, 3\}$, CCP1 with index 4 and CCP2 with index 5 in the matrices and vectors below. Formally,

$$\bar{p}^{\text{R1}} = \begin{pmatrix} 0 & 0 & 0 & 3 & 2 \\ 0 & 0 & 0 & 0 & 0 \\ 0 & 0 & 0 & 0 & 0 \\ 0 & 3 & 0 & 0 & 0 \\ 0 & 0 & 2 & 0 & 0 \end{pmatrix}, \quad m = \begin{pmatrix} 0 & 0 & 0 & 1 & 1 \\ 0 & 0 & 0 & 0 & 0 \\ 0 & 0 & 0 & 0 & 0 \\ 0 & 0 & 0 & 0 & 0 \\ 0 & 0 & 0 & 0 & 0 \end{pmatrix}, \quad b = (2.5, 0, 0, 0, 0)^\top.$$

The joint clearing member M1 is the only node in fundamental default, i.e., $\mathcal{F} = \{1\} = \{\text{M1}\}$.

We assume that $\gamma_i^{(1)}, \gamma_i^{(2)} \in [0, 1]$ for all $i \in \mathcal{N}$ and assume that $\alpha = 0$.

Then, if we use clearing with pro rata payments, i.e., by using Φ^{R1} and Φ^{R2} in (1) and (3) respectively, then both CCPs default. In particular, here

$$p^{*,\text{R1}} = \begin{pmatrix} 0 & 0 & 0 & \frac{8}{3} & \frac{11}{6} \\ 0 & 0 & 0 & 0 & 0 \\ 0 & 0 & 0 & 0 & 0 \\ 0 & \frac{8}{3} & 0 & 0 & 0 \\ 0 & 0 & \frac{11}{6} & 0 & 0 \end{pmatrix},$$

and $\Delta = 2$, i.e., all initial margins are used in the first round. Therefore, no initial margins are returned in round 2 and therefore $\Gamma = 0$ and $p^{*,\text{R2}} = 0$. The total shortfall is $S = 1$. Assuming illiquid collateral ($\alpha > 0$) increases the shortfall, but cannot lead to more defaults because all nodes with payment obligations are already in default.

If, however, clearing is done using a pecking order of the clearing members, i.e., by using $\Phi^{\text{R1, pecking}}$ and $\Phi^{\text{R2, pecking}}$ in (13) and (17) respectively – where clearing members rank CCPs according to the size of their payment obligations – then only CCP2 defaults. In particular, clearing member M1 ranks CCP1 on rank 1 of its pecking order and CCP2 on rank 2, because M1's payment obligations to CCP1 are larger than those to CCP2. Then,

$$p^{*,\text{R1, pecking}} = \begin{pmatrix} 0 & 0 & 0 & 3 & 1.5 \\ 0 & 0 & 0 & 0 & 0 \\ 0 & 0 & 0 & 0 & 0 \\ 0 & 3 & 0 & 0 & 0 \\ 0 & 0 & 1.5 & 0 & 0 \end{pmatrix},$$

and $\Delta = 2$, i.e., all initial margins are used in the first round. Therefore, no initial margins are returned in round 2 and therefore $\Gamma = 0$ and $p^{*,\text{R2, pecking}} = 0$. The the total shortfall is the same as before ($S = 1$).

Hence, this is an example in which the pecking order causes a smaller number of contagious defaults. This is not always the case. Here, CCP1 is on rank 1 in M1's pecking order. Hence, all available assets are used to pay CCP1 first, before CCP2 is paid. In this example, this results in CCP1 being paid in full (all initial margins are used), but now there is a payment shortfall of $1/2$ from M1 to CCP2. With pro-rata payments this shortfall was only $1/6$.

If M3 has payment obligations, the higher shortfall can cause additional contagious default, as the next example shows.

D.3.2 Example #2: Clearing with a pecking order can increase the number of contagious defaults

For this example, we add one more CCP and one more clearing member to the previous situation. Figure 17 provides a graphical illustration. Formally,

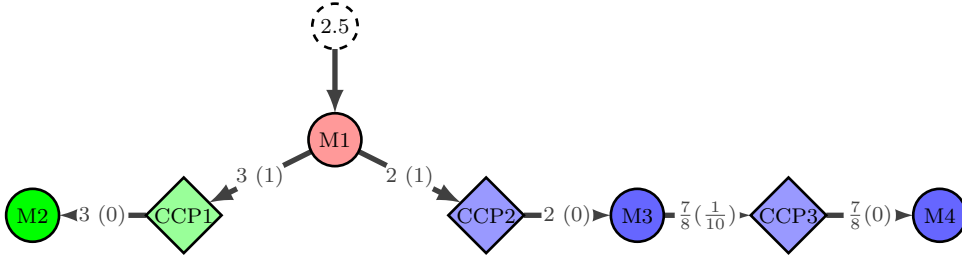


Figure 17: Example in which clearing with a pecking order can increase the number of contagious defaults.

$$\bar{p}^{R1} = \begin{pmatrix} 0 & 0 & 0 & 0 & 3 & 2 & 0 \\ 0 & 0 & 0 & 0 & 0 & 0 & 0 \\ 0 & 0 & 0 & 0 & 0 & 0 & \frac{7}{8} \\ 0 & 0 & 0 & 0 & 0 & 0 & 0 \\ 0 & 3 & 0 & 0 & 0 & 0 & 0 \\ 0 & 0 & 2 & 0 & 0 & 0 & 0 \\ 0 & 0 & 0 & \frac{7}{8} & 0 & 0 & 0 \end{pmatrix}, \quad m = \begin{pmatrix} 0 & 0 & 0 & 0 & 1 & 1 & 0 \\ 0 & 0 & 0 & 0 & 0 & 0 & 0 \\ 0 & 0 & 0 & 0 & 0 & 0 & 0.1 \\ 0 & 0 & 0 & 0 & 0 & 0 & 0 \\ 0 & 0 & 0 & 0 & 0 & 0 & 0 \\ 0 & 0 & 0 & 0 & 0 & 0 & 0 \\ 0 & 0 & 0 & 0 & 0 & 0 & 0 \end{pmatrix}, \quad b = (2.5, 0, 0, 0, 0, 0, 0)^\top.$$

Then, if we use clearing with pro rata payments, i.e., by using Φ^{R1} and Φ^{R2} in (1) and (3) respectively, then as before CCP1, CCP2 are the only contagious defaults. In particular, here

$$p^{*,R1} = \begin{pmatrix} 0 & 0 & 0 & 0 & \frac{8}{3} & \frac{11}{6} & 0 \\ 0 & 0 & 0 & 0 & 0 & 0 & 0 \\ 0 & 0 & 0 & 0 & 0 & 0 & \frac{7}{4} \\ 0 & \frac{8}{3} & 0 & 0 & 0 & 0 & 0 \\ 0 & 0 & \frac{11}{6} & 0 & 0 & 0 & 0 \\ 0 & 0 & 0 & \frac{7}{4} & 0 & 0 & 0 \end{pmatrix},$$

and $\Delta = 2$. Furthermore, $\Gamma = 0$ and $p^{*,R2} = 0$. The total shortfall is $S = 1$.

If, however, clearing is done using a pecking order of the clearing members, i.e., by using $\Phi^{R1, \text{pecking}}$ and $\Phi^{R2, \text{pecking}}$ in (13) and (17) respectively, then CCP1 no longer defaults, CCP2 still defaults and now additionally both CCP3 and M4 default.

In particular, here

$$p^{*,R1, \text{pecking}} = \begin{pmatrix} 0 & 0 & 0 & 0 & 3 & 1.5 & 0 \\ 0 & 0 & 0 & 0 & 0 & 0 & 0 \\ 0 & 0 & 0 & 0 & 0 & 0 & 1.6 \\ 0 & 0 & 0 & 0 & 0 & 0 & 0 \\ 0 & 3 & 0 & 0 & 0 & 0 & 0 \\ 0 & 0 & 1.5 & 0 & 0 & 0 & 0 \\ 0 & 0 & 0 & 1.6 & 0 & 0 & 0 \end{pmatrix},$$

and $\Delta = 2.1$, i.e., all initial margins are used in the first round. Therefore, no initial margins are returned in round 2 and therefore $\Gamma = 0$ and $p^{*,R2, \text{pecking}} = 0$. The total shortfall has now increased to $S = 1.3$. Hence, this is an example in which using a pecking order for clearing can increase the total shortfall.

D.4 Pecking order: a case study

We now consider an example of clearing in IRS. The stress scenario is chosen such that Deutsche Bank and the Royal Bank of Scotland are the only fundamental defaults. Figure 18 shows the difference between the shortfall from clearing with a pecking order (where clearing members rank CCPs according to the size of payment obligations) and clearing using the pro rata rule. For both clearing models we assume liquid collateral and no additional frictions. We find that there are winners and losers when using a pecking order. The winner here is LCH Swap Clear which receives more payments from Deutsche Bank. CME and JSCC, however, receive less payments under the pecking order rule. When comparing the total shortfall in the system, clearing with a pecking order results in a slightly larger shortfall of $S = 5,920,148$ (million USD), which compares to $S = 5,919,408$ (million USD) under the pro rata rule.

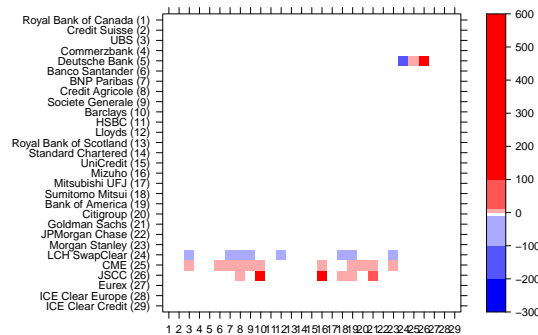


Figure 18: Difference in the shortfalls obtained from using a pecking order and a pro rata rule. Blue cells represent winners under the pecking order (i.e., smaller shortfalls), red cells represent losers under the pecking order (i.e., higher shortfalls).

We also investigate the impact of clearing with pecking order when conducting a stress test as before, by wiping out the liquidity buffers of different pairs of clearing members. Figure 19 shows the difference in shortfall between clearing with pecking order and clearing pro rata for different combinations of clearing member pairs being shocked. Here, we assume that collateral is liquid and that there are no further frictions. We find that in the large majority of cases, clearing with a pecking order results in a slightly larger shortfall in the system.

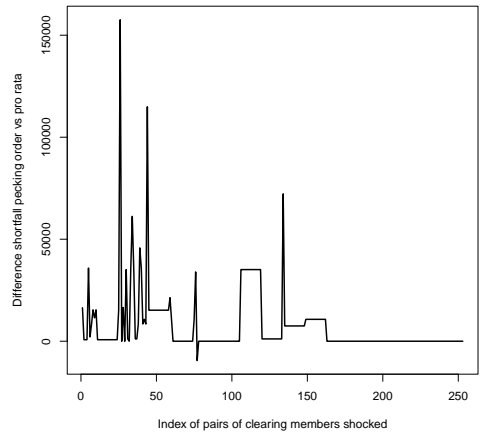


Figure 19: Difference in shortfall when clearing members use a pecking order ($\Phi^{R1, \text{pecking}}$ and $\Phi^{R2, \text{pecking}}$) rather than the pro-rata repayment (Φ^{R1} and Φ^{R2}) when different pairs of clearing members are shocked. All numbers in million USD.

References

- Amini, H., Filipović, D. & Minca, A. (2015). Systemic risk and central clearing counterparty design. Swiss Finance Institute Research Paper No. 13-34. Available at SSRN: <https://ssrn.com/abstract=2275376>.
- Amini, H., Filipović, D. & Minca, A. (2016). Uniqueness of equilibrium in a payment system with liquidation costs. *Operations Research Letters* **44**, 1–5.
- Basel Committee on Banking Supervision (2018). Stress testing principles. Available on <https://www.bis.org/bcbs/publ/d450.htm>.
- BCBS-CPMI-FSB-IOSCO (2018). Analysis of central clearing interdependencies. Tech. Rep. 181, Basel Committee on Banking Supervision - Committee on Payments and Market Infrastructures - Financial Stability Board - International Organization of Securities Commissions.
- Biais, B., Heider, F. & Hoerova, M. (2016). Risk-sharing or risk-taking? Counterparty risk, incentives, and margins. *The Journal of Finance* **71**, 1669–1698.
- Bignon, V. & Vuillemeys, G. (2020). The failure of a clearinghouse: Empirical evidence. *Review of Finance* **24**, 99–128.
- Boissel, C., Derrien, F., Ors, E. & Thesmar, D. (2017). Systemic risk in clearing houses: Evidence from the European repo market. *Journal of Financial Economics* **125**, 511–536.
- Cifuentes, R., Shin, H. S. & Ferrucci, G. (2005). Liquidity risk and contagion. *Journal of the European Economic Association* **3**, 556–566.
- Cont, R. (2017). Central clearing and risk transformation. Working Paper Norges Bank Research 3/2017.
- Cont, R. & Kokholm, T. (2014). Central clearing of OTC derivatives: bilateral vs multilateral netting. *Statistics & Risk Modeling* **31**, 3–22.
- CPMI-IOSCO (2018). Framework for supervisory stress testing of central counterparties (ccps). Publication by the Committee on Payments and Market Infrastructures (CPMI), Board of the International Organization of Securities Commissions (IOSCO); available on www.bis.org.
- CPMI-IOSCO (2020). Central counterparty default management auctions – issues for consideration. Publication by the Committee on Payments and Market Infrastructures (CPMI), Board of the International Organization of Securities Commissions (IOSCO); available on www.bis.org.
- Demange, G. & Piquard, T. (2021). On the market structure of central counterparties in the EU. Preprint available at <https://halshs.archives-ouvertes.fr/halshs-03107812>.
- Duffie, D. (2014). Resolution of failing central counterparties. Research Papers 3256, Stanford University, Graduate School of Business.
- Duffie, D. & Zhu, H. (2011). Does a central clearing counterparty reduce counterparty risk? *Review of Asset Pricing Studies* **1**, 74–95.
- Eisenberg, L. & Noe, T. H. (2001). Systemic risk in financial systems. *Management Science* **47**, 236–249.
- Elsinger, H. (2011). Financial networks, cross holdings, and limited liability. Tech. rep., Oesterreichische Nationalbank Working Paper 156.

- ESMA (2020). Report, 3rd EU-wide stress test. European Securities and Markets Authority (ESMA), ESMA-151-3186.
- ESRB (2020). Mitigating the procyclicality of margins and haircuts in derivatives markets and securities financing transactions. Tech. rep., European Systemic Risk Board.
- Faruqui, U., Huang, W. & Takáts, E. (2018). Clearing risks in OTC derivatives markets: the CCP-bank nexus. *BIS Quarterly Review* .
- Ferrara, G., Li, X. & Marszalec, D. (2020). Central counterparty auction design. *Journal of Financial Market Infrastructures* .
- Gandy, A. & Veraart, L. A. M. (2017). A Bayesian methodology for systemic risk assessment in financial networks. *Management Science* **63**, 4428–4446.
- Garratt, R. & Zimmerman, P. (2015). Does central clearing reduce counterparty risk in realistic financial networks? *Federal Reserve Bank of New York - Staff Reports* 1–18.
- Ghamami, S., Glasserman, P. & Young, H. P. (2022). Collateralized networks. *Management Science* **68**, 2202–2225.
- Glasserman, P., Moallemi, C. C. & Yuan, K. (2015). Hidden illiquidity with multiple central counterparties. *Operations Research* **64**, 1143–1158.
- Gregory, J. (2014). *Central counterparties: Mandatory Central Clearing and Initial Margin Requirements for OTC Derivatives*. Wiley Finance.
- Huang, W. (2019). Central counterparty capitalization and misaligned incentives. BIS Working Papers 767, Bank for International Settlements.
- Huang, W. & Takats, E. (2020). Model risk at central counterparties: Is skin-in-the-game a game changer? BIS Working Papers 866, Bank for International Settlements.
- Huang, W. & Zhu, H. (2021). CCP auction design. BIS Working Paper No 938, Bank for International Settlements.
- ISDA (2013). CCP loss allocation at the end of the waterfall. Tech. rep., International Swaps and Derivatives Association.
- Lopez, J. A. C., Harris, J. H., Hurlin, C. & Pérignon, C. (2017). Comargin. *Journal of Financial and Quantitative Analysis* **52**, 2183–2215.
- Menkveld, A. J. & Vuillemeij, G. (2021). The economics of central clearing. *Annual Review of Financial Economics* **13**, 153–178.
- Newman, M. E. J. (2010). *Networks - An Introduction*. Oxford University Press.
- Paddrik, M., Rajan, S. & Young, H. P. (2020). Contagion in derivatives markets. *Management Science* **66**, 3603–3616.
- Paddrik, M. & Young, H. P. (2021). How safe are central counterparties in credit default swap markets? *Mathematics and Financial Economics* **15**, 41–57.
- Rogers, L. & Veraart, L. A. M. (2013). Failure and rescue in an interbank network. *Management Science* **59**, 882–898.

- Tarski, A. (1955). A lattice theoretical fixed point theorem. *Pacific Journal of Mathematics* **5**.
- Veraart, L. A. M. (2022). When does portfolio compression reduce systemic risk? *Mathematical Finance* **32**, 727–778.
- Wang, J. J., Capponi, A. & Zhang, H. (2022). A theory of collateral requirements for central counterparties. *Management Science* .

Previous volumes in this series

1051 November 2022	How capital inflows translate into new bank lending: tracing the mechanism in Latin America	Carlos Cantú, Catherine Casanova, Rodrigo Alfaro, Fernando Chertman, Gerald Cisneros, Toni dos Santos, Roberto Lobato, Calixto Lopez, Facundo Luna, David Moreno, Miguel Sarmiento and Rafael Nivin
1050 November 2022	Population aging and bank risk-taking	Sebastian Doerr, Gazi Kabaş and Steven Ongena
1049 November 2022	Crypto trading and Bitcoin prices: evidence from a new database of retail adoption	Raphael Auer, Giulio Cornelli, Sebastian Doerr, Jon Frost and Leonardo Gambacorta
1048 November 2022	Is the Covid-19 pandemic fast-tracking automation in developing countries? Evidence from Colombia	Leonardo Bonilla, Luz A Flórez, Didier Hermida, Francisco Lasso, Leonardo Fabio Morales, Juan Jose Ospina and José Pulido
1047 November 2022	What drives inflation? Disentangling demand and supply factors	Sandra Eickmeier and Boris Hofmann
1046 November 2022	The case for convenience: how CBDC design choices impact monetary policy pass-through	Rodney Garratt, Jiaheng Yu and Haoxiang Zhu
1045 October 2022	The term structure of carbon premia	Dora Xia and Omar Zulaica
1044 October 2022	Gender diversity in bank boardrooms and green lending: evidence from euro area credit register data	Leonardo Gambacorta, Livia Pancotto, Alessio Reghezza and Martina Spaggiari
1043 October 2022	The scarring effects of deep contractions	David Aikman, Mathias Drehmann, Mikael Juselius and Xiaochuan Xing
1042 September 2022	Emerging market bond flows and exchange rate returns	Peter Hördahl and Giorgio Valente
1041 September 2022	The impact of fintech lending on credit access for U.S. small businesses	Giulio Cornelli, Jon Frost, Leonardo Gambacorta and Julapa Jagtiani
1040 September 2022	Quantifying the role of interest rates, the Dollar and Covid in oil prices	Emanuel Kohlscheen

All volumes are available on our website www.bis.org.